Geotechnical uncertainties and reliability-based assessments of dykes

Varkey, Divya

DOI
10.4233/uuid:48460103-30a0-4338-8c4a-ebc80c73c2d3

Publication date
2020

Document Version
Final published version

Citation (APA)
Varkey, D. (2020). *Geotechnical uncertainties and reliability-based assessments of dykes*. [Dissertation (TU Delft), Delft University of Technology]. https://doi.org/10.4233/uuid:48460103-30a0-4338-8c4a-ebc80c73c2d3

GEOTECHNICAL UNCERTAINTIES AND RELIABILITY-BASED ASSESSMENTS OF DYKES

GEOTECHNICAL UNCERTAINTIES AND RELIABILITY-BASED ASSESSMENTS OF DYKES

Dissertation

for the purpose of obtaining the degree of doctor
at Delft University of Technology
by the authority of the Rector Magnificus, prof. dr. ir. T.H.J.J. van der Hagen,
chair of the Board for Doctorates,
to be defended publicly on
Thursday 24 September 2020 at 10:00 o'clock

by

Divya VARKEY

Master of Technology in Soil Dynamics, Indian Institute of Technology Roorkee, India
born in Bhilai, India

This dissertation has been approved by the promotors.

Composition of the doctoral committee:

Rector Magnificus	chairperson
Prof. dr. M. A. Hicks	Delft University of Technology, promotor
Dr. P. J. Vardon	Delft University of Technology, promotor
Independent members:	
Prof. dr. J. Ching	National Taiwan University
Dr. T. L. L. Orr	Trinity College Dublin
Ir. H. van Hemert	Rijkswaterstaat, STOWA
Prof. dr. ir. S. N. Jonkman	Delft University of Technology
Prof. dr. ir. P. H. A. J. M. van Gelder	Delft University of Technology

Keywords: Hetereogeneity, Reliability, RFEM, Slope stability, Statistical analysis

Printed by: Ipskamp printing

Front & Back: Based on Section 3.4.1 of this dissertation.

ISBN 978-94-6366-298-7

An electronic version of this dissertation is available at
http://repository.tudelft.nl/.

To my parents

CONTENTS

SUMMARY

This thesis utilises the random finite element method (RFEM) to provide practical guidance and tools for geotechnical engineers to account for the influence of soil spatial variability. This has involved: (a) practical insight and guidance on the choice of characteristic soil property values and scales of fluctuation; (b) a robust approach to reliability assessment and design that obviates the need for explicit calculation of characteristic values; and (c) the benchmarking and improving of simpler analysis tools.

The presence of uncertainties, due to both insufficient knowledge and irreducible uncertainties, significantly influences the design and performance assessment of geotechnical structures. As such, a common engineering practice is to carry out deterministic assessments of structures based on characteristic soil property values. These are often derived as cautious estimates of property (or mean property) values, based on the Eurocode 7 guidelines requiring a 95% structural reliability. Although the Eurocode promotes the use of statistical methods, it gives limited guidance on how to derive the characteristic values; in particular, given their problem-dependent nature, which can make their determination rather subjective. As a simple default, engineers sometimes resort to a deterministic approach based on 5-percentile soil property values, ensuring a (over) conservative solution. This thesis proposes to close this knowledge gap by using a fully probabilistic RFEM to calculate safety factors at the target reliability level recommended in Eurocode 7, hence by-passing the need to explicitly calculate the characteristic values. This thesis demonstrates the advantages of a full probabilistic analysis, by comparing the safety assessment of an existing dyke, founded on a layered soil, in the Netherlands using the two approaches, i.e the full probabilistic and deterministic approaches. The results facilitate a better understanding of reliability-based characteristic values, by explicitly accounting for uncertainties and by reducing over-conservatism in designs. The results of this research are a clear demonstration of how the advantages of a more accurate RFEM solution in a practical setting may outweigh any disadvantages relating to computational time.

The influence of accounting for the out-of-plane (i.e. along the dyke) correlation structure of shear strength properties has begun to receive increasing attention in research. This is because a 3D reliability assessment enables modelling the complete soil correlation structure, and the results are usually found to be significantly different compared to equivalent 2D assessments. This thesis investigates the influence of various forms of geometric uncertainties on reliability assessments of dykes. Specifically, for an idealised 3D embankment slope, the influence of uncertainties in the external slope geometry, in the depth of the boundary between the slope and foundation materials, and in the spatial variability of shear strength properties within soil layers has been investigated. The results indicate that soil spatial variability is the most influential factor, whereas the influence of uncertainties in the external geometry and inter-layer boundaries were very small to negligible. The influence of anisotropic soil spatial variability on the reliability of the slope

and on the consequences of failure have also been investigated. It was demonstrated that the correlation structure along the embankment length had a greater influence on the computed response than that perpendicular to the embankment length. It was also demonstrated that using an isotropic horizontal correlation length based on the critical value of the correlation length along the embankment gave reasonably conservative solutions. A range of critical values of the correlation length were identified, hence bypassing the need to accurately determine the in-situ horizontal spatial variability in some cases.

For very long geotechnical structures like dykes, the computational requirements of a full RFEM analysis may increase by several orders of magnitude, thereby limiting its application. Nevertheless, there are simpler semi-analytical methods which give fast and convenient solutions for 3D slope reliability assessments. Hence, there is a need to benchmark these simpler methods to identify when the results are comparable to the more robust RFEM solution and when they are not. This thesis compares the performance of RFEM with Vanmarcke's method, a simpler method that predicts the reliability of heterogeneous 3D slopes based on certain simplifying yet significant assumptions. The ranges of the scale of fluctuation of the shear strength properties for which the two methods give similar results, and for which they give significantly different results, were identified, and the reasons behind the differences investigated. Three significant areas were identified as requiring improvement in the simpler method. These errors were corrected in this thesis by proposing an alternative relationship for the predicted failure length and two correction factors (to account for the overestimated end-resistance and the overestimated averaged shear strength) that modify the original formulation of the Vanmarcke method. The proposed modifications resulted in solutions that were in good agreement to the computationally expensive RFEM solutions for the entire range of correlation lengths and slope geometries considered in this research.

The combination of approaches developed and demonstrated in this thesis makes several significant steps in making reliability-based design a practical and valuable tool in geotechnical engineering.

SAMENVATTING

Dit proefschrift gebruikt de random finite element method (RFEM) om praktische richtlijnen en hulpmiddelen voor geotechnische ingenieurs te geven om rekening te houden met de invloed van ruimtelijke variatie. Het werk bestaat uit: (a) praktisch inzicht en sturing voor een keuze in karakteristieke grondparameters en ruimtelijke correlatie; (b) een robuuste methode voor toetsing en ontwerp die het berekenen van karakteristieke waarden overbodig maakt; en (c) het benchmarken en verbeteren van eenvoudigere analysemethoden.

De aanwezigheid van onzekerheden als gevolg van onvoldoende kennis en niet-reduceerbare onzekerheden hebben een significante invloed op het ontwerp en de toetsing van geotechnische constructies. Hierdoor is het gebruikelijk om in de praktijk determinische analyses van constructies uit te voeren op basis van karakteristieke grondparameters. Deze waarden zijn vaak afgeleid als een voorzichtige schatting van de parameterwaarden (of gemiddelde waarden), gebaseerd op de Eurocode 7-norm waarin een 95% betrouwbaarheid geëist wordt. Hoewel de Eurocode het gebruik van statistische methoden toestaat, geeft het weinig richtlijnen over hoe de karakteristieke waarde afgeleid dient te worden; in het bijzonder, omdat de waarden probleemafhankelijk zijn is de afleiding zeer subjectief. Gebruikelijk gaan ingenieurs ervan uit dat een deterministische aanpak, gebaseerd op de 5-procent grondparameter, voldoende conservatief is. Dit proefschrift gebruikt een volledig statistische RFEM analyse om de kennisleemte te overbruggen en de veiligheidsfactoren te berekenen aan de hand van de betrouwbaarheidseis die wordt gesteld in Eurocode 7. Hiermee is het niet meer nodig expliciet te karakteristieke waarden te berekenen.

Dit proefschrift toont de voordelen van van een volledig probabilistische analyse met de vergelijking van de veiligheidstoetsing van een bestaande Nederlandse dijk die rust op een gelaagde ondergrond. Deze vergelijking behelst twee methodes; een volledig proabilistische en een deterministische. De resultaten leiden tot een beter begrip van de op betrouwaarheids-niveau gebaseerde karakteristieke waarden, door onzekerheden expliciet mee te nemen en door de reductie van over-conservatisme in het ontwerp. De resultaten van dit onderzoek tonen duidelijk aan hoe de voordelen van een nauwkeuriger RFEM berekening in de praktijk kan opwegen tegen de nadelen gerelateerd aan de rekentijd.

De invloed van het meenemen van de out-of-plane (i.e. parallel aan de dijk) ruimtelijke correlatie van de schuifsterkte-materiaaleigenschappen krijgt steeds meer aandacht in wetenschappelijk onderzoek. Dit gebeurt omdat in 3D betrouwbaarheidsanalyses de gehele ruimtelijke correlatie structuur gemodelleerd kan worden, en vaak wordt er een significant verschil gevonden in vergelijking met vergelijkbare 2D analyses. Dit proefschrift onderzoekt het effect van verschillende vormen van geometrische onzekerheden op de betrouwbaarheidsanalyses van dijken. Vanuit een geidealiseerd 3D hellingsmodel is de invloed van onzekerheden in de externe geometrie, in de laagscheidingsdiepte en in de

ruimtelijke variabiliteit van de sterkte eigenschappen onderzocht. Hieruit is gebleken dat de onzekerheid in de ruimtelijke variatie de meeste invloed heeft, terwijl de invloed van de externe geometrie en de laagscheidingsgrens tussen de helling en de fundering relatief klein tot verwaarloosbaar is. Ook zijn de invloed van anisotropische ruimtelijke variatie op de betrouwbaarheidsanalyse en de consequenties voor het faalmechanisme onderzocht. Hieruit volgt dat de invloed van de ruimtelijke variatie in de langsrichting van de dijk groter is dan de invloed van de ruimtelijke variatie dwars op de dijk. Ook is aangetoond dat wanneer het gebruik van een isotrope horizontale correlatielengte wordt gebaseerd op de kritische correlatielengte, dit redelijk conservatieve waarden geeft. Vanuit de benchmarkanalyses zijn kritische waarden voor correlatielengtes vastgesteld, waardoor niet voor alle gevallen de ruimtelijke variatie met metingen hoeft worden vastgesteld.

Voor lange geotechnische constructies zoals dijken neemt de benodigde rekencapaciteit van een volledige RFEM analyse toe met meerdere ordes van grootte. Dit limiteerd de bruikbaarheid. Echter geven eenvoudige semi-analytische methodes voor de betrouwbaarheidsanalyse van 3D hellingen snelle en bruikbare resultaten. Hierdoor ontstaat de noodzaak deze eenvoudigere methoden te benchmarken en te analyseren wanneer de methoden overeenkomen met de RFEM oplossing. In dit proefschrift worden de resultaten van RFEM vergeleken met de methode van Vanmarcke , een eenvoudigere methode om de betrouwbaarheid van 3D hellingen te voorspellen die uitgaat van significante vereenvoudigingen en aannames. Het interval waarin de ruimtelijke variatie van de sterkte-eigenschappen voor beide methoden overeenkomen, en waar de resultaten significante verschillen vertonen, zijn geinventairseerd en de redenen waarom de antwoorden verschillen zijn verder onderzocht. Er zijn drie onderdelen geïdentificeerd waar de eenvoudigere methode significant verbeterd kan worden. In dit proefschrift is een voorstel gedaan voor het corrigeren van de Vanmarcke methode door middel van een alternatieve relatie voor de lengte van het faalmechanisme en twee correctiefactoren (ter correctie van de overschatting van de kopweerstand en van de gemiddelde sterkte). De resultaten van de voorgestelde aanpassingen zijn in goede overeenstemming met de berekeningintensieve RFEM methode voor het gehele scala aan ruimtelijke correlatielengtes en hellinggeometrieën binnen dit onderzoek.

De combinatie van de methoden die worden gebruikt en gedemonstreerd in dit proefschrift maken de betekenis in het beschikbaar maken van praktische betrouwbareheidsanalyses als hulpmiddel in de geotechnische adviespraktijk.

LIST OF SYMBOLS

ACRONYMS

1D	1 Dimensional
2D	2 Dimensional
3D	3 Dimensional
cdf	Cumulative Density Function
COV	Coefficient of Variation
CPT	Cone Penetration Test
EC7	Eurocode 7
ERD	Effective Random Dimensions 7
FEM	Finite Element Method
FORM	First Order Reliability Method
FOSM	First Order Second Moment method
HHNK	Hoogheemraadschap Hollands Noorderkwartier (Water Board Hollands Noorderkwartier)
HLRF	Hasofer-Lind Rackwitz Fiessler
IPO	Interprovinciaal Overleg
LAS	Local Average Subdivision
MVM	Modified Vanmarcke's Method
NWO	Nederlandse Organisatie voor Wetenschappelijk Onderzoek (Netherlands Organisation for Scientific Research)
pdf	Probability Density Function
PEM	Point Estimate Method
QVM	Quantile Value Method
RFEM	Random Finite Element Method
RSM	Response Surface Method
SORM	Second Order Reliability Method
TTW	Toegepaste en Technische Wetenschappen (Applied and Engineering Sciences)
VM	Vanmarcke's Method

LATIN SYMBOLS

a	factor accounting for quality of tests and levels of expertise
a^i	weighting coefficient for stage i of LAS
a_W	lever arm of centre of gravity of a sliding mass
A	area of resisting end-section
$\mathbf{A}$	decomposed covariance matrix

b	predicted length of failure
b_c	critical length of failure
b_i	coefficient of variable X_i in the linearised performance function
c'	effective cohesion
c_i	standard deviation of white noise term at stage i of LAS
C	covariance function; crest width
d	effective width of a resisting end-section
D	domain size
E	Young's modulus
E[.]	expectation
$f_X(x)$	joint pdf of X
F	factor of safety
$\overline{F_2}$	2D F based on the mean values of the soil parameters
F_b	3D F of a slope failing over a length b
$g(x)$	limit state function in x-space
$G(u)$	$g(x)$ transformed to standard normal space
H	height of slope
H_b	height of berm
i	direction; stage of LAS
I	indicator function
j,k,m	cell locations in LAS
k_r	standard score
k_X	standard score representing the level of cautious estimate of X
l_{h}	horizontal component of failure length
l_{v}	vertical component of failure length
L	length of slope
L_a	length of cross-sectional failure arc
$\mathbf{L}$	lower triangular matrix obtained by decomposition of $\mathbf{R}$
n	number of cell values
N	number of realisations or variables
P_f	probability of failure
$\mathbf{Q}$	matrix of orthogonal eigenvectors
r	realisation
r'	effective rotation arm for the resisting end-sections
r_b	lever arm of the resisting moment
R	reliability
R_e	resisting moment of end-sections
$\mathbf{R}$	correlation matrix
s	point shear strength
s_1	averaged strength along unit length
s_b	averaged strength along b

s_e	shear strength over resisting end-section
$\boldsymbol{t}$	location in Cartesian space
T	toe width
U	standard normal random number
W	weight per unit length of sliding mass
W_d	inter-ditch spacing
X	random variable in physical space
X_{d}	design value of X
X_{extr}	extreme value of X
X_{k}	characteristic value of X
X_{m}	mean value of X
X^*_{m}	mean value of effective distribution of X
Z	local averaged cell value in standard normal space
$\boldsymbol{Z}$	vector of n un-correlated Gaussian random variables

GREEK SYMBOLS

α	correction factor for overestimated averaged shear strength
β	correction factor for overestimated end-resistance
β_M	Markov covariance function
β_R	reliability index
γ	unit weight
γ_{M}	partial factor on material properties
Γ^2	variance reduction factor
Γ^2_i	Γ^2 along i-direction; Γ^2 for variable X_i
η	percentile of the underlying distribution corresponding to X_k
θ	scale of fluctuation or correlation length
θ_{h}	horizontal component of θ
θ_i	component of θ along i-direction
θ_{v}	vertical component of θ
μ	mean
ν	Poisson's ratio
$\boldsymbol{\xi}$	vector of n correlated Gaussian random variables
ρ	correlation function or coefficient
$\rho_{X_1X_2}$	linear product moment cross-correlation coefficient between variables X_1 and X_2
σ	standard deviation
σ_n	stress normal to failure surface
τ	lag distance
ϕ'	effective friction angle
Φ	standard normal cumulative distribution function
$\boldsymbol{\Lambda}$	diagonal matrix of eigenvalues
ψ	dilation angle

1

INTRODUCTION

1

1.1. BACKGROUND AND MOTIVATION

The ultimate engineering target is to come up with economical designs to build safe structures. Traditionally, engineering practice relied on the concept of a factor of safety (F) of a structure, which was expressed as the ratio of resisting to disturbing forces (or moments). In recent years, computers have transformed engineering practice by speeding-up traditional calculation methods and by allowing the use of more complex numerical techniques, such as the finite element method (FEM). However, although a better understanding of the behavior of soil and implementation of constitutive relations are crucial aspects for design, geotechnical engineering practice relies heavily on engineering judgment when conducting ground investigation and calibrating design property values. Hence, due to a lack of proper understanding of the associated uncertainties and their impacts on a structure, conservative property values are usually chosen, resulting in $F >> 1$ and thereby leading to overconservative and uneconomic designs. Moreover, such a deterministic approach does not allow for a quantifiable assessment of the impact of uncertainties on the calculated F. There can be uncertainty associated with a subjective lack of knowledge (e.g. sampling, testing and calibrating) as well as uncertainty due to irreducible unknowns, such as the inherent soil spatial variability, which may be quantified using a parameter called the scale of fluctuation.

Dyke assessments in the Netherlands are based on using reliability-based characteristic values of geotechnical parameters and partial factors for the resistances and/or actions. Based on the recommendation of the Eurocodes, the National Annexes provide guidance for the values of the partial factors, with the intention to address uncertainties on an individual basis. On the other hand, reliability-based characteristic values may be derived using statistical methods based on the definition in Eurocode 7 (CEN, 2004), which is a significant shift from traditional design methods based on global factors of safety. However, although the code recognises the need for adequate representation of in-situ variability through the choice of the characteristic values, it does not give much guidance on how to determine them. Approximate approaches are available for calculating characteristic values, some of which indirectly incorporate the spatial correlations by reducing the variance of the underlying property distributions. However, for simplicity, geotechnical engineering practice often uses the 5-percentile soil property value as the characteristic value for reliability-based design, and often ignores the impact of any local spatial correlations, thereby leading to uneconomic structures.

There is clearly a need to better understand the concept of characteristic values and to reduce over-conservatism in design. This thesis proposes to close this knowledge gap by using a fully robust random finite element method (RFEM) to calculate reliability-based safety factors for embankment slopes, as well as to back-calculate characteristic soil property values and compare them with those obtained using simplified approaches reported in the literature. The thesis also investigates the influence of spatial variability of the soil properties in the third dimension, as well as variabilities in the geometry of the problem itself, which is especially relevant for reliability-based assessments of long geotechnical structures such as dykes. Moreover, a semi-analytical method for faster predictions of 3D slope reliability, compared to the computationally expensive RFEM, is proposed. This has been developed by extending an existing semi-analytical method by Vanmarcke (1977).

The main motivation of this thesis is to utilise RFEM to provide practical guidance and tools for industry. This involves:

1. Practical insight and guidance on the choice of characteristic soil property values and scales of fluctuation.

2. A new and robust approach to reliability-based assessment and design that obviates the need for explicit calculation of characteristic values.

3. The benchmarking (and improving where applicable) of simpler analysis tools.

1.2. OBJECTIVES OF THE THESIS

Spatial variability of shear strength parameters is an aleatoric form of uncertainty and its quantification is not a trivial task, although some guidance regarding the possible range of values of spatial correlations may be found in the literature. Much research has been done on the influence of the spatial variability of soil shear strength parameters, both drained and undrained, on the stability of slopes in 2D. Efficient probabilistic tools have been successfully applied for assessments of low failure probability events. RFEM has also been widely adopted in research for reliability-based assessments of geotechnical structures, although only a limited number of applications, mostly in an academic setting, have been carried out in 3D owing to its large computational requirements. Conditional random fields, which efficiently use available field data, are now being adopted in research for 2D slope reliability assessments, although there are only a few examples of the technique being adopted for 3D slope reliability assessments.

Although RFEM has been widely used by researchers, it has seldom found its way into practice due to its complexity, required input data and large computational requirements. Instead, geotechnical engineering practice often resorts to a simplified deterministic approach based on characteristic values for reliability-based assessments of geotechnical structures. These characteristic values are derived either by ignoring the spatial nature of soil variability, or by incorporating the soil spatial variability in the form of easy-to-use equations. A thorough comparative analysis of the responses obtained using this simplified approach with the responses obtained at the target reliability level using an RFEM analysis will highlight the advantages, if any, of the computationally expensive RFEM and will give better insights on characteristic values.

The significance of considering the out-of plane spatial correlation structure in the reliability assessments of dykes has been well researched by assuming isotopic correlation in the horizontal plane. In recent years, the uncertainty arising due to stratigraphic heterogeneity between different material zones in 2D geotechnical problems has received increasing attention, although the influence of such a form of uncertainty on the reliability of dykes has not been fully investigated. Also, for long geotechnical structures such as dykes, even for a constant designed cross-section, variations in geometry are generally observed along its length. A detailed investigation combining all these forms of uncertainty could give a better insight into the relative impact of each on the structural response.

Carrying out a full RFEM analysis, as mentioned above, is computationally expensive and is even more so for problems extended to 3D. Alternative simplified semi-analytical

solutions are available in the literature, which, based on certain assumptions, give quick and convenient solutions for 3D slope reliability problems. Hence, there is a need to benchmark these simplified approaches, to identify when they work well and when they do not, and thereby to improve them where appropriate.

In the light of the above, the main objectives of this thesis are:

1. To gain better insights into reliability-based characteristic soil property values, based on probabilistic analyses that fully account for the spatial nature of soil variability.

2. To investigate the relative performance of alternative simpler methods for calculating characteristic values, some of which indirectly incorporate the soil spatial variability by reducing the variance of the underlying property distribution.

3. To model and investigate the relative impact of various forms of spatial uncertainty (i.e. embankment geometry, subsurface stratigraphy and shear strength properties within layers) on 3D slope reliability.

4. To investigate the influence of horizontal anisotropy in the spatial variability of shear strength parameters on the response of slopes in 3D, and to identify worst case correlation scales that may be used in the absence of detailed field data.

5. To benchmark a semi-analytical solution for 3D slope reliability assessments and identify the range of scales of fluctuation of the shear strength parameters over which it gives satisfactory results.

6. To upgrade the semi-analytical solution for 3D slope reliability assessments so that it gives satisfactory results for the entire range of possible scales of fluctuation of the shear strength parameters.

This thesis was funded by the Netherlands Organisation for Scientific Research (NWO) domain Applied and Engineering Sciences (TTW) under the project name Reliable Dykes (13864). The project, with 4 PhDs and 1 post-doctoral researcher, focused on providing a better understanding and quantification of uncertainties and of their impact in stability assessments, and aimed to provide industry with scientific insights and guidance relating to regional dykes. The first PhD project (de Gast, 2020) focused on the characterisation of a site using in-situ (CPT) data, on the monitoring, implementation and evaluation of a full-scale dyke failure test, and on a back-analysis of the field test; the second PhD project (Muraro, 2019) focused on describing pre-failure and failure mechanisms, a better understanding of the mechanical behaviour of peat and providing guidance on the selection of material parameters; the third PhD project is this thesis; the fourth PhD project (e.g. Jamalinia *et al.* (2019)) focused on investigating the soil-atmosphere interaction and hydraulic conditions in the regional dykes; and the post-doctoral researcher (e.g. van den Eijnden & Hicks (2017)), working closely with the 4 PhDs, was responsible for the development of practical assessment tools and facilitating the integration of these tools within industrial codes of practice.

1.3. OVERVIEW OF THE THESIS

This thesis is divided into the following chapters:

Chapter 2 gives an overview of the background literature relevant to this thesis. The chapter describes the various available approaches for the discretisation of random fields and the various reliability-based design methods in geotechnical engineering. Additional topic-specific literature reviews are discussed in the subsequent chapters.

Chapter 3 briefly describes the derivation of characteristic soil property values based on the definition in Eurocode 7. The chapter then reports a case study involving the re-assessment and re-design of a dyke section in the Netherlands. The stability of a representative cross-section of the dyke section was first assessed using characteristic soil property values derived based on a frequent (simpler) interpretation of Eurocode 7, ignoring the spatial nature of the variability of the soil properties. The advantages of carrying out an RFEM analysis, which fully accounts for the spatial variability of soil properties, are then demonstrated. Firstly, various simplified approaches for calculating reliability-based characteristic values are reviewed, and these are then used to derive characteristic values for the dyke cross-section. The factors of safety computed using deterministic analyses based on these characteristic values are compared with the target reliability-based factor of safety computed using RFEM. This chapter does not consider the soil spatial variability in the third dimension and thereby ignores any influence of it on the dyke response.

Chapter 4 extends the general problem to 3D by investigating the influence of uncertainties in dyke geometry, inter-layer boundary between the dyke and foundation layers, and anisotropic heterogeneity in the shear strength properties within layers on the reliability of slopes that are long in the third dimension. The chapter describes the strategy adopted for modelling these forms of uncertainties, which were then combined with finite elements within the Monte Carlo framework. The relative influence of these forms of uncertainties were investigated by comparing the responses obtained for an idealised 3D embankment slope. Moreover, the influence of different levels of anisotropy in the soil spatial variability on the horizontal plane, on the embankment reliability and failure consequences, has also been investigated.

Having established the significant influence of horizontal spatial variability of shear strength properties in the third dimension on the reliability, and considering the large computational requirements for RFEM, Chapter 5 benchmarks a simpler (and more efficient) semi-analytical model of Vanmarcke. This chapter compares the performance of RFEM with the semi-analytical method for the reliability assessment of an idealised 3D slope. Specifically, the mean and standard deviation of the 3D safety factor, as well as the expected failure lengths obtained for a range of horizontal scales of fluctuation of the soil shear strength parameters, have been compared. The range of horizontal scales of fluctuation over which the two methods give similar results, as well as the range over which they differ significantly, are identified. After establishing the reasons behind the differences, the chapter proposes an improved semi-analytical method which gives computationally inexpensive and satisfactory results over the entire possible range of scales of fluctuation of the shear strength parameters. The methodology adopted for calibrating the correction factors in the improved semi-analytical method has been described and the limitations of the improved method have also been discussed.

Chapter 6 concludes this thesis by highlighting the major findings and contributions of this research and gives recommendation for further research.

In order to carry out this PhD research, the author has inherited stand–alone codes developed in Fortran for 1D and 2D random field generation using the Local Average Subdivision (LAS) method by Samy (2003), followed by an extension to 3D LAS by Spencer (2007), parallelisation by Nuttall (2011) and high-performance implementation by Li (2017) using Grid computing technologies. The factors of safety within the probabilistic framework are calculated by finite elements using the strength reduction method (Smith & Griffiths, 2005).

REFERENCES

CEN (2004). Eurocode 7: Geotechnical design. Part 1: General rules, EN 1997-1. *European Committee for Standardisation*.

de Gast, T. (2020). *Dykes and Embankments: a Geostatistical Analysis on Soft Terrain*. Ph.D. thesis, Delft University of Technology, The Netherlands.

Jamalinia, E., Vardon, P. J. & Steele-Dunne, S. C. (2019). The effect of soil–vegetation–atmosphere interaction on slope stability: a numerical study. *Environmental Geotechnics* doi:10.1680/jenge.18.00201, online, ahead of print.

Li, Y. (2017). *Reliability of long heterogeneous slopes in 3D*. Ph.D. thesis, Delft University of Technology, The Netherlands.

Muraro, S. (2019). *The deviatoric behaviour of peat: A route between past empiricism and future perspectives*. Ph.D. thesis, Delft University of Technology, The Netherlands.

Nuttall, J. D. (2011). *Parallel implementation and application of the random finite element method*. Ph.D. thesis, University of Manchester, UK.

Samy, K. (2003). *Stochastic analysis with finite elements in geotechnical engineering*. Ph.D. thesis, University of Manchester, UK.

Smith, I. M. & Griffiths, D. V. (2005). *Programming the finite element method*. 4 edn., John Wiley & Sons.

Spencer, W. A. (2007). *Parallel stochastic and finite element modelling of clay slope stability in 3D*. Ph.D. thesis, University of Manchester, UK.

van den Eijnden, A. P. & Hicks, M. A. (2017). Efficient subset simulation for evaluating the modes of improbable slope failure. *Computers and Geotechnics* **88**, 267–280.

Vanmarcke, E. H. (1977). Reliability of earth slopes. *Journal of the Geotechnical Engineering Division* **103**, No. 11, 1247–1265.

2

LITERATURE REVIEW

Section 2.4.1 is based on Varkey *et al.* (2018).

2.1. INTRODUCTION

Uncertainty is inevitable in geotechnical engineering due to the inherently heterogeneous nature of soils. There may also be uncertainties associated with in-situ measurements, model parameter estimates, modelling techniques and with the idealised geometry of the model itself. There are several sources of uncertainty in the estimation of model parameters, such as: measurement errors caused by the equipment and/or procedure followed; statistical uncertainty associated with the number of measurements (Student, 1908) and the observed variances between them; transformation errors introduced when field or laboratory measurements are transformed into model parameters (Ching & Phoon, 2015; Wang *et al.*, 2017; van der Krogt *et al.*, 2019); and the inherent spatial variability of soil that arises due to a combination of various geological, environmental and physico-chemical processes (Phoon & Kulhawy, 1999a,b). A comprehensive study of the coefficient of variation (COV = standard deviation/mean) of shear strength property values (cohesion c' and friction angle ϕ') is available in Arnold (2016) and is summarised in Table 2.1.

Of the various sources of uncertainty mentioned above, the spatial nature of soil variability is an aleatoric property while the others are epistemic in nature. The soil spatial variability may be quantified using a parameter called the scale of fluctuation (θ), which approximately defines the distance over which property values are significantly correlated. Some guidance regarding the possible range of values of θ are available in Jaksa *et al.* (1999), Hicks & Onisiphorou (2005), Nie *et al.* (2015), Li (2017), Ching *et al.* (2018), de Gast (2020) and de Gast *et al.* (2020b).

This chapter, through the following 3 sections, provides an overview of the background literature relevant to this thesis. In particular, it considers various topics that are needed in order to propagate the effects of uncertainty at the material property level to the system (i.e. structure) level. Section 2.2 describes various available approaches for the discretisation of random fields, which are used for the modelling of spatial variability. Section 2.3 describes the various reliability-based design methods for dealing with uncertainties in geotechnical engineering. Section 2.4 gives a literature review of the random finite element method for the stability analysis of 2D and 3D slopes. Additional topic-specific literature reviews are included within Chapters 3 to 5.

2.2. RANDOM FIELD DISCRETISATION METHODS

Spatial variability can be mathematically represented using random fields (Vanmarcke, 1983), which are defined as the joint probability distribution defining the simultaneous variation of a random process (X) within a domain. Gaussian random fields have been used in this research, as has often been adopted in the literature because of their wide applicability due to the Central Limit Theorem. Gaussian random fields are completely characterised by the mean and autocovariance function. If the expectation $\mathrm{E}[X(t_i)] = \mu(t_i)$ and $\mathrm{Var}[X(t_i)] = \sigma^2(t_i)$ are the mean (μ) and variance (σ^2) of the random field at location $t = t_i$, then the covariance $C(X(t_i), X(t_j))$ between field values $X(t_i)$ and $X(t_j)$ at $t = t_i$ and $t = t_j$, respectively, is defined as:

$$\mathrm{C}(X(t_i), X(t_j)) = \mathrm{E}[(X(t_i) - \mu(t_i)) \cdot (X(t_j) - \mu(t_j))] \tag{2.1}$$

and the correlation function between $X(t_i)$ and $X(t_j)$ is defined as:

Table 2.1: Range of coefficient of variation of effective shear strength parameters available in the literature (based on Arnold (2016))

Property	COV	Soil type	Reference
c'	0.259–0.316	clayey silt	Lumb (1966)
	0.263	clayey coarse sand	Lumb (1970)
	0.435	clayey silt	Lumb (1970)
	0.684	silty coarse sand	Lumb (1970)
	0.1–0.7	-	Cherubini (1997, 2000)
	0.02–0.07	-	Rackwitz (2000)
	0.10–0.15	-	Baker & Calle (2006)
$\tan\phi'$	0.138	silty sand	Lumb (1966)
	0.148	clayey silt	Lumb (1966)
	0.058	silt coarse sand	Lumb (1970)
	0.064	clayey coarse sand	Lumb (1970)
	0.086	clayey silt	Lumb (1970)
	0.073	sand	Schultze (1971)
	0.05–0.14	sand	Phoon *et al.* (1995)
	0.06–0.46	clay and silt	Phoon *et al.* (1995)
	0.1–0.2	-	Baker & Calle (2006)
ϕ'	0.053	sand	Schultze (1971)
	0.10–0.15	-	Becker (1996)
	0.037–0.093	sand	Wolff *et al.* (1996)
	0.02–0.05	sand	Lacasse & Nadim (1996)
	0.05–0.11	sand	Phoon *et al.* (1995)
	0.04–0.50	clay and silt	Phoon *et al.* (1995)
	0.05–0.15	sand and clay	Phoon & Kulhawy (1999a)
	0.10–0.50	clay	Cherubini (2000)
	0.05–0.15	sand	Cherubini (2000)
	0.05–0.25	silt	Cherubini (2000)

$$\rho(X(t_i), X(t_j)) = \frac{\mathrm{E}[(X(t_i) - \mu(t_i)) \cdot (X(t_j) - \mu(t_j))]}{\sigma(t_i)\sigma(t_j)} = \frac{\mathrm{C}[X(t_i), X(t_j)]}{\sigma(t_i)\sigma(t_j)} \tag{2.2}$$

The field is said to be a wide-sense stationary random field if $\mathrm{E}[X(t_i)] = \mu$ and $\mathrm{Var}[X(t_i)] = \sigma^2$ for all t, such that the covariance is independent of the absolute location and depends only on the vector separation of t_i and t_j. Also, if the covariance depends only on the absolute distance between t_i and t_j, and not on direction, the field is said to be an isotropic random field.

The various methods of discretising a continuous random field, in order to integrate it with the spatial discretisation of the problem, can broadly be divided into the various groups briefly discussed below.

2.2.1. POINT DISCRETISATION METHODS

The midpoint method (Der Kiureghian & Ke, 1988) approximates a random field at the centroid of the zone of interest, e.g. an element in an FE mesh. In this method, the random variables are the selected values of the field at certain points in the finite element

mesh, resulting in realisations that are piecewise constant with discontinuities at the element boundaries. The shape function method (Liu *et al.*, 1986a,b) approximates the random field in each element using the nodal field values and shape functions associated with the finite element. These methods have been shown to over-represent the variability (Li & Der Kiureghian, 1993). The optimal linear estimation method (Li & Der Kiureghian, 1993) approximates the random field by a linear function of nodal values, in which the coefficients of the function are determined by minimising the error in the variance at each point.

2.2.2. SERIES EXPANSION METHODS

The Karhunen-Loeve (K-L) expansion method (Huang *et al.*, 2001) is based on the spectral decomposition of the auto-covariance function in terms of its eigenvalues and eigenvectors. The approximation of the field over a domain is carried out by truncating the series after a finite number of terms, which strongly depends on the correlation length with respect to the domain size and on the desired level of accuracy. This discretisation method gives an efficient representation of random fields and has several useful properties, as explained in detail by Sudret & Der Kiureghian (2000). The orthogonal series expansion method and the expansion optimal linear estimation method are the other two methods which fall into this group, where the latter is an extension of the optimal linear estimation method.

2.2.3. SPATIAL AVERAGE METHODS

In these methods, the domain is subdivided into cells, with each cell containing, for example, an FEM integration point. The spatial average methods (Vanmarcke, 1983) approximate the random field in each cell as the average of the random field values over the cell area (or volume). For example, for the following exponential correlation function,

$$\rho(\tau_i) = \exp\left(-\frac{2|\tau_i|}{\theta_i}\right) \tag{2.3}$$

where τ_i is the width of the averaging domain and θ_i is the scale of fluctuation in the direction i. The variance reduction factor (Γ^2) due to averaging over τ_i is given by:

$$\Gamma^2(\tau_i) = \frac{\theta_i^2}{2\tau_i^2}\left(\frac{2|\tau_i|}{\theta_i} + \exp\left(-\frac{2|\tau_i|}{\theta_i}\right) - 1\right) \tag{2.4}$$

LOCAL AVERAGE SUBDIVISION METHOD

The Local Average Subdivision (LAS) method (Fenton & Vanmarcke, 1990) is a top-down recursive approach. It begins with selecting a random number (the global mean for that realisation) from the standard normal distribution and assigning it to a domain, such that the variance obtained from local average theory is equal to the variance of the underlying standard normal field multiplied by Γ^2. Following this assignment, the cells are subdivided while preserving the global mean value. The subdivision process continues until the variance of the approximated field achieves the target value.

The cell values (Z) at an arbitrary subdivision stage $i+1$ can therefore be derived based on the known cell values at the previous stage i (see Figure 2.1) by using the following

	j - 1		j		j + 1		stage i
	$2j$ - 3	$2j$ - 2	$2j$ - 1	$2j$	$2j$ + 1	$2j$ + 2	stage i + 1

Figure 2.1: Indexing in 1D LAS (based on Fenton & Vanmarcke (1990))

equation:

$$Z_{2j}^{i+1} = \left\{ a_{-1}^{i} Z_{j-1}^{i} + a_{0}^{i} Z_{j}^{i} + a_{1}^{i} Z_{j+1}^{i} \right\} + c^{i+1} U_{j}^{i+1} \tag{2.5}$$

where a_{-1}^{i}, a_{0}^{i} and a_{1}^{i} are the weighting coefficients for the cell values at stage i, and c^{i+1} is the standard deviation of the white noise term U.

To calculate the unknown coefficients, multiplying the above equation by an arbitrary cell value (Z_{m}^{i}) at stage i and taking expectations, followed by simplification (i.e. $\mathrm{E}[U] = 0$), gives

$$\mathrm{E}\left[Z_{2j}^{i+1} Z_{m}^{i}\right] = \sum_{k=j-1}^{j+1} a_{k-j}^{i} \mathrm{E}\left[Z_{k}^{i} Z_{m}^{i}\right] \tag{2.6}$$

where the cross-stage covariance term can be evaluated using

$$\mathrm{E}\left[Z_{2j}^{i+1} Z_{m}^{i}\right] = \frac{1}{2}\left(\mathrm{E}\left[Z_{2j}^{i+1} Z_{2m-1}^{i+1}\right] + \mathrm{E}\left[Z_{2j}^{i+1} Z_{2m}^{i+1}\right]\right) \tag{2.7}$$

and the covariance terms can be calculated using

$$\mathrm{E}\left[Z_{k}^{i} Z_{m}^{i}\right] = \frac{\sigma^2}{2}\left[(p-1)^2\Gamma^2\left((p-1)D^{i}\right) - 2p^2\Gamma^2\left(pD^{i}\right) + (p+1)^2\Gamma^2\left((p+1)D^{i}\right)\right] \tag{2.8}$$

In the above equation, $\mathrm{E}\left[Z_{k}^{i} Z_{m}^{i}\right]$ is the covariance of the cells k and m separated by p cells at stage i, and D^{i} is the cell size at stage i. Squaring and taking expectations for Equation (2.5) leads to

$$\left(c^{i+1}\right)^2 = \mathrm{E}\left[\left(Z_{2j}^{i+1}\right)^2\right] - \sum_{k=j-1}^{k=j+1} a_{k-j}^{i} \mathrm{E}\left[Z_{2j}^{i+1} Z_{k}^{i}\right] \tag{2.9}$$

Since the weighting coefficients and the standard deviation of the white noise term are independent of the actual values of the local averages for a stationary random process, they can be determined a priori and used for all the realisations.

COVARIANCE MATRIX DECOMPOSITION METHOD

The covariance matrix decomposition method makes use of the orthogonality of the decomposed covariance matrix. Here, an FEM integration point is assigned the averaged cell value of the underlying random field, consistent with the spatial average theory (Vanmarcke, 1983). In this method, the vector of a standard normal random field is expressed as

the product of the decomposed covariance matrix and a vector of uncorrelated standard normal random numbers ($\boldsymbol{U}$):

$$\boldsymbol{Z} = \mathbf{A}\boldsymbol{U} \tag{2.10}$$

where $\mathbf{A}$ is a decomposition of the covariance matrix. Since the covariance matrices are usually positive definite, they can be decomposed using Cholesky decomposition or by using the eigen-decomposition method. In the latter case, $\boldsymbol{Z}$ will be given by

$$\boldsymbol{Z} = \mathbf{Q}\boldsymbol{\Lambda}^{1/2}\boldsymbol{U} \tag{2.11}$$

where $\mathbf{Q}$ is the matrix of orthogonal eigenvectors and $\boldsymbol{\Lambda}$ is the diagonal matrix of the eigenvalues. As in LAS, the decomposition of the covariance matrix can be carried out prior to generation of the random field realisations. An advantage of the covariance matrix decomposition method over LAS is that the former has fewer restrictions on the mesh discretisation. However, the method becomes computationally expensive with an increase in the number of discretisation cells.

2.3. RELIABILITY-BASED DESIGN METHODS AND APPLICATIONS TO SLOPES

There are various ways of dealing with uncertainties in geotechnical engineering, including: semi-probabilistic approaches, which account for uncertainties within a deterministic design by applying partial factors to characteristic values of strength parameters to achieve a target reliability level; approximate probabilistic methods, which estimate the probability of failure (P_f) of a problem by approximating the performance function around design points which maximise the failure probability; response surface methods, which use an explicit, approximate functional relationship between the random numbers corresponding to the uncertainty in the soil parameters along a slip surface and the structure response; and fully probabilistic methods, which compute the P_f numerically by random sampling of discrete sets of variables from their joint distributions. These methods are briefly described in the following subsections.

2.3.1. DETERMINISTIC METHOD

Although reliability-based design methods are yet to find their way into everyday geotechnical applications, they are (indirectly) incorporated in the safety assessments of geotechnical structures. For instance, a characteristic value and partial factor based approach is widely adopted for dyke safety assessments in the Netherlands. In this semi-probabilistic method, following the guidelines of Eurocode 7 (CEN, 2004), the characteristic value (X_k) of a soil property X is chosen as a cautious estimate of the mean value (X_m) of a limited set of parameters:

$$X_\mathrm{k} = X_\mathrm{m}(1 - k_X \times \mathrm{COV}) \tag{2.12}$$

where k_X is a standard score representing the level of cautious estimate of X. The design value X_d is then given by

$$X_{\mathrm{d}} = X_{\mathrm{k}}/\gamma_{\mathrm{M}} \tag{2.13}$$

where γ_{M} is the partial factor for the material property and recommended values are usually given in the national standards.

If the influence of spatial variability on the structure response is ignored, X_k corresponds to the 5 percentile of the soil property distribution in order to achieve the target structural reliability level requirement of Eurocode 7, i.e. $k_X = 1.645$ for a normally distributed X. Additionally, there are several simplified approaches to calculate a value of k_X that accounts for variance reduction due to spatial averaging of soil properties (Orr, 2017; Schneider, 1997; Schneider & Schneider, 2012). However, the effectiveness of such equations in predicting the target reliability of the structure has not been fully investigated, for example by comparing with a full random finite element analysis which directly calculates the reliability-based F, by-passing the need to calculate X_{k}.

2.3.2. APPROXIMATE METHODS

The First Oder Second Moment method (FOSM) (Baecher & Christian, 2003) uses the Taylor series expansion to approximate the performance function ($g = F - 1$) using the mean and variance of the associated variables. The Point Estimate Method (PEM) (Rosenblueth, 1981) uses 2^N sampling points to discretise a performance function involving N variables. Both these methods (FOSM and PEM) are independent of the type of distribution of the variables and hence are invariant to transformation, which can be problematic for cross-correlated variables.

If a vector of variables $\boldsymbol{X}$ is described by a joint probability density function (pdf) $f_X(x)$, the probability of failure is given by:

$$P_f = \int_{\{x:g(x)<0\}} f_X(x)\,dx \tag{2.14}$$

where $g(x)$ is the limit state function. Thus, $x : g(x) > 0$ and $x : g(x) < 0$ correspond to the safe and failure domains, respectively, while $x : g(x) = 0$ corresponds to points along the limit state surface.

The First Order Reliability method (FORM) (Hasofer & Lind, 1974) solves Equation (2.14) numerically by linearly approximating the limit state surface locally at a point. The procedure involves transforming the variables from their physical space (x) to standard normal space (u) and linearisation of the limit state surface at the most probable failure point (U^* in standard normal space), also called the design point. An illustration of FORM is shown in Figure 2.2. In Figure 2.2b, $G(u)$ is the limit state function evaluated in standard normal space. The distance from the origin to the design point is known as the reliability index (β_R), and is related to P_f by

$$\beta_R \approx -\Phi^{-1}(P_f) \tag{2.15}$$

where Φ is the standard normal cumulative distribution function. For a linear limit state function in standard normal space, the above approximation becomes exact. The Second Order Reliability Method (SORM) (Der Kiureghian & de Stefano, 1991) has also been

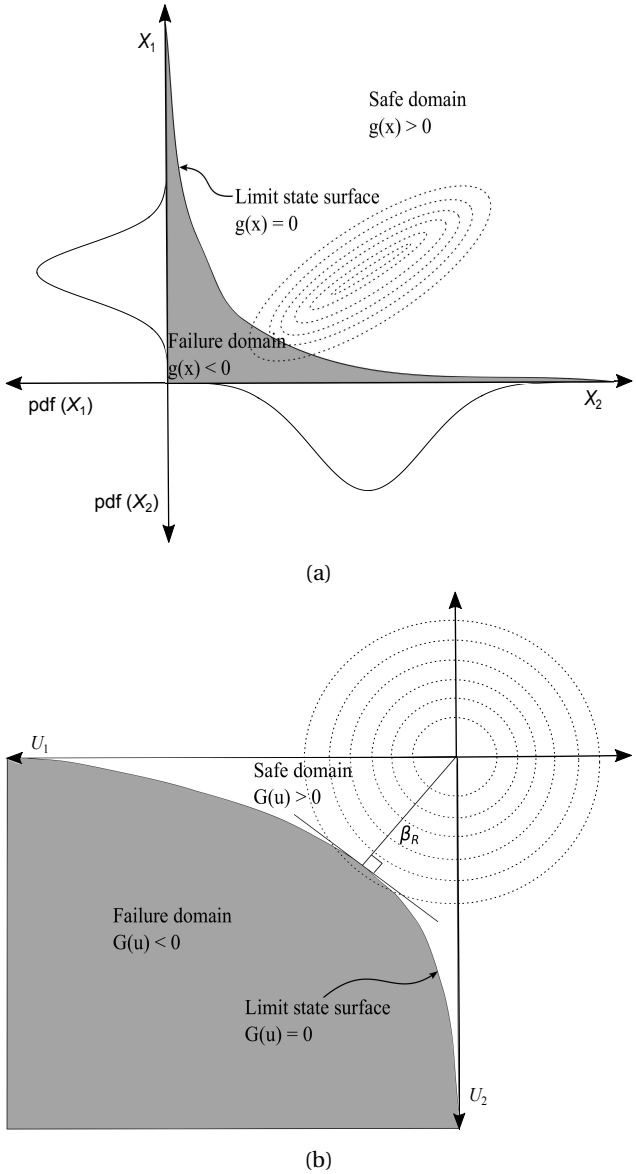

Figure 2.2: Graphical representation of FORM involving 2 variables. Variables defined in (a) physical space and (b) standard normal space

proposed to improve the precision, which extends FORM by approximating the limit state surface using a higher order function.

The partial factor method, FORM and SORM are increasingly receiving a wider acceptance in geotechnical applications due to their ease of use. Low & Tang (1997) introduced

an Excel spreadsheet platform that performed efficient FORM procedures and could easily be applied to various geotechnical problems. The combination of reliability index and the design point, as an outcome of a FORM analysis, gives useful information to design engineers for the reliability-based assessment of slopes. However, a limitation of this method is that spatial variability of parameters was not incorporated, which was later shown to cause misleading predictions regarding the failure probability or reliability of a structure. Later attempts to include spatial variation were done through using reduced variances of the parameters, to account for the spatial averaging of property values along potential failure surfaces. Also, since traditional FORM was defined in standard normal space, it was not straightforward to implement the method for correlated non-Gaussian type variables.

Low & Tang (2004, 2007) re-explained FORM in the physical space of the variables, based on the perspective of an expansion ellipsoid, and proposed another spreadsheet algorithm to solve problems using FORM in x-space. Recently, Ji & Kodikara (2015) proposed an invariant of FORM, in the x-space of the variables, by modifying the original Hasofer-Lind Rackwitz Fiessler (HLRF) algorithm. Ji *et al.* (2018) explicitly modelled the spatial variability of shear strength properties using the point discretisation method and combined it with the invariant of FORM in x-space to investigate the influence of soil spatial variability on the assessments of slopes in 2D. Further improvements to FORM were proposed by Ji *et al.* (2019), by introducing a simplified iterative HLRF algorithm. However, if the number of variables is too large, a disadvantage with FORM is that a 'fake' local minimum could be mistaken for the global minimum while determining the design point (Wang *et al.*, 2011).

2.3.3. RESPONSE SURFACE METHOD

The Response Surface Method (RSM) approximates the performance function using a computationally efficient model, following which a reliability analysis is carried out. The classical RSM approximates the performance function by identifying the most critical slip surface. Recently, system slope reliability analysis has been gaining increasing attention (Chowdhury & Xu, 1955; Huang *et al.*, 2010; Li *et al.*, 2011; Zhang *et al.*, 2011), in which the system (or overall) failure probability of a slope is defined in terms of a system of numerous potential slip surfaces and is shown to be greater than the failure probability along any individual (critical) potential slip surface. Li & Chu (2016) and Zhang & Huang (2016) proposed that the correlation between values of F from different potential slip surfaces should be considered, to identify the most representative ones resulting in the maximum failure probability and risk. Recently, Li *et al.* (2019) proposed a method to efficiently incorporate multiple slip surfaces into the risk assessments of slopes.

RSM has been widely used to carry out efficient reliability analyses of slopes. Xu & Low (2006) used RSM to approximate the performance function and used the response surface to combine numerical packages with spreadsheet-based reliability analysis. Cho (2009) proposed a numerical procedure for integrating a probabilistic slope stability analysis with a commercial finite difference method. The author proposed an artificial neural network-based RSM to approximate the limit state function and calculated the probability of failure using the first and second order reliability methods. Zhao (2008) and Li *et al.* (2013) proposed a support vector machine-based RSM to approximate the performance

function. Luo *et al.* (2012) and Zhang *et al.* (2013a) proposed a Kriging-based response surface to approximate the performance function and demonstrated its applicability to geotechnical problems. To overcome convergence difficulties in classical RSM, Zhang *et al.* (2015) proposed an efficient and robust RSM for geotechnical reliability analysis and combined it with a commercial geotechnical program for automated reliability analysis.

Jiang *et al.* (2015) and Li *et al.* (2015a) proposed multiple RSMs for evaluating slope reliability considering soil spatial variability. Liu *et al.* (2018) proposed a simplified framework for the efficient reliability analysis of slopes in spatially variable soils, based on multiple RSMs and Monte Carlo simulation. However, the RSM can be inefficient with an increase in the number of variables defining the surface, especially with random fields associated with the spatially variable properties. A detailed review and comparison of response surface methods for slope reliability analysis are given in Li *et al.* (2016c).

2.3.4. SIMULATION-BASED METHODS

The principle of the Monte Carlo method, which is a fully probabilistic method, is to simulate a large number of samples from the distributions of random variables, compute independently the response for each sample and carry out a statistical analysis of the responses. In this method, the probability of failure is calculated numerically by simulating a sequence of N independent variables from the joint probability density function $f_X(x)$ of the variables in $\boldsymbol{X}$:

$$P_f \approx \frac{1}{N}\sum_{i=1}^{N} I_i \tag{2.16}$$

where I is the indicator function: $I_i = 1$ if $g(x_i) \leq 0$ and $I_i = 0$ if $g(x_i) > 0$. The accuracy of a Monte Carlo simulation is measured using the COV of P_f, given by

$$\mathrm{COV}(P_f) \approx \sqrt{\frac{1-P_f}{P_f(N-1)}} \tag{2.17}$$

As can be seen from Equation (2.17), the $\mathrm{COV}(P_f)$ decreases with an increase in the number of samples N.

EFFICIENT PROBABILISTIC METHODS

A disadvantage of the fully probabilistic method is that a large number of samples are required to achieve a high confidence level in the estimation of a low P_f. For example, based on Equation (2.17), 10^5 samples would be required to achieve a target $\mathrm{COV}(P_f) \leq 0.1$ for $P_f = 0.001$. However, a number of efficient sampling methods are available, for example, importance sampling, directional simulation, Latin Hypercube sampling and subset simulation. Subset simulation (Au & Beck, 2001) stems from the idea that a rare event can be expressed as a Bayesian sequence of intermediate events, thereby making a small probability event a more frequent one. This method uses Markov Chain Monte Carlo simulation to generate conditional samples of the intermediate failure events until the target failure probability is reached. This method has been applied to geotechnical systems by Santoso *et al.* (2011), Wang *et al.* (2011), Li *et al.* (2016b) and Huang *et al.* (2017) for modelling the spatial variability of undrained shear strength in soils and for

quantifying its effects on the stability of slopes at low probability levels. It was observed that the number of realisations required to reach this high level of reliability was much smaller compared to using a direct Monte Carlo simulation.

The efficiency of subset simulation was improved by introducing a new response conditioning method (Au, 2007). This method makes use of a conditioning response, also termed preliminary response, which is a simplified assumption to approximate the more complex target response. Li *et al.* (2016a) and Xiao *et al.* (2016) used Auxiliary-RFEM, which was based on the principles of efficient subset simulation proposed by Au (2007), to model the spatial variability of undrained shear strength in 2D and 3D slope reliability, respectively. The authors made use of responses from the limit equilibrium method and coarse mesh FE analysis to generate conditioning responses. The critical slip surface for determining the conditioning response in the limit equilibrium analysis was based on the mean property values, and hence the final results may have been biased towards this presumed slip surface.

The subset simulation method was further improved by modifying the basic Markov Chain Monte Carlo algorithm for a faster acceptance rate of the generated candidate states (Papaioannou *et al.*, 2015). van den Eijnden & Hicks (2017) proposed a modified version of subset simulation, which based the selection criteria on performance rather than on the usual probability-based selection, and illustrated the efficiency of the proposed algorithm by applying it to an idealised slope.

2.4. RANDOM FINITE ELEMENT METHOD

The Random Finite Element Method (RFEM) combines random fields with FEM within a Monte Carlo framework. RFEM has proven to be an effective method, as it does not make any assumptions regarding the shape or location of the failure surface and nor does it make any assumption regarding the sampling strategy. RFEM has been adopted for reliability-based analyses of a wide range of geotechnical problems including slopes. Hicks & Samy (2002a,b) used RFEM for reliability assessments of an idealised slope in 2D and highlighted the importance of considering the spatial nature of soil variability. The authors modelled the anisotropy in spatial variability by squashing and/or stretching an isotropic random field until the required level of anisotropy was achieved. It was observed that, for a given vertical scale of fluctuation, assuming isotropic spatial variability severely underestimated the probability of failure. Hicks & Samy (2002a, 2004) compared the responses obtained from a strongly stationary random field with that from a weakly stationary random field that had a depth trend in the mean undrained shear strength, and observed that the reliability of the slope was lower in the latter case. Griffiths *et al.* (2009a), Griffiths *et al.* (2011), Huang *et al.* (2010) and Le (2014) compared FORM and RFEM results for a 2D $c-\phi$ soil slope, for different cross–correlation coefficients and at different slope inclinations. The results highlighted the importance of including cross–correlations between shear strength parameters, as it was observed that a positive correlation coefficient had a destabilising effect on slopes. Arnold & Hicks (2011) looked at the influence of spatial variability in the mechanical and hydraulic properties of soils, both correlated and uncorrelated, on 2D slope reliability. Javankhoshdel & Bathurst (2014) and Javankhoshdel *et al.* (2016) modified existing stability charts for cohesive and cross–correlated c–ϕ soils using closed form solutions and Monte Carlo simulations. Javankhoshdel &

Bathurst (2016) compared the results obtained using 2D RFEM and the 2D random limit equilibrium method, and highlighted various cases of slope inclination and degree of anisotropy of the soil spatial variability where the solutions using the two methods were similar, as well as those cases where they were significantly different. Recently, de Gast *et al.* (2020a) used RFEM for reliability assessment of a controlled dyke failure in the Netherlands.

Spencer (2007), Hicks *et al.* (2008), Griffiths *et al.* (2009b) and Hicks & Spencer (2010) investigated the influence of 3D spatial variability of undrained shear strength parameters on the reliability of an idealised slope. They found that assuming perfect spatial correlation in the out-of-plane direction (i.e. along the slope length), as in a 2D stochastic analysis, may underestimate the probability of failure. Hicks & Spencer (2010) and Hicks *et al.* (2014) modelled anisotropy in the spatial variability by assuming one scale of fluctuation in the horizontal plane and a much smaller scale of fluctuation in the vertical direction, to reflect the long-term depositional characteristics of soils. They observed that anisotropy in the spatial variability significantly influenced the location, number and shape of the failure mechanisms, and thereby the reliability of the slopes and associated risks. Hicks *et al.* (2014) quantified the risk by developing a threshold-crossing technique to estimate the length and volume of a sliding mass, based on a threshold value obtained as a percentage of the maximum out–of–face displacement of the sliding mass. They also observed that very low and very high levels of anisotropy resulted in solutions that were equivalent to solutions obtained with 2D deterministic and 2D stochastic slope stability analyses, respectively. Hence, they proposed three categories of failure mode corresponding to different levels of anisotropy in the spatial variability of the undrained shear strength with respect to the height and length of the slope. Huang *et al.* (2013) quantified the failure consequence in terms of sliding volume by using the K–means clustering method, in which the whole soil domain was classified into stable and sliding masses based on the nodal displacement vector and using an iterative scheme to classify the domain.

2.4.1. CROSS-CORRELATED RANDOM FIELDS

Random fields of different material properties may be cross-correlated to account for parameter interdependency. For random variables Z_i and Z_j, the linear product-moment cross-correlation coefficient ($\rho_{Z_i Z_j}$) between the variables at the same point in space is given by

$$\rho_{Z_i Z_j} = \frac{\mathrm{E}[Z_i, Z_j] - \mathrm{E}[Z_i]\mathrm{E}[Z_j]}{\sigma_{Z_i}\sigma_{Z_j}} \tag{2.18}$$

where $\rho_{Z_i Z_j}$ varies between -1.0 and 1.0, implying perfectly negative and perfectly positive linear correlations, respectively. If $\boldsymbol{Z}$ and $\boldsymbol{\xi}$ are the vectors of n uncorrelated and correlated Gaussian random variables, respectively, then $\boldsymbol{\xi}$ can be derived from $\boldsymbol{Z}$ using

$$\boldsymbol{\xi} = \mathbf{L}\boldsymbol{Z} \tag{2.19}$$

where $\mathbf{L}$ is the lower triangular matrix obtained by the Cholesky decomposition of the correlation matrix $\mathbf{R}$, given by

$$\mathbf{R} = \begin{bmatrix} 1 & \rho_{Z_1 Z_2} & .. & \rho_{Z_1 Z_n} \\ \rho_{Z_2 Z_1} & 1 & .. & \rho_{Z_2 Z_n} \\ .. & .. & .. & .. \\ \rho_{Z_n Z_1} & \rho_{Z_n Z_2} & .. & 1 \end{bmatrix} \tag{2.20}$$

The results obtained by RFEM strength reduction analyses of an idealised 45°, 5 m high and 50 m long slope are briefly discussed here (Varkey *et al.*, 2018). A vertical scale of fluctuation (θ_v) of 1 m was used for both the parameters (i.e. c' and ϕ'). Figure 2.3 shows the F obtained in each realisation of RFEM analyses using (a) perfectly positive and (b) perfectly negative cross-correlated c'–ϕ' fields, against F obtained from uncorrelated c'–ϕ' fields for a horizontal scale of fluctuation (θ_h) of 12 m for both the parameters. Extreme values of $\rho_{c'\phi'}$ compared to values reported in literature have been chosen, in order to highlight the differences between the solutions. For positively cross-correlated fields of the shear strength parameters, the weak zones (and the strong zones) of the shear strength are exaggerated compared to the uncorrelated fields. Hence, the positive cross-correlation decreases (or increases) the safety factor for each realisation and increases the range of possible solutions. In contrast, a negative cross-correlation between the shear strength parameters reduces the range of possible solutions.

Figure 2.4 compares the distributions of F for different values of θ_h, for different $\rho_{c'\phi'}$. In Figure 2.4b, for the case of $\theta_h = 12$ m, i.e., for a value of θ_h lying between the slope height and half of the slope length, there is the possibility of discrete weak zones generated within each realisation. This results in the mean F being lower than the deterministic solution ($F = 1.4$), which is also the case for other values of θ_h lying in this range (not shown in the figures). For positive values of $\rho_{c'\phi'}$, the failure can propagate through even weaker zones and the mean F reduces further below the deterministic solution. In contrast, for negatively cross-correlated fields of c' and ϕ', the average mobilised shear strength over all the realisations increases. This results in the mean F tending towards the deterministic F for $\rho_{c'\phi'} = -1$. Also, the range of possible solutions decreases considerably compared to the uncorrelated and positively cross-correlated fields, and the variance of F reduces accordingly.

For the case of a very large θ_h relative to the slope length (Figure 2.4c), there is a wide range of possible solutions for uncorrelated fields and an even wider range for positively correlated fields. This wide range is due to the relative locations of very extensive weak zones through which the failure propagates. For very small scales of fluctuation relative to the slope height, as in Figure 2.4a, considerable spatial averaging takes place and there is thus a negligible difference between responses for different values of $\rho_{c'\phi'}$.

2.4.2. CONDITIONAL RANDOM FIELDS

In order to make efficient use of available field data, conditional simulation techniques may be adopted to reduce the uncertainty and increase confidence in a project. In this method, the generated random fields are conditioned (or constrained) at the locations of actual measurements. Lloret-Cabot *et al.* (2012) applied the Kriging interpolation technique to get the best linear estimates of random fields between known locations. Wang *et al.* (2013) utilised field measurements to improve the estimation of soil parameters, using the maximum likelihood method which estimates the most likely set of

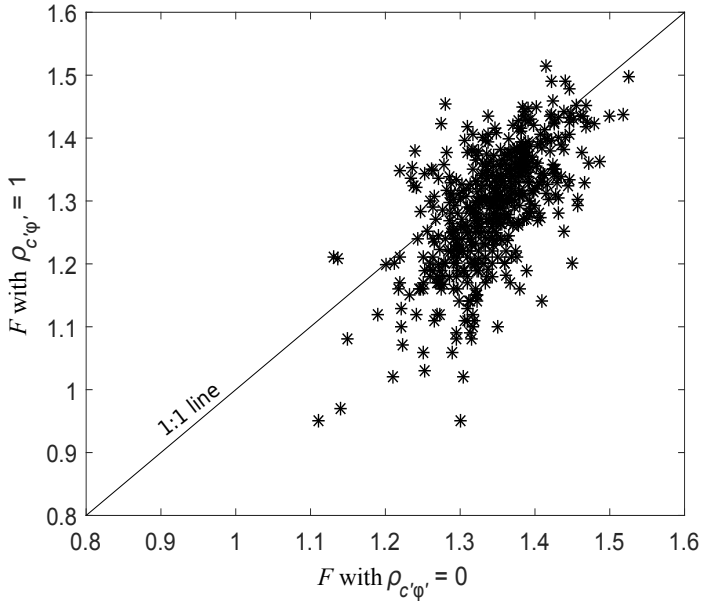

(a)

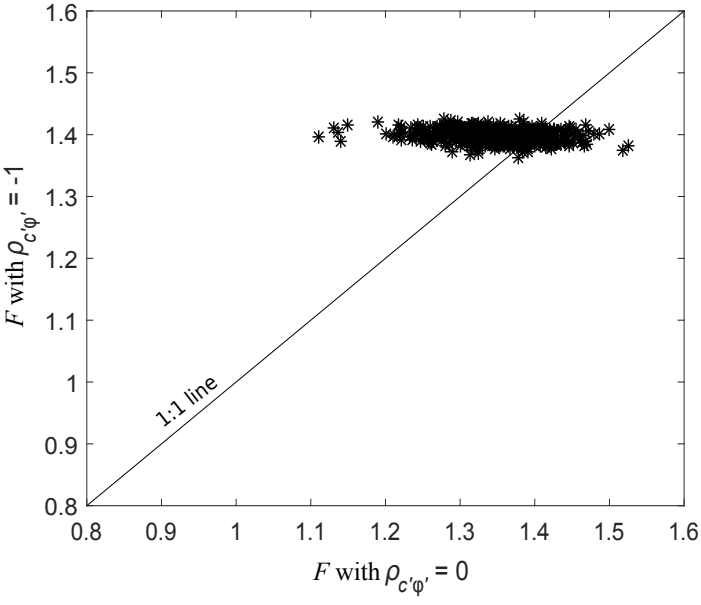

(b)

Figure 2.3: F obtained with (a) $\rho_{c'\phi'} = 1$, and (b) $\rho_{c'\phi'} = -1$ against F obtained with $\rho_{c'\phi'} = 0$, for $\theta_h = 12\,\mathrm{m}$

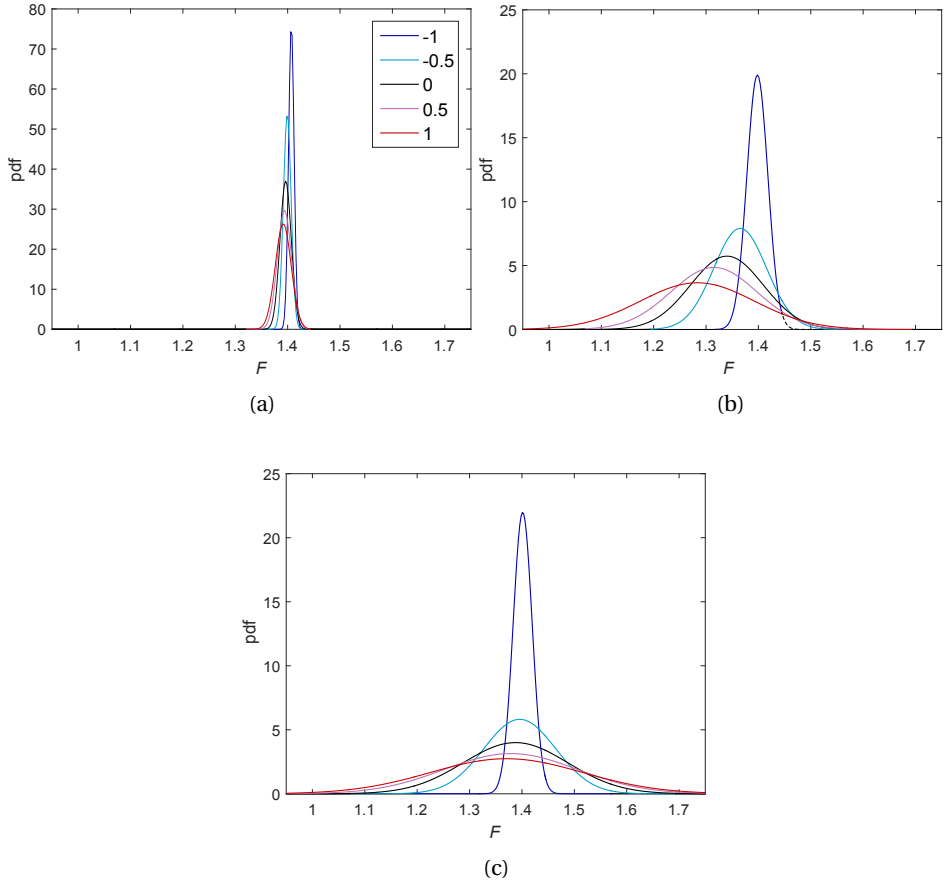

Figure 2.4: Probability density functions of F for different values of $\rho_{c'\phi'}$: (a) $\theta_h = 1\,m$, (b) $\theta_h = 12\,m$, and (c) $\theta_h = 2000\,m$

parameters based on the measurements. Lloret-Cabot *et al.* (2014) used information from conditional random fields for the estimation of scale of fluctuation and highlighted the efficiency of this method in estimating the scale of fluctuation with relatively few data. Li *et al.* (2016d) extended the work of Lloret-Cabot *et al.* (2012) to apply conditional simulation in a three dimensional space. They developed an approach to identify the best locations to carry out field testing for a given number of boreholes, thereby directing field exploration programmes and developing a more efficient way to condition the random fields. They combined conditional 3D random fields with finite element analysis for the stability assessments of slopes, and compared responses obtained with conditional and unconditional random fields for slopes with different slope angles.

Zhang *et al.* (2013b) back–calculated hydraulic parameters by utilising measurements of pore water pressure and investigated the effect of uncertainties in the hydraulic parameters on the prediction of slope stability. Vardon *et al.* (2016) took the analogy one step further by considering the spatial variability of hydraulic parameters. They utilised

an inverse analysis method to better estimate the hydraulic conductivity field and then correlated this field with the soil shear strength parameters to assess the stability of a slope.

2.4.3. RFEM COMPARED TO SEMI-ANALYTICAL METHODS FOR 3D SLOPE RELIABILITY ASSESSMENTS

RFEM, due to its large computational requirements and complexity in implementation, is seldom used in practice. Alternative semi-analytical methods, such as those proposed by Vanmarcke (1977) and Calle (1985), give quick and convenient solutions based on certain simplifying assumptions. Vanmarcke (1977) pioneered 3D slope reliability assessments by extending a 2D slip surface to a 3D failure surface with resisting end-sections within a probabilistic framework. In his method, the variance of the average mobilised shear strength is calculated as the variance of the underlying distribution multiplied by a reduction factor to account for the averaging of property values over the failure surface. Moreover, this method also predicts the critical width of the failure surface which maximises the probability of failure. The original method considered the spatial variability in undrained shear strength, and it was later extended to include the variability in drained shear strength along with several other extensions (Vanmarcke, 1980). The details of the method are discussed in detail in Chapter 5. Li *et al.* (2015b) compared the performance of this method with RFEM for computing the reliability of an idealised 3D slope. They highlighted those instances in which the two methods gave similar solutions and those in which the solutions were significantly different. Hicks & Li (2018) investigated the length-dependency of the responses of a long idealised slope. They compared the solutions obtained using RFEM (which allowed the possibility of multiple discrete failures along the slope length) with those obtained using the first crossing method in Vanmarcke (1977) and the "2.5 D" method of Calle (1985).

REFERENCES

Arnold, P. (2016). *Probabilistic modelling of unsaturated slope stability accounting for heterogeneity*. Ph.D. thesis, University of Manchester, UK.

Arnold, P. & Hicks, M. A. (2011). A stochastic approach to rainfall-induced slope failure. In *Proceedings of 3rd International Symposium on Safety and Risk*, Munich, pp. 107–115.

Au, S.-K. (2007). Augmenting approximate solutions for consistent reliability analysis. *Probabilistic Engineering Mechanics* **22**, 77–87.

Au, S.-K. & Beck, J. L. (2001). Estimation of small failure probabilities in high dimensions by Subset Simulation. *Probabilistic Engineering Mechanics* **16**, 263–277.

Baecher, G. B. & Christian, J. T. (2003). *Reliability and statistics in geotechnical engineering*. John Wiley & Sons.

Baker, J. & Calle, E. (2006). JCSS Probabilistic Model Code, Section 3.7: Soil Properties. *Joint Committee on Structural Safety*, Zurich, Switzerland.

Becker, D. E. (1996). Eighteens Canadian Geotechnical Colloquium: Limit States Design for Foundations. Part II. Development for the National Building Code of Canada. *Canadian Geotechnical Journal* **33**, No. 9, 984–1007.

Calle, E. (1985). Probabilistic analysis of stability of earth slopes. In *Proceedings of 11th International Conference on Soil Mechanics and Foundation Engineering*, California, pp. 809–812.

CEN (2004). Eurocode 7: Geotechnical design. Part 1: General rules, EN 1997-1. *European Committee for Standardisation.*

Cherubini, C. (1997). Data and considerations on the variability of geotechnical properties of soil. In *Proceedings of the International Conference on Safety and Reliability 97*, Lisbon, Portugal, pp. 1583–1591.

Cherubini, C. (2000). Reliability evaluation of shallow foundation bearing capacity on *c'*, ϕ' soils. *Canadian Geotechnical Journal* **37**, No. 1, 264–269.

Ching, J. & Phoon, K.-K. (2015). Reducing the transformation uncertainty for the mobilized undrained shear strength of clays. *Journal of Geotechnical and Geoenvironmental Engineering* **141**, No. 2, 04014103.

Ching, J., Wu, T.-J., Stuedlein, A. W. & Bong, T. (2018). Estimating horizontal scale of fluctuation with limited CPT soundings. *Geoscience Frontiers* **9**, No. 6, 1597–1608.

Cho, S. E. (2009). Probabilistic stability analyses of slopes using the ann-based response surface. *Compuers and Geotechnics* **36**, 787–797.

Chowdhury, R. N. & Xu, D. W. (1955). Geotechnical system reliability of slopes. *Reliability Engineering and System Safety* **47**, 141–151.

de Gast, T. (2020). *Dykes and Embankments: a Geostatistical Analysis on Soft Terrain*. Ph.D. thesis, Delft University of Technology, The Netherlands.

de Gast, T., Hicks, M. A., van den Eijnden, A. P. & Vardon, P. J. (2020a). On the reliability assessment of a controlled dyke failure. *Géotechnique* Symposium in Print: Linear Infrastructure.

de Gast, T., Vardon, P. J. & Hicks, M. A. (2020b). Assessment of soil spatial variability for linear infrastructure using cone penetration tests. *Géotechnique* Under review.

Der Kiureghian, A. & de Stefano, M. (1991). Efficient algorithms for second order reliability analysis. *Journal of Engineering Mechanics* **117**, No. 12, 2906–2923.

Der Kiureghian, A. & Ke, J.-B. (1988). The stochastic finite element method in structural reliability. *Probabilistic Engineering Mechanics* **3**, No. 2, 83–91.

Fenton, G. A. & Vanmarcke, E. H. (1990). Simulation of random fields via local average subdivision. *Journal of Engineering Mechanics* **116**, No. 8, 1733–1749.

Griffiths, D. V., Huang, J. & Fenton, G. A. (2009a). Influence of spatial variability on slope reliability using 2-D random fields. *Journal of Geotechnical and Geoenvironmental Engineering* **135**, No. 10, 1367–1378.

Griffiths, D. V., Huang, J. & Fenton, G. A. (2009b). On the reliability of earth slopes in three dimensions. In *Proceedings of the Royal Society of London A: Mathematical, Physical and Engineering Sciences*, vol. 465, The Royal Society, pp. 3145–3164.

Griffiths, D. V., Huang, J. & Fenton, G. A. (2011). Probabilistic infinite slope analysis. *Computers and Geotechnics* **38**, 577–584.

Hasofer, A. M. & Lind, M. C. (1974). An exact and invariant first order reliability format. *Journal of Engineering Mechanics* **100**, 111–121.

Hicks, M. A., Chen, J. & Spencer, W. A. (2008). Influence of spatial variability on 3D slope failures. In *Proceedings of 6th International Conference on Computer Simulation in Risk Analysis and Hazard Mitigation*, Kefalonia, pp. 335–342.

Hicks, M. A. & Li, Y. (2018). Influence of length effect on embankment slope reliability in 3D. *International Journal for Numerical and Analytical Methods in Geomechanics* **42**, 891–915.

Hicks, M. A., Nuttall, J. D. & Chen, J. (2014). Influence of heterogeneity on 3D slope reliability and failure consequence. *Computers and Geotechnics* **61**, 198–208.

Hicks, M. A. & Onisiphorou, C. (2005). Stochastic evaluation of static liquefaction in a predominantly dilative sand fill. *Géotechnique* **55**, No. 2, 123–133.

Hicks, M. A. & Samy, K. (2002a). Influence of heterogeneity on undrained clay slope stability. *Quarterly Journal of Engineering Geology and Hydrogeology* **35**, No. 1, 41–49.

Hicks, M. A. & Samy, K. (2002b). Reliability-based characteristic values: A stochastic approach to Eurocode 7. *Ground Engineering* **35**, No. 12, 30–34.

Hicks, M. A. & Samy, K. (2004). Stochastic evaluation of heterogeneous slope stability. *Italian Geotechnical Journal* **38**, No. 2, 54–66.

Hicks, M. A. & Spencer, W. A. (2010). Influence of heterogeneity on the reliability and failure of a long 3D slope. *Computers and Geotechnics* **37**, No. 7, 948–955.

Huang, J., Fenton, G. A., Griffiths, D. V., Li, D.-Q. & Zhou, C.-B. (2017). On the efficient estimation of small failure probability in slopes. *Landslides* **14**, No. 2, 491–498.

Huang, J., Griffiths, D. V. & Fenton, G. A. (2010). System reliability of slopes by RFEM. *Soils and Foundations* **50**, No. 3, 343–353.

Huang, J., Lyamin, A. V., Griffiths, D. V., Krabbenhoft, K. & Sloan, S. W. (2013). Quantitative risk assessment of landslide by limit analysis and random fields. *Computers and Geotechnics* **53**, 60–67.

Huang, S. P., Quek, S. T. & Phoon, K.-K. (2001). Convergence study of the truncated karhunen-loeve expansion for simulation of stochastic processes. *International Journal for Numerical Methods in Engineering* **52**, No. 9, 1029–1043.

Jaksa, M. B., Kaggwa, W. S. & Brooker, P. I. (1999). Experimental evaluation of the scale of fluctuation of a stiff clay. In *Proceedings of 8th International Conference on the application of statistics and probability in Civil Engineering*, Sydney, pp. 415–422.

Javankhoshdel, S. & Bathurst, R. J. (2014). Simplified probabilistic slope stability design charts for cohesive and $c-\phi$ soils. *Canadian Geotechnical Journal* **51**, 1033–1045.

Javankhoshdel, S. & Bathurst, R. J. (2016). Influence of cross-correlation between soil parameters on probability of failure of simple cohesive and $c-\phi$ slopes. *Canadian Geotechnical Journal* **53**, No. 5, 839–853.

Javankhoshdel, S., Luo, N. & Bathurst, R. J. (2016). Probabilistic analysis of simple slopes with cohesive soil strength using rlem and rfem. *Georisk: Assessment and Management of Risk for Engineered Systems and Geohazards* **10**, 1–16.

Ji, J. & Kodikara, J. (2015). Efficient reliability method for implicit limit state surface with correlated non-gaussian variables. *International Journal for Numerical and Analytical Methods in Geomechanics* **39**, No. 17, 1898–1911.

Ji, J., Zhang, C., Gao, Y. & Kodikara, J. (2018). Efficient reliability method for implicit limit state surface with correlated non-gaussian variables. *Geoscience Frontiers* **9**, 1631–1638.

Ji, J., Zhang, C., Gao, Y. & Kodikara, J. (2019). Reliability-based design for geotechnical engineering: An inverse fom approach for practice. *Computers and Geotechnics* **111**, 22–29.

Jiang, S.-H., Li, D.-Q., Cao, Z.-J., Zhou, C.-B. & Phoon, K.-K. (2015). Efficient system reliability analysis of slope stability in spatially variable soils using monte carlo simulation. *Journal of Geotechnical and Geoenvironmental Engineering* **141**, No. 2, 04014096.

Lacasse, S. & Nadim, F. (1996). Reliability and probabilistic methods. In *Uncertainty in the Geologic Environment: from Theory to Practice, Proceeding of Uncertainty '96, Geotechnical Special Publication No. 58*, Wisconsin, US, pp. 49–75.

Le, T. M. H. (2014). Reliability of heterogeneous slopes with cross-correlated shear strength parameters. *Georisk: Assessment and Management of Risk for Engineered Systems and Geohazards* **8**, No. 4, 250–257.

Li, C.-C. & Der Kiureghian, A. (1993). Optimal discretisation of random fields. *Journal of Engineering Mechanics* **119**, No. 6, 1136–1154.

Li, D.-Q., Jiang, S.-H., Cao, Z.-J., Zhou, W., Zhou, C.-B. & Zhang, L.-M. (2015a). A multiple response-surface method for slope reliability analysis considering spatial variability of soil properties. *Engineering Geology* **187**, 60–72.

Li, D.-Q., Jiang, S.-H., Chen, Y.-F. & Zhou, C.-B. (2011). System reliability analysis of rock slope stability involving correlated failure modes. *KSCE Journal of Civil Engineering* **15**, No. 8, 1349–1359.

Li, D.-Q., Xiao, T., Cao, Z.-J., Phoon, K.-K. & Zhou, C.-B. (2016a). Efficient and consistent reliability analysis of soil slope stability using both limit equilibrium analysis and finite element analysis. *Applied Mathematical Modelling* **40**, 5216–5229.

Li, D.-Q., Xiao, T., Cao, Z.-J., Zhou, C.-B. & Zhan, L.-M. (2016b). Enhancement of random finite element method in reliability analysis and risk assessment of soil slopes using Subset Simulation. *Landslides* **13**, 293–303.

Li, D.-Q., Yang, Z.-Y., Cao, Z.-J. & Zhang, L.-M. (2019). Area failure probability method for slope system failure risk assessment. *Compuers and Geotechnics* **107**, 36–44.

Li, D.-Q., Zheng, D., Cao, Z.-J., Tang, X.-S. & Phoon, K.-K. (2016c). Response surface methods for slope reliability analysis: Review and comparison. *Engineering Geology* **203**, 3–14.

Li, L. & Chu, X. (2016). Locating the multiple failure surfaces for slope stability using monte carlo technique. *Geotechnical and Geological Engineering* **34**, No. 5, 1475–1486.

Li, S. J., Zhao, H. B. & Ru, Z. L. (2013). Slope reliability analysis by updated support vector machine and monte carlo simulation. *Natural Hazards* **65**, No. 1, 707–722.

Li, Y. (2017). *Reliability of long heterogeneous slopes in 3D*. Ph.D. thesis, Delft University of Technology, The Netherlands.

Li, Y., Hicks, M. A. & Nuttall, J. D. (2015b). Comparative analyses of slope reliability in 3D. *Engineering Geology* **196**, 12–23.

Li, Y., Hicks, M. A. & Vardon, P. J. (2016d). Uncertainty reduction and sampling efficiency in slope designs using 3D conditional random fields. *Computers and Geotechnics* **79**, 159–172.

Liu, L.-L., Deng, Z.-P., Zhang, S.-H. & Cheng, Y.-M. (2018). Simplified framework for system reliability analysis of slopes in spatially variable soils. *Engineering Geology* **239**, 330–343.

Liu, W.-K., Belytschko, T. & Mani, A. (1986a). Probabilistic finite elements for nonlinear structural dynamics. *Computer Methods in Applied Mechanics and Engineering* **56**, No. 1, 61–81.

Liu, W.-K., Belytschko, T. & Mani, A. (1986b). Random field finite elements. *International Journal for Numerical Methods in Engineering* **23**, No. 10, 1831–1845.

Lloret-Cabot, M., Fenton, G. A. & Hicks, M. A. (2014). On the estimation of scale of fluctuation in geostatistics. *Georisk: Assessment and Management of Risk for Engineered Systems and Geohazards* **8**, No. 2, 129–140.

Lloret-Cabot, M., Hicks, M. A. & van den Eijnden, A. P. (2012). Investigation of the reduction in uncertainty due to soil variability when conditioning a random field using Kriging. *Géotechnique Letters* **2**, No. 3, 123–127.

Low, B. A. & Tang, W. H. (1997). Efficient reliability evaluation using spreadsheet. *Journal of Engineering Mechanics* **123**, No. 7, 749–752.

Low, B. A. & Tang, W. H. (2004). Reliability analysis using object-oriented constrained optimization. *Structural Safety* **26**, No. 1, 69–89.

Low, B. A. & Tang, W. H. (2007). Efficient spreadsheet algorithm for first-order reliability method. *Journal of Engineering Mechanics* **133**, No. 12, 1378–1387.

Lumb, P. (1966). The variability of natural soils. *Canadian Geotechnical Journal* **3**, 105–112.

Lumb, P. (1970). Safety factors and probability distribution of soil strength. *Canadian Geotechnical Journal* **7**, No. 3, 225–242.

Luo, X., Li, X., Zhao, J. & Cheng, T. (2012). A kriging-based hybrid optimization algorithm for slope reliability analysis. *Structural Safety* **34**, No. 1, 401–406.

Nie, X., Zhang, J., Huang, H., Liu, Z. & Lacasse, S. (2015). Scale of fluctuation for geotechnical probabilistic analysis. In *Proceedings of 5th International Symposium on Safety and Risk*, Rotterdam, The Netherlands, pp. 834–840.

Orr, T. L. L. (2017). Defining and selecting characteristic values of geotechnical parameters for designs to Eurocode 7. *Georisk: Assessment and Management of Risk for Engineered Systems and Geohazards* **11**, No. 1, 103–115.

Papaioannou, I., Betz, W., Zwirglmaier, K. & Straub, D. (2015). MCMC algorithms for Subset Simulation. *Probabilistic Engineering Mechanics* **41**, 89–103.

Phoon, K.-K. & Kulhawy, F. H. (1999a). Characterization of geotechnical variability. *Canadian Geotechnical Journal* **36**, No. 4, 612–624.

Phoon, K.-K. & Kulhawy, F. H. (1999b). Evaluation of geotechnical property variability. *Canadian Geotechnical Journal* **36**, No. 4, 625–639.

Phoon, K.-K., Kulhawy, F. H. & Grigoriu, M. D. (1995). Reliability-Based Design of Foundations for Transmission and Line Structures. *Technical Report Final Report EPRI TR-105000, Research Project 1493-04*, Electric Power Research Institute, Palo Alto, California, US.

Rackwitz, R. (2000). Reviewing probabilistic soils modelling. *Computers and Geotechnics* **26**, No. 3–4, 199–223.

Rosenblueth, E. (1981). Two-point estimates in probabilities. *Applied Mathematical Modelling* **5**, No. 5, 329–335.

Santoso, A. M., Phoon, K.-K. & Quek, S. T. (2011). Effects of soil spatial variability on rainfall induced landslides. *Probabilistic Engineering Mechanics* **89**, No. 11, 893–900.

Schneider, H. R. (1997). Definition and characterization of soil properties. In *Proceedings of the XIV International Conference on Soil Mechanics and Geotechnical Engineering*, Hamburg, Germany, pp. 273–281.

Schneider, H. R. & Schneider, M. A. (2012). Dealing with uncertainties in EC7 with emphasis on determination of characteristic soil properties. In *In: Arnold, P., G. A. Fenton, M. A. Hicks, T. Schweckendiek, and B. Simpson (Eds.), Modern Geotechnical Design Codes of Practice: Development, Calibration and Experiences*, IOS Press, pp. 87–101.

Schultze, E. (1971). Frequency distributions and correlation of soil properties. In *Proceedings of the 1st International Conference on Applications of Statistics and Probability in Soil and Structural Engineering*, Hong Kong, pp. 371–387.

Spencer, W. A. (2007). *Parallel stochastic and finite element modelling of clay slope stability in 3D*. Ph.D. thesis, University of Manchester, UK.

Student (1908). The probable error of a mean. *Biometrika* **6**, No. 1, 181–190.

Sudret, B. & Der Kiureghian, A. (2000). *Stochastic finite element methods and reliability: a state-of-the-art report*. Department of Civil and Environmental Engineering, University of California Berkeley.

van den Eijnden, A. P. & Hicks, M. A. (2017). Efficient subset simulation for evaluating the modes of improbable slope failure. *Computers and Geotechnics* **88**, 267–280.

van der Krogt, M. G., Schweckendiek, T. & Kok, M. (2019). Uncertainty in spatial average undrained shear strength with a site-specific transformation model. *Georisk: Assessment and Management of Risk for Engineered Systems and Geohazards* **13**, No. 3, 181–190.

Vanmarcke, E. H. (1977). Reliability of earth slopes. *Journal of the Geotechnical Engineering Division* **103**, No. 11, 1247–1265.

Vanmarcke, E. H. (1980). Probabilistic stability analysis of earth slopes. *Engineering Geology* **16**, No. 1-2, 29–50.

Vanmarcke, E. H. (1983). *Random fields: analysis and synthesis*. The MIT Press, Cambridge, Massachussets.

Vardon, P. J., Liu, K. & Hicks, M. A. (2016). Reduction of slope stability uncertainty based on hydraulic measurement via inverse analysis. *Georisk: Assessment and Management of Risk for Engineered Systems and Geohazards* **10**, No. 3, 223–240.

Varkey, D., Hicks, M. A. & Vardon, P. J. (2018). 3D slope stability analysis with spatially variable and cross-correlated shear strength parameters. In *Proceedings of 9th European Conference on Numerical Methods in Geotechnical Engineering*, Porto, Portugal, pp. 498–503.

Wang, C.-H., Osorio-Murillo, C. A., Zhu, H. & Rubin, Y. (2017). Bayesian approach for calibrating transformation model from spatially varied CPT data to regular geotechnical parameter. *Computers and Geotechnics* **85**, 262–273.

Wang, L., Hwang, J. H., Luo, Z., Juang, C. H. & Xiao, J. (2013). Probabilistic back analysis of slope failure – A case study in Taiwan. *Computers and Geotechnics* **51**, 12–23.

Wang, Y., Cao, Z. & Au, S.-K. (2011). Practical reliability analysis of slope stability by advanced Monte Carlo simulations in a spreadsheet. *Canadian Geotechnical Journal* **48**, No. 1, 162–172.

Wolff, T. F., Demsky, E. C., Schauer, J. & Perry, E. (1996). Reliability assessment of dike and levee embankments. In *Uncertainty in the Geologic Environment: from Theory to Practice, Proceeding of Uncertainty '96, Geotechnical Special Publication No. 58*, Wisconsin, US, pp. 636–650.

Xiao, T., Li, D.-Q., Cao, Z.-J., Au, S.-K. & Phoon, K.-K. (2016). Three-dimensional slope reliability and risk assessment using auxiliary random finite element method. *Computers and Geotechnics* **79**, 146–158.

Xu, B. & Low, B. K. (2006). Probabilistic stability analyses of embankments based on finite element method. *Journal of Geotechnical and Geoenvironmental Engineering* **132**, No. 11, 1444–1454.

Zhang, J., Chen, H. Z., Huang, H. W. & Luo, Z. (2015). Efficient response surface method for practical geotechnical reliability analysis. *Compuers and Geotechnics* **69**, 496–505.

Zhang, J. & Huang, H. W. (2016). Risk assessment of slope failure considering multiple slip surfaces. *Compuers and Geotechnics* **74**, 188–195.

Zhang, J., Huang, H. W. & Phoon, K.-K. (2013a). Application of the kriging-based response surface method to the system reliability of soil slopes. *Journal of Geotechnical and Geoenvironmental Engineering* **139**, No. 4, 651–655.

Zhang, J., Zhang, L.-M. & Tang, W.-H. (2011). New methods for system reliability analysis of soil slopes. *Candian Geotechnical Journal* **48**, No. 7, 1138–1148.

Zhang, L. L., Zhuo, Z. B., Ye, G. L., Jeng, D. S. & Wang, J. H. (2013b). Probabilistic parameter estimation and predictive uncertainty based on field measurements for unsaturated soil slope. *Computers and Geotechnics* **48**, 72–81.

Zhao, H. B. (2008). Slope reliability analysis using a support vector machine. *Compuers and Geotechnics* **35**, No. 3, 459–467.

3

CHARACTERISTIC VALUES AND RELIABILITY-BASED ASSESSMENT OF A DYKE

.

A case study involving the assessment and re-design of an existing dyke, founded on a layered soil, has compared deterministic analysis based on 5-percentile property values and a reliability-based RFEM analysis consistent with the requirements of Eurocode 7. The results show that a consideration of the spatial nature of soil variability generally leads to higher computed factors of safety and, for those dyke sections requiring remedial action, to more economic designs. Characteristic values back-figured from the RFEM analysis are compared with those calculated using various simplified approaches. The deterministic stability analyses based on the characteristic values show that the simplified methods accounting for variance reduction due to averaging of property values mostly give factors of safety within 10% of the RFEM solution, whereas the factor of safety based on the 5-percentile material properties is significantly over-conservative.

This chapter is based on Hicks *et al.* (2019); Varkey *et al.* (2019, 2020a,b)

3.1. INTRODUCTION

Around 1 billion euros per year are required to maintain and upgrade the Dutch dyke network, which protects around 40% of the Netherlands from inundation. This includes 14.000 km of rural dykes, which are currently maintained and upgraded using rules mainly derived from research on primary dykes (a very different type of structure). Although there are several approaches proposed for the determination of characteristic values, the current strategy for determining when maintenance and/or upgrading are needed is based on assessment using partial factors and reliability-based characteristic values derived only from the point statistics of the material properties. This chapter reports a recent reliability-based assessment of a dyke ring in the west of the Netherlands, based on statistics derived from laboratory and site investigation data. In particular, for a selected dyke cross-section, deterministic solutions for the factor of safety are compared with probability distributions of factor of safety based on reliability analyses using (a) only the point statistics, and (b) random fields. Additionally, the relative performances of various simplified approaches to determining characteristic values have also been investigated.

3.2. BACKGROUND

Dutch stability assessments of rural dykes are based on the Eurocode 7 (EC7) philosophy of partial factors and characteristic values of soil properties, in which the partial factors are defined by the code and the characteristic values are chosen by the engineer (CEN, 2004). In particular, they adopt a statistical approach to deriving characteristic values.

Table 3.1: Clause (11) extracted from Section 2.4.5.2 of Eurocode 7 (CEN, 2004)

(11)	If statistical methods are used, the characteristic value should be derived such that the calculated probability of a worse value governing the occurrence of the limit state under consideration is not greater than 5%". NOTE: In this respect, a cautious estimate of the mean value is a selection of the mean value of the limited set of geotechnical parameter values, with a confidence level of 95%; where local failure is concerned, a cautious estimate of the low value is a 5% fractile.

Extracts from Section 2.4.5.2 of EC7, "Characteristic values of geotechnical parameters", were reviewed by Hicks (2012) and Hicks & Nuttall (2012). In particular, they highlighted Clause (11), which gives guidelines for when statistical methods are used (see Table 3.1). It infers that characteristic values should be selected so as to give a minimum confidence level or reliability of at least 95% with respect to the system response. Although this appears to be contradicted by the two parts of the footnote, the first part of which refers to mean values and the second part of which refers to the soil property distribution, it was demonstrated that the clause and both parts of the footnote are entirely consistent, and explained by a consideration of the scale of fluctuation θ (the distance over which soil properties are significantly correlated) and the size of the problem domain D (e.g. the extent of the failure surface), relative to a modified 'effective'property distribution governing the limit state. In Figure 3.1, which, for simplicity, shows a single soil property X represented by a normal distribution, three scenarios are possible for the characteristic

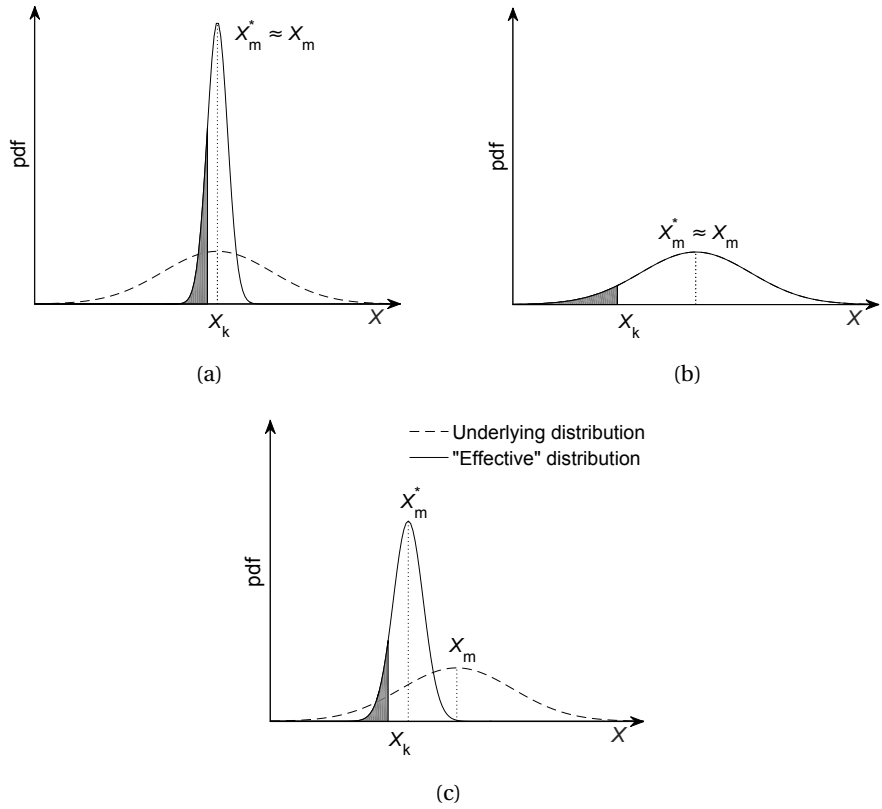

Figure 3.1: Derivation of characteristic property values satisfying EC7 (based on Hicks (2012) and Hicks & Nuttall (2012)): underlying distribution of X, and 'effective' distribution accounting for influence of spatial correlation and problem being analysed: (a) $\theta/D << 1$, (b) $\theta/D >> 1$, and (c) intermediate values of θ/D

value X_k:

1. For very small values of θ/D, there is considerable averaging of soil property values over the potential failure surface. This leads to a narrow 'effective' property distribution centred about the mean (X_m) of the underlying distribution. In this case, the 5 percentile of the modified distribution represents a cautious estimate of the mean (cf. part 1 of footnote).

2. For very large values of θ/D, failures tend to be local and there is a large range of possible solutions. This leads to the 'effective' distribution tending towards the underlying distribution, from which the characteristic value is the 5 percentile (cf. part 2 of footnote).

3. For intermediate values of θ/D (i.e. the usual scenario), X_k is problem-dependent and there are two competing factors: (a) the averaging of soil properties over the potential failure surface leads to a narrower 'effective' property distribution; (b) the

tendency for failure to be attracted to semi-continuous weaker zones leads to a reduced mean (X^*_{m}) relative to the underlying distribution.

Note that Scenario 3, as illustrated in Figure 3.1c, is the general case, whereas Scenarios 1 and 2 (Figures 3.1a and 3.1b, respectively) are the limiting cases. Moreover, although the mean is reduced in Scenario 3, because the modified distribution is narrower than the underlying distribution, the 5 percentile of the modified distribution representing the characteristic value is generally greater than in Scenario 2; that is, relative to the underlying distribution, X_{k} corresponds to a percentile (η) greater than 5 %.

Various approaches have been proposed for selecting the characteristic values of soil properties; for example, as reported by Orr (2017) and Shen *et al.* (2019). However, for reasons of simplicity, engineering practice sometimes uses the 5 percentile of the underlying distribution as the characteristic value, regardless of the value of θ/D or the geotechnical application. The implications of this simplification are investigated below, through use of a reliability-based random finite element approach consistent with the requirements of Eurocode 7.

3.3. PROBLEM DESCRIPTION

The Starnmeer polder is situated in the province of North Holland and is managed by the water board Hoogheemraadschap Hollands Noorderkwartier (HHNK). It was originally drained in 1643, covers an area of 580 hectares, and is contained within a dyke ring of around 13 km in length. Recently, HHNK initiated a stability assessment of the dyke. This was performed by dividing the dyke into 10 sections and, for each section, the factor of safety (F) against slope failure was determined for a representative cross-section using the limit equilibrium software D-Geo Stability (Deltares, 2018). This revealed that 5 of the 10 sections do not comply with current safety requirements. Indeed, not only did they return factors of safety below the required F; in some cases, factors of safety as low as 0.5 were reported even though the dyke has remained stable for hundreds of years.

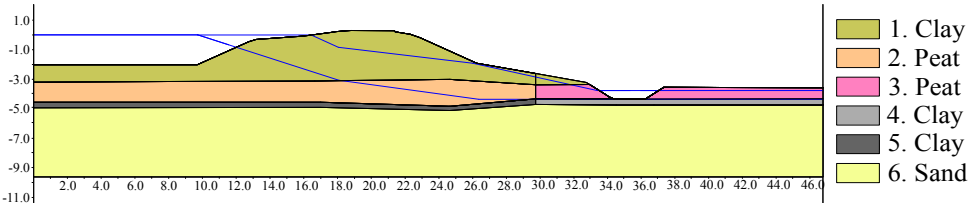

Figure 3.2: Dyke cross-section (scale in metres). The higher phreatic surface relates to layers 1-5 and the bottom phreatic surface relates to layer 6

In this chapter, the assumptions made in analysing the dyke cross-section which returned a factor of safety of 0.59 based on design property values have been investigated. Figure 3.2 shows that the 3.8 m high dyke, loaded by a stable water level, is composed of clay, and is founded on a peat layer underlain by a thin clay layer and a thick sand layer. Table 3.2(a) summarises the unit weights and shear strength properties used in the original assessment, based on the results of extensive laboratory (triaxial and direct simple shear) tests on soils from Starnmeer (Kames, 2015). In this table, the mean and

5-percentile values for the cohesion (c') and tangent of the friction angle (tan ϕ'), for each material zone indicated in Figure 3.2, are reported, as well as the respective partial factors and design property values used in the stability analysis (in which the design value is equal to the characteristic value divided by the partial factor). Also shown in the table are the COVs of c' and tan ϕ', which have been back-figured from the respective mean and 5-percentile values assuming a log-normal distribution, and are on the conservative (high) side due to soil samples coming from the Starnmeer area as a whole rather than from the specific cross-section being analysed. Note that no test results were reported for the bottom (sand) layer, and that the 5-percentile value of tan ϕ' adopted for this layer is the value suggested by NEN 9997-1 (2011) for a moderately packed sand.

3.4. RE-ANALYSIS OF DYKE STABILITY

Table 3.3 summarises the results of a re-evaluation of the stability of the dyke section. These results have been obtained using an in-house finite element software, developed at TU Delft, that computes the factor of safety using the strength reduction method, and they are based on the same cross-sectional geometry and material properties used previously. Moreover, the same external water level and phreatic surfaces as in the original assessment have been assumed here (represented by the blue lines in Figure 3.2), in which the higher phreatic surface relates to all soil layers, except for layer 6 for which the lower phreatic surface is used. Figure 3.3 illustrates the significance of the underlying peat layer, by showing the computed failure mechanism based on homogeneous soils.

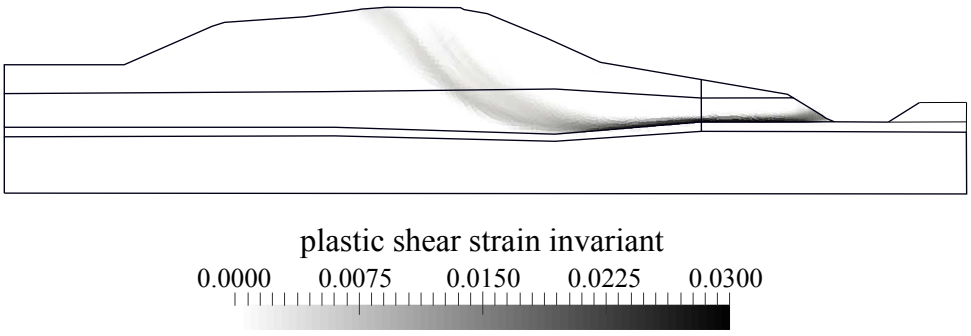

Figure 3.3: Plastic shear strain invariant contours at failure based on homogeneous soil layers. (Refer to Figure 3.2 for the soil layers)

Firstly, Table 3.3 lists the deterministic factors of safety obtained using the mean, 5-percentile and design property values for the different material zones (from Table 3.2(a)). Based on the design properties, $F = 0.54$, which compares favourably with the D-Geo Stability solution of 0.59, as well as with an F of 0.56 obtained by using the commercial finite element code PLAXIS. Each of these solutions takes account of the uncertainty in the design property values by basing them on characteristic values representing the 5-percentile of the property distribution; that is, by adopting the approach called Scenario 2 in Section 3.2. However, as discussed, this is not consistent with the intention of EC7, as

Table 3.2: Unit weights and shear strength parameter values used in analysis of dyke cross-section for: (a) layers 1 – 6; (b) layers 7 – 8. (Layers 1 – 6 refer to Figure 3.2; layers 7 – 8 refer to Figure 3.5.)

Layer	γ (kN/m^3)	c'					$\tan\phi'$				
		Mean (kPa)	5-percentile value (kPa)	COV	Partial factor	Design value (kPa)	Mean	5-percentile value	COV	Partial factor	Design value
						(a)					
1	13.9 *	4.4	1.1	0.773	1.20	0.917	0.580	0.506	0.081	1.15	0.429
2	9.8	3.2	1.0	0.656	1.20	0.833	0.398	0.361	0.058	1.15	0.310
3	9.9	2.0	0.5	0.775	1.20	0.417	0.358	0.279	0.145	1.15	0.241
4	15.0	4.5	1.7	0.544	1.20	1.417	0.559	0.547	0.012	1.15	0.465
5	15.0	5.4	2.9	0.352	1.20	2.417	0.601	0.594	0.007	1.15	0.503
6	20.0	0.0	0.0	0.000	-	0.000	0.637	0.637	0.000	1.20	0.531
						(b)					
7	17.0	6.2	1.6	0.773	1.20	1.333	0.531	0.463	0.081	1.15	0.403
8	20.0	0.0	0.0	0.000	-	0.000	0.637	0.637	0.000	1.20	0.531

* $\gamma = 6.9\,\text{kN/m}^3$ above phreatic surface.

Table 3.3: Factors of safety F for dyke cross-section based deterministic and stochastic analyses

Deterministic analyses		Stochastic analysis		
			F corresponding to cdf of 0.05	
Property values	F	θ_h (m)	without partial factors	with partial factors
Mean	1.31	0.5	1.10	-
5-percentile	0.66	6.0	0.98	0.85
Design	0.54	12.0	0.98	-

illustrated in Figure 3.1, in that the characteristic values take no account of the spatial nature of the soil variability nor of the problem being analysed.

Hence, Table 3.3 also shows stochastic results accounting for the spatial variability of soil property values within the material zones. These have been computed with the same in-house finite element software, but now using RFEM implemented within a Monte Carlo simulation. The random fields have here been generated by covariance matrix decomposition using a Markov auto-correlation function; see van den Eijnden & Hicks (2017) for details. The RFEM process uses the same point statistics as listed in Table 3.2, but additionally, for each soil property and each material zone, vertical and horizontal scales of fluctuation are specified to quantify the distance over which property values are significantly correlated. As insufficient data are available for the cross-section, the vertical scale of fluctuation (θ_v) has been taken as 0.5 m for all properties and all material zones. This is a conservative (high) estimate based on a range of 0.2 – 0.5 m reported by de Gast *et al.* (2017) for similar soils found at the Leendert de Boerspolder site in South Holland. Three values for the horizontal scale of fluctuation (θ_h) have initially been considered; 0.5 m, 6.0 m and 12.0 m, to investigate the sensitivity of the solution to this statistical measure. For each value of θ_h, an RFEM analysis involving 500 realisations has been conducted, in which, for each realisation, the point and spatial statistics have been used to generate uncorrelated random fields of c' and $\tan\phi'$ for each material zone, and the factor of safety of the dyke then computed using the strength reduction method. This gives 500 factors of safety, from which a cumulative distribution (cdf) of F can be plotted.

Figure 3.4 shows the cdf of F computed using RFEM for each value of θ_h (as a solid curve), based on the soil property statistics given in Table 3.2(a). Also indicated in the figure are the factors of safety obtained from deterministic analyses based only on the mean, median and 5-percentile values, as well as that obtained based on the design property values. The cdf of F from a stochastic analysis based only on the point statistics (i.e. with no spatial averaging) is included, to highlight the significance of spatial averaging in the RFEM analyses.

Figure 3.4 shows that, corresponding to the 5-percentile system response, a conservative estimate of $F = 0.98$ is obtained when $\theta_h = 6$ m. In order to determine the value of F corresponding to the design property values, for each material zone the property distribution for c' has been scaled down by a partial factor of 1.20 and the property distribution for $\tan\phi'$ has been scaled down by a partial factor of 1.15 (or 1.20, in the case of the sand layer). These "design" property distributions have then been used in a further RFEM analysis (with $\theta_h = 6$ m), to give a new cdf (shown as a broken curve in Figure 3.4) and a value of $F = 0.85$ corresponding to 5 percentile of that cdf (see Table 3.3). This value

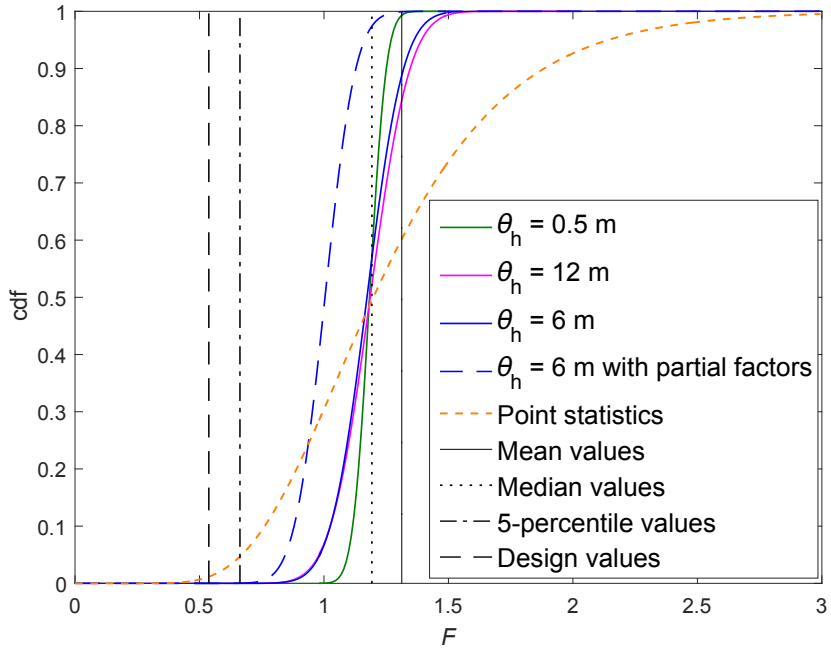

Figure 3.4: Comparison of deterministic and stochastic solutions for factor of safety

represents a significant (57%) increase in F when accounting for the spatial nature of the soil variability, although, as it is still less than the $F = 0.95$ safety requirement (based on the IPO-class, i.e. design class, this dyke section belongs to (Kames, 2015)), some upgrading of the dyke section is needed. While a value of $F < 1$ usually implies failure, the required $F = 0.95$ takes into account the economic implications of inundation in addition to material uncertainties (de Gast, 2020).

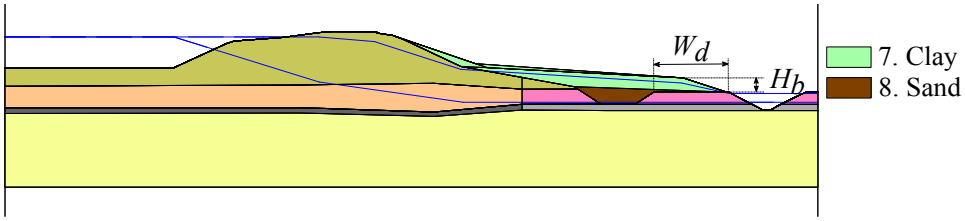

Figure 3.5: Initial re-design for dyke cross-section

3.4.1. RE-DESIGN OF THE DYKE SECTION

Figure 3.5 shows an initial proposal for the re-design of the dyke section, following on from the original stability assessment of $F = 0.59$ (using D-Geo Stability). This involves moving

the ditch further away, infilling the original ditch with sand, and constructing a clay berm over the sloping face to increase the resistance against failure. The unit weights and shear strength properties for the sand infill and clay fill are summarised in Table 3.2(b). This led to increased deterministic factors of safety, based on the design property values, of $F = 1.33$ using D-Geo Stability and $F = 1.21$ using the in-house software. However, an RFEM analysis based on the design property distributions, $\theta_v = 0.5\,\text{m}$, and $\theta_h = 6\,\text{m}$, for the cross-section in Figure 3.5, gave $F = 1.53$ corresponding to the 5-percentile system response, an increase of 27% relative to the deterministic in-house solution.

Table 3.4 shows the results of further RFEM analyses, corresponding to a range of berm heights and berm widths (as quantified by the distance between old and new ditches), see Figure 3.5. These results show how F corresponding to the 5-percentile system response, with and without partial factors, varies as a function of the berm geometry. In particular, it highlights how a berm with a height of $H_b/2$ and inter-ditch spacing of $W_d/3$ gives a factor of safety (with partial factors) satisfying the safety requirement (i.e. $F = 1.015 > 0.95$). This represents a significant saving relative to the original re-design (Figure 3.5), both in terms of volume of fill required (75% less than the volume of fill required in the original re-design) and impact on neighbouring property.

3.5. CHARACTERISTIC VALUES

The above analysis and re-design of the dyke section using RFEM is fully consistent with EC7, in that it is based on soil property values giving a 5-percentile system response, factored down by the required partial factors. Note that, even though the characteristic soil properties have not been calculated explicitly during the analyses (i.e. the 5 percentile of the 'effective' distribution), it is the reliability-based factor of safety that is needed in the safety assessment. Moreover, calculating characteristic values for a problem in which there are two soil properties and multiple soil layers is not straightforward. In contrast to the simple illustration given in Figure 3.1, in which the characteristic property is a single value, for this dyke section the characteristic values for each material zone are represented by a surface in c'-tan ϕ' space; in other words, there are many combinations of c' and tan ϕ' that give the same reliability for the structure. Nonetheless, it is informative to back-calculate percentiles of the underlying property distributions (η) representing the characteristic values.

3.5.1. SINGLE CHARACTERISTIC PERCENTILE

For illustrative purposes, a simple approach to back-calculate percentiles has here been adopted. Specifically, a single value of η has been back-figured, which, when applied to the distributions of c' and tan ϕ' for each material zone, gives characteristic values that return the correct factor of safety corresponding to the 5-percentile system response. This percentile has been determined by conducting multiple deterministic analyses, in which, for any given realisation, the shear strength parameters for all material zones are sampled from the same percentile location in the respective property distributions (i.e. each material zone is treated as homogeneous). Thus, in realisation r, the input $(X_i)_r$ for a parameter X_i (i.e. either c' or tan ϕ') is calculated using

$$(X_i)_r = \exp(\mu_{\ln X_i} + \sigma_{\ln X_i} \times k_r) \tag{3.1}$$

Table 3.4: Factors of safety corresponding to the 5-percentile system response for various berm designs

	H_b	$2H_b/3$	$3H_b/5$		$H_b/2$		$0H_b$	
	without partial factors	without partial factors	without partial factors	with partial factors	without partial factors	with partial factors	without partial factors	with partial factors
W_d	1.789	1.461	1.268	1.083	1.197	1.027	0.968	0.826
$2W_d/3$	1.736	1.377	1.265	1.080	1.193	1.021	-	-
$W_d/2$	1.724	1.375	1.259	1.079	1.186	1.016	-	-
$W_d/3$	1.647	1.360	1.249	1.071	1.181	1.015	-	-

where $\mu_{\ln X_i}$ and $\sigma_{\ln X_i}$ are the mean and standard deviation of the natural logarithm of X_i, respectively, and k_r is the standard score, computed using

$$k_r = \Phi^{-1}(r/N) \tag{3.2}$$

where Φ^{-1} is the inverse of the standard normal cumulative distribution function and N is the total number of realisations.

Figure 3.6 compares the cdf of F obtained using this approach with the cdf of F obtained using RFEM with $\theta_v = 0.5$ m and $\theta_h = 6$ m, for the original dyke cross-section in Figure 3.2. For $F = 0.98$, corresponding to the 5-percentile system response in the RFEM analysis, the value of r/N is 0.34. Hence, for this particular dyke section and loading conditions, the characteristic percentile that may be used for both the c' and tan ϕ' distributions (for all material zones) is 34%.

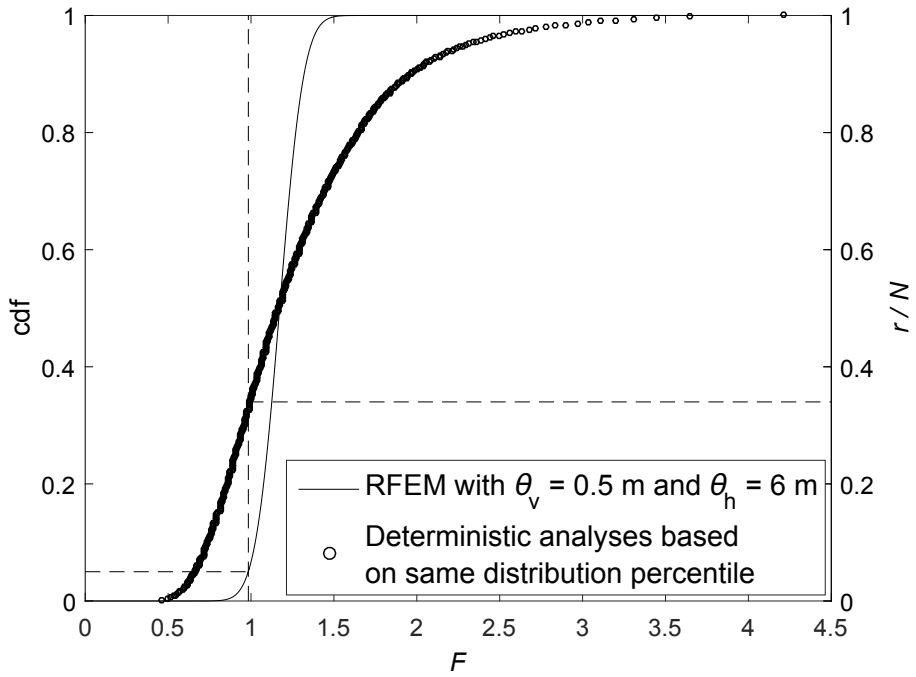

Figure 3.6: Comparison of factor of safety distribution obtained using RFEM with deterministic analyses based on same distribution percentile

3.5.2. 5-PERCENTILE DESIGN POINT

The 5-percentile design point is here defined as the most likely combination of parameters on the "characteristic" surface (i.e., the 5-percentile system response surface, corresponding to $F = 0.98$). (Note that this 5-percentile design point is not the same as the design value in EC7, which is calculated as the characteristic value divided by the partial

Table 3.5: Most likely combination of characteristic soil property values corresponding to the 5-percentile system response ($F = 0.98$) of the dyke section, the respective percentiles of the underlying distributions (η) and the sensitivity indices of the variables

Layer	c'			$\tan\phi'$		
	5-percentile design point, X_k (kPa)	η (%)	Sensitivity index	5-percentile design point, X_k	η (%)	Sensitivity index
1	2.688	35.27	0.27	0.577	49.70	0.00
2	1.863	27.27	0.58	0.396	46.98	0.01
3	1.285	38.11	0.14	0.354	49.70	0.00

factor). The 5-percentile design point was evaluated using the HLRF algorithm (Hasofer & Lind, 1974; Rackwitz & Fiessler, 1978), with the performance function ($G = F - 0.98$) being evaluated by the finite element method without accounting for spatial variability. Based on the location of the shear strain invariant contours observed in the previous RFEM analyses, six variables were considered in defining the 5-percentile design point; i.e., two variables (c' and $\tan\phi'$) from each of the three most influential soil layers (1, 2 and 3).

Table 3.5 shows the most likely combination of characteristic values, the respective percentiles of the underlying property distributions and the sensitivity indices of the variables. The results imply that F is less sensitive to $\tan\phi'$ for all layers, with the characteristic values of $\tan\phi'$ corresponding to η values approaching 50%. Conversely, F is most sensitive to c' from the underlying peat layer (layer 2); the characteristic value for c' from this layer corresponds to $\eta = 27.27\%$.

Note that no correlation has been assumed between c' and $\tan\phi'$ in this research, although previous studies have mainly suggested a negative correlation between these two parameters, which would result in a narrower cdf of F (Vardon *et al.*, 2016) and thereby a higher characteristic percentile. Thus, the characteristic percentiles computed for this particular dyke section are likely to be a conservative estimate.

3.5.3. CHARACTERISTIC VALUES FOR THE DYKE SECTION COMPUTED USING VARIOUS ANALYTICAL EQUATIONS

The approaches described above to back-calculate the characteristic values require a reliability-based F from a fully stochastic analysis, e.g., using RFEM. However, several simpler (albeit more approximate) solutions exist. Hence, characteristic values for c' and $\tan\phi'$ from layers $1-3$ of the dyke section have been calculated using the methods reviewed below, and, using the computed X_k values for these layers and mean values (X_m) for the other (not influential) layers, deterministic slope stability assessments have been carried out using finite elements with the strength reduction method.

SCHNEIDER (1997) EQUATION

Schneider (1997) proposed:

$$X_k = X_m \times (1 - \text{COV} \times 0.5) \tag{3.3}$$

The resulting characteristic values, value of η and value of F are listed in Table 3.6. This shows that the X_k values are mostly underestimated relative to the 5-percentile design

Table 3.6: Characteristic soil property values for the dyke section computed using Equation (3.3) (Schneider, 1997), value of η and resulting value of F

Layer	c'		$\tan\phi'$		F
	X_k (kPa)	η (%)	X_k	η (%)	
1	2.472	30.85	0.555	30.85	
2	1.984	30.85	0.386	30.85	0.96
3	1.122	30.85	0.329	30.85	

point values, especially for $\tan\phi'$, resulting in a slightly conservative value of F (i.e., relative to $F = 0.98$).

SCHNEIDER & SCHNEIDER (2012) EQUATION

Schneider & Schneider (2012) extended Equation (3.3) to include variance reduction (Γ^2) (Vanmarcke, 1977) due to averaging of soil property values along the failure surface. The derivation was based on the total coefficient of variation $\mathrm{COV}_{\mathrm{total}}$ (Phoon & Kulhawy, 1999):

$$\mathrm{COV}_{\mathrm{total}} = \sqrt{\mathrm{COV}^2 \times \Gamma^2 + {\mathrm{COV}_{\mathrm{m}}}^2 + {\mathrm{COV}_{\mathrm{t}}}^2 + {\mathrm{COV}_{\mathrm{s}}}^2} \tag{3.4}$$

Assuming that the COVs due to measurement (m), transformation (t) and statistical (s) errors are negligible, so that $\mathrm{COV}_{\mathrm{total}} \approx \mathrm{COV} \times \Gamma$, Schneider & Schneider (2012) proposed the following equations for X_k. When X is modelled as a normal distribution

$$X_{\mathrm{k}} = X_{\mathrm{m}} \times \left(1 - \mathrm{COV} \times \Gamma \times 1.645\right) \tag{3.5}$$

whereas for a log-normal distribution of X,

$$X_{\mathrm{k}} = X_{\mathrm{m}} \times \left(0.192^{\sqrt{\ln(1+\mathrm{COV}^2 \times \Gamma^2)}} / \sqrt{1 + \mathrm{COV}^2 \times \Gamma^2}\right) \tag{3.6}$$

where $\Gamma^2 = \Gamma_x^2 \times \Gamma_y^2 \times \Gamma_z^2$ is the variance reduction due to the averaging of property values over the failure length l_i in the direction i, given by

$$\begin{aligned} \Gamma_i^2 &= \left(\frac{\theta_i}{l_i} \times \left(1 - \frac{\theta_i}{3 \times l_i}\right)\right);\ \theta_i \le l_i \\ \Gamma_i^2 &= \left(1 - \frac{l_i}{3 \times \theta_i}\right);\ \theta_i \ge l_i \end{aligned} \tag{3.7}$$

Equations (3.5) and (3.6) imply that X_{k} is the 5 percentile of a distribution with a COV that is reduced relative to the underlying distribution. Although this aspect is similar to the concept of 'effective' property distribution described in Section 3.2, Equations (3.5) and (3.6) do not consider the reduction in the mean of the distribution arising from the influence of weak zones. Moreover, they require the estimation of Γ_i^2 and thereby l_i, which may not be straightforward.

In order to calculate the variance reduction for the dyke section, a deterministic analysis based on mean soil properties was used to provide a representative failure mechanism

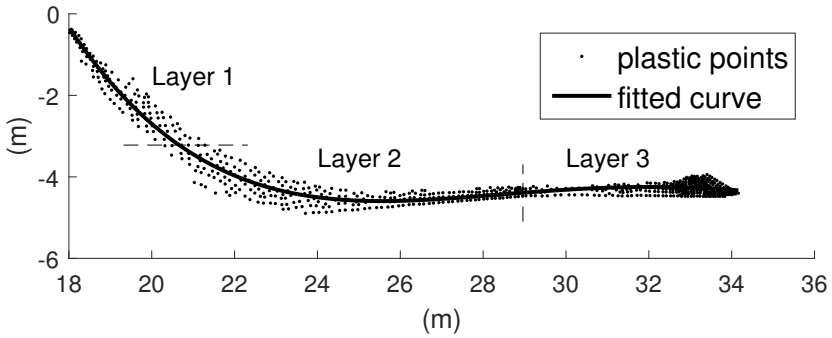

Figure 3.7: Failure surface fitted through plastic points (obtained using deterministic analysis of the dyke section based on mean soil property values) in order to calculate variance reduction using Equation (3.7)

Table 3.7: Characteristic soil property values for the dyke section computed using Equation (3.6) (Schneider & Schneider, 2012), η values and resulting value of F

Layer	l_h (m)	l_v (m)	Γ	c'		$\tan\phi'$		F
				X_k (kPa)	η (%)	X_k	η (%)	
1	3.1	2.7	0.380	2.627	34.04	0.551	27.66	
2	8.3	1.0	0.478	1.842	26.63	0.380	22.16	0.89
3	5.1	0.0	0.845	0.624	8.77	0.290	8.43	

(Figure 3.3). The length of the failure surface was calculated based on the curve fitted through the failure points in Figure 3.7. The estimated lengths of the horizontal and vertical components of the surface passing through each soil layer are given in Table 3.7, along with the respective values of Γ (Equation (3.7)), the X_k values (Equation (3.6)), and resulting value of F. The characteristic values and thereby η values are greatly underestimated for layer 3, resulting in a conservative estimate of F. Although it is unsurprising that a failure length smaller than θ, as in layer 3, would result in X_k tending towards the 5-percentile (as has been computed by Equation (3.6)), the higher η values of the 5-percentile design point for layer 3 (Table 3.5) are due to the lower relative influence of layer 3 on the failure mechanism.

EQUATION PROPOSED BY CEN (ORR, 2017)

An evolution committee of CEN, the European Committee for Standardisation, which plans to publish a revised version of EC7, has proposed (Orr, 2017):

$$X_k = X_m - a \times (X_m - X_{extr}) \times \sqrt{\theta_v / l_v} \tag{3.8}$$

where X_{extr} is the expected extreme value which Orr (2017) proposed to be at a distance of 3 standard deviations from the mean, l_v is the vertical component of the failure length, and a is a factor accounting for the extent and quality of field and laboratory investigations and levels of expertise (with lower values of a corresponding to high quality tests and reliable results).

Table 3.8: Characteristic soil property values for the dyke section computed using Equation (3.8) (Orr, 2017), η values and resulting value of F, for different values of a: (a) $a = 0.5$; (b) $a = 0.75$; (c) $a = 1.0$

(a)

Layer	l_v (m)	c'			tan ϕ'			F
		X_{extr} (kPa)	X_k (kPa)	η (%)	X_{extr}	X_k	η (%)	
1	2.7	0.447	3.548	51.10	0.454	0.553	28.95	1.04
2	1.0	0.445	2.226	37.92	0.334	0.375	16.30	
3	0.0	0.202	1.101	29.89	0.230	0.294	9.76	

(b)

Layer	l_v (m)	c'			tan ϕ'			F
		X_{extr} (kPa)	X_k (kPa)	η (%)	X_{extr}	X_k	η (%)	
1	2.7	0.447	3.122	43.67	0.454	0.539	19.40	0.89
2	1.0	0.445	1.739	23.56	0.334	0.364	6.54	
3	0.0	0.202	0.651	9.81	0.230	0.262	1.81	

(c)

Layer	l_v (m)	c'			tan ϕ'			F
		X_{extr} (kPa)	X_k (kPa)	η (%)	X_{extr}	X_k	η (%)	
1	2.7	0.447	2.696	35.43	0.454	0.525	11.90	0.69
2	1.0	0.445	1.252	10.21	0.334	0.353	1.99	
3	0.0	0.202	0.202	0.13	0.230	0.230	0.13	

Based on the values of a suggested by Orr (2017), the characteristic soil property values computed using Equation (3.8) and resulting values of F are listed in Table 3.8 (a)–(c). Note that, in using Equation (3.8), an upper limit for θ_v / l_v of 1.0 has been implemented here in order to avoid the possibility of unrealistically low values of X_k (i.e. $X_k < X_{extr}$). The table shows that the X_k values for tan ϕ' are greatly underestimated (even though, as indicated by the 5-percentile design point, the dyke section is less sensitive to tan ϕ'). Conversely, the X_k values for c' for layer 1 are overestimated, due to a relatively smaller value of θ_v / l_v leading to greater spatial averaging. Table 3.8 shows that X_k values are very sensitive to the value of a and F varies from moderately unconservative to extremely conservative, depending on a.

ERD-QVM (CHING *et al.*, 2020)

A method to approximate the 5 percentile of the system response function (G) directly, through the reformulation of the characteristic values based on the concept of number of effective random dimensions (ERD) in a quantile value method (QVM), was recently proposed by Ching *et al.* (2020). The method relies on the linearisation of G around the

parameter means:

$$b_i = G(\mu_1, ..., \mu_i + 0.5 \times \sigma_i, ..., \mu_n) - G(\mu_1, ..., \mu_i - 0.5 \times \sigma_i, ..., \mu_n) \tag{3.9}$$

where b_i is the coefficient of variable X_i in the linearised G, and μ_i and σ_i are the mean and standard deviation of X_i.

For uncorrelated variables, ERD is then calculated as

$$\text{ERD} = \frac{(|b_1| + |b_2| + ... + |b_n|)^2}{\sum_i b_i^2} \tag{3.10}$$

The required η that achieves the target exceedance probability of 5% is then

$$\eta = \Phi\left(\frac{\Phi^{-1}(0.05)}{\sqrt{\text{ERD}}}\right) \tag{3.11}$$

Applying this method to the six variables gives ERD = 2.93, η = 17% and thereby $F = 0.82$. Due to the need for linearisation against all variables, the method does not allow the direct inclusion of spatial variability.

ERD-QVM-Γ (PROPOSED IN THIS THESIS)

Combining the ERD-QVM with the method by Schneider & Schneider (2012) to account for spatial variability, Equations (3.9) and (3.11) can be modified to:

$$b_i = G(\mu_1, ..., \mu_i + 0.5 \times \sigma_i \times \Gamma_i, ..., \mu_n) - G(\mu_1, ..., \mu_i - 0.5 \times \sigma_i \times \Gamma_i, ..., \mu_n) \tag{3.12}$$

$$\eta_i = \Phi\left(\frac{\Phi^{-1}(0.05)}{\sqrt{\text{ERD}}} \times \Gamma_i\right) \tag{3.13}$$

where Γ_i^2 is the variance reduction for X_i.

Applying this method to the six variables and using Γ_i from Table 3.7 gives ERD = 3.08, and thereby the η values listed in Table 3.9 and $F = 0.96$.

Table 3.9: Characteristic soil property values for the dyke section computed using ERD-QVM-Γ, η values and resulting value of F

Layer	c'			$\tan\phi'$			F
	b	X_k (kPa)	η (%)	b	X_k	η (%)	
1	0.064	2.728	36.10	0.002	0.562	36.10	0.96
2	0.136	2.046	32.70	0.010	0.387	32.70	
3	0.097	0.918	21.40	0.005	0.316	21.40	

3.5.4. COMPARISON OF METHODS

Figure 3.8 illustrates, in standard normal space, the characteristic values of c' computed for layers 1–3 using the different methods. The values corresponding to the single characteristic percentile and the 5-percentile design point lie on the characteristic surface of

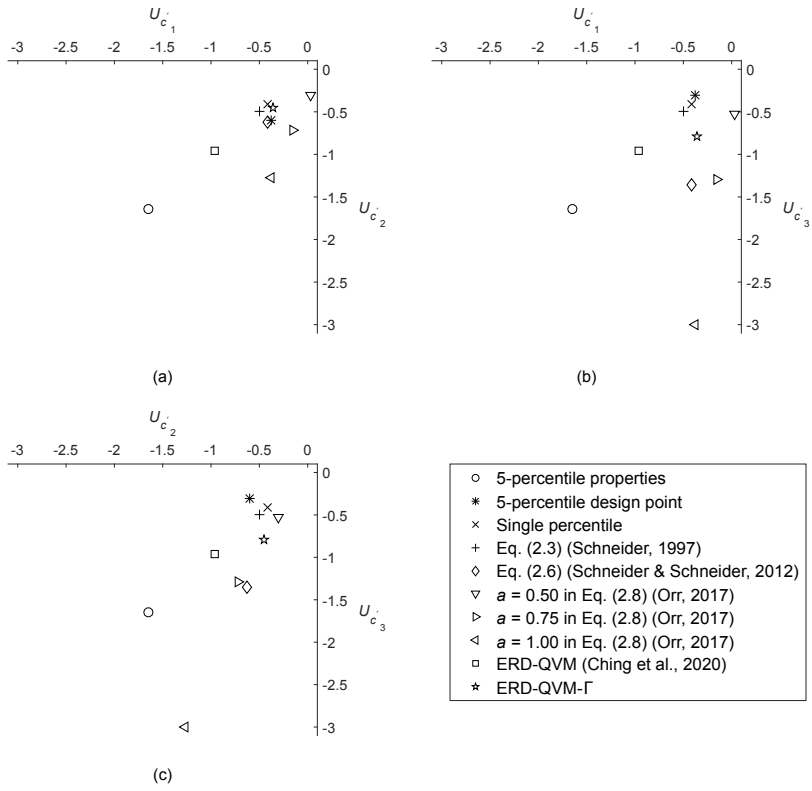

Figure 3.8: Characteristic values in standard normal space of c_1', c_2' and c_3' for layers 1, 2 and 3, respectively, computed using various methods: (a) layers 1 and 2; (b) layers 1 and 3; (c) layers 2 and 3

points resulting in $F = 0.98$. Figure 3.9 shows that the values computed using $a = 0.50$ in Equation (3.8) lies on the unconservative side ($F > 0.98$) of the characteristic surface, whereas the values computed using other simplified methods are on the conservative side ($F < 0.98$). Although there are other variables that define the characteristic surface (i.e. $\tan \phi'$ from layers 1–3), these have not been illustrated in Figure 3.8 for reasons of clarity.

Figure 3.9 compares the factors of safety obtained by the finite element method using the characteristic soil properties obtained by the various simplified methods, and compares them with $F = 0.98$ obtained using RFEM (corresponding to the 5-percentile system response). Aside from the over-conservative values of F computed using 5-percentile property values, ERD-QVM and Equation (3.8) by Orr (2017) when based on unreliable data, all other methods give values of F within 10% of the benchmark solution (both conservative and unconservative). In this study, Schneider (1997) equation and ERD-QVM-Γ give the best approximation, although which method is the best will be problem-dependent.

The more rigorous RFEM approach is computationally intensive; however, it by-passes the need to explicitly determine characteristic values, is completely general and can lead to economy of design, so it may be prudent to use such an approach in larger projects.

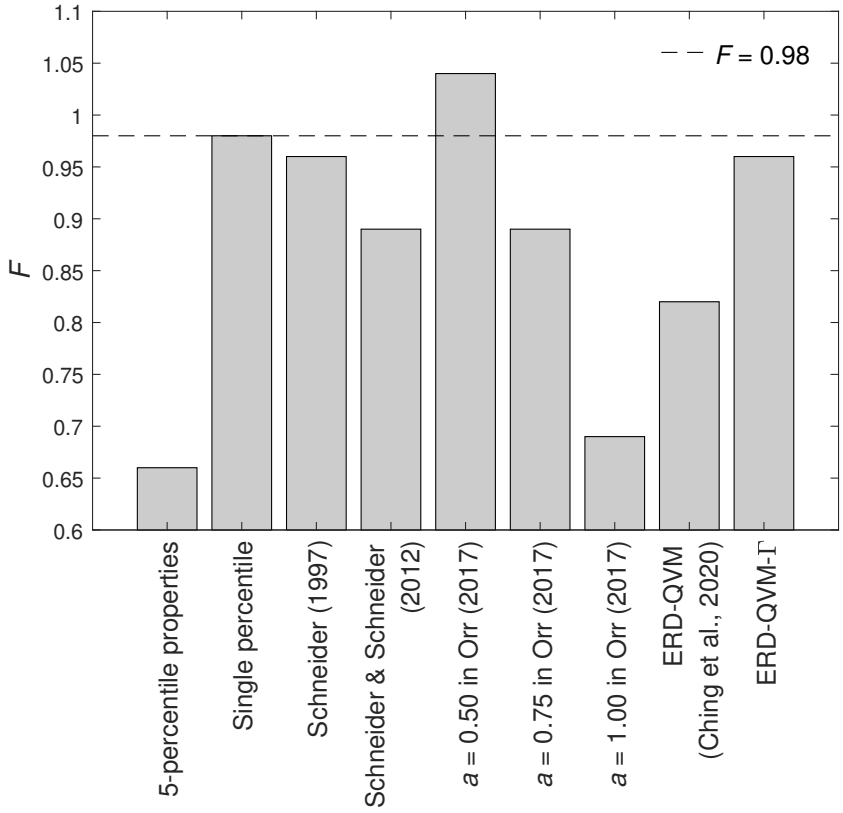

Figure 3.9: Comparison of factors of safety obtained by the various methods with $F = 0.98$ (corresponding to the 5-percentile system response based on RFEM)

3.6. CONCLUSIONS

A comparison has been made between using a deterministic assessment method and the random finite element method to assess the stability and re-design of an historic dyke in the Netherlands, based on a reliability-based framework consistent with Eurocode 7. It has been shown that a proper consideration of spatial variability, such as with the random finite element method, can lead to higher factors of safety and, for those structures requiring attention, to less costly and less intrusive mitigation measures. The advantage of the proposed approach is that it satisfies the requirements of Eurocode 7 without the need to explicitly select or calculate the characteristic property values.

Nevertheless, for the particular dyke section analysed in this chapter, characteristic soil property values consistent with Eurocode 7 were back-calculated and compared with those calculated using available simpler approaches. It was observed that the back-calculated characteristic values represented a significant increase in strength capacity over simpler interpretations of Eurocode 7 based only on the point statistics, i.e. based on 5-percentile property values. Other simpler methods, some of which account for variance reduction due to averaging of property values, mostly gave F within 10% of the benchmark solution (both conservative and unconservative). However, given the problem-dependent nature of characteristic values, as well as the desire for simpler validated approaches amenable to practice, further (case) studies are recommended for a more general insight.

REFERENCES

CEN (2004). Eurocode 7: Geotechnical design. Part 1: General rules, EN 1997-1. *European Committee for Standardisation*.

Ching, J., Phoon, K.-K., Chen, K.-F., Orr, T. L. L. & Schneider, H. R. (2020). Statistical determination of multivariate characteristic values for Eurocode 7. *Structural Safety* **82**, 101893.

de Gast, T. (2020). *Dykes and embankments: A geostatistical analysis on soft terrain*. Ph. D. thesis, Delft University of Technology, The Netherlands.

de Gast, T., Vardon, P. J. & Hicks, M. A. (2017). Estimating spatial correlations under man-made structures on soft soils. In *Proceedings of 6th International Symposium on Geotechnical Safety and Risk*, Colorado, USA, pp. 382–389.

Deltares (2018). D-Geo Stability. URL https://www.deltares.nl/en/software/d-geo-stability-2/.

Hasofer, A. M. & Lind, M. C. (1974). An exact and invariant first order reliability format. *Journal of Engineering Mechanics* **100**, 111–121.

Hicks, M. A. (2012). An explanation of characteristic values of soil properties in eurocode 7. In *In: Arnold, P., G. A. Fenton, M. A. Hicks, T. Schweckendiek, and B. Simpson (Eds.), Modern Geotechnical Design Codes of Practice: Development, Calibration and Experiences*, IOS Press, pp. 36–45.

Hicks, M. A. & Nuttall, J. D. (2012). Influence of soil heterogeneity on geotechnical performance and uncertainty: a stochastic view on ec7. In *Proceedings of 10th International Probabilistic Workshop*, Stuttgart, Germany, pp. 215–227.

Hicks, M. A., Varkey, D., van den Eijnden, A. P., de Gast, T. & Vardon, P. J. (2019). On characteristic values and the reliability-based assessment of dykes. *Georisk: Assessment and Management of Risk for Engineered Systems and Geohazards* **13**, No. 4, 313–319.

Kames, J. (2015). Veiligheidstoets boezemkaden. *Technical Report 14.0046944*, Hollands Noorderkwartier.

NEN 9997-1 (2011). Geotechnical Design of Structures - Part 1: General Rules. *The Royal Dutch Standardisation Institute*.

Orr, T. L. L. (2017). Defining and selecting characteristic values of geotechnical parameters for designs to Eurocode 7. *Georisk: Assessment and Management of Risk for Engineered Systems and Geohazards* **11**, No. 1, 103–115.

Phoon, K.-K. & Kulhawy, F. H. (1999). Characterization of geotechnical variability. *Canadian Geotechnical Journal* **36**, No. 4, 612–624.

Rackwitz, R. & Fiessler, B. (1978). Structural reliability under combined random load sequences. *Computers & Structures* **9**, No. 5, 489–494.

Schneider, H. R. (1997). Definition and characterization of soil properties. In *Proceedings of the XIV International Conference on Soil Mechanics and Geotechnical Engineering*, Hamburg, Germany, pp. 273–281.

Schneider, H. R. & Schneider, M. A. (2012). Dealing with uncertainties in EC7 with emphasis on determination of characteristic soil properties. In *In: Arnold, P., G. A. Fenton, M. A. Hicks, T. Schweckendiek, and B. Simpson (Eds.), Modern Geotechnical Design Codes of Practice: Development, Calibration and Experiences*, IOS Press, pp. 87–101.

Shen, M., Khoshnevisan, S., Tan, X., Zhang, Y. & Juang, C. H. (2019). Assessing characteristic value selection methods for design with LRFD – A design robustness perspective. *Canadian Geotechnical Journal* **56**, No. 10, 1475–1485.

van den Eijnden, A. P. & Hicks, M. A. (2017). Efficient subset simulation for evaluating the modes of improbable slope failure. *Computers and Geotechnics* **88**, 267–280.

Vanmarcke, E. H. (1977). Reliability of earth slopes. *Journal of the Geotechnical Engineering Division* **103**, No. 11, 1247–1265.

Vardon, P. J., Liu, K. & Hicks, M. A. (2016). Reduction of slope stability uncertainty based on hydraulic measurement via inverse analysis. *Georisk: Assessment and Management of Risk for Engineered Systems and Geohazards* **10**, No. 3, 223–240.

Varkey, D., Hicks, M. A., van den Eijnden, A. P. & Vardon, P. J. (2020a). On characteristic values for calculating factors of safety for dyke stability. *Géotechnique letters* **10**, No. 2, 353–359.

Varkey, D., Hicks, M. A., Vardon, P. J. & van den Eijnden, A. P. (2019). Influence of spatial variability of shear strength parameters on reliability-based assessment of dykes. In *Proceedings of the 27th European Young Geotechnical Engineers Conference*, Bodrum, Turkey, pp. 153–160.

Varkey, D., others *et al.* (2020b). Reliability-based assessment of a dyke section in the Netherlands. *Geotechniek* To be submitted.

4

UNCERTAINTIES IN GEOMETRY, MATERIAL BOUNDARY AND SHEAR STRENGTH PROPERTIES OF A 3D SLOPE

This chapter investigates the influence of three forms of uncertainty on the reliability of an idealised 3D embankment slope. These are due to 1D spatial variability in the external geometry of the slope along its length, 2D spatial variability in the depth of the boundary between the embankment material and the foundation layer, and 3D spatial variability in the shear strength properties of the slope and foundation materials. The relative influence of each uncertainty has been investigated using RFEM. The results indicate that the soil spatial variability has a much greater influence than uncertainties relating to embankment geometry and inter-layer boundaries. Moreover, it is demonstrated that the spatial correlation of material properties along the length of embankment has a greater influence on embankment reliability and failure consequences than the spatial correlation of properties perpendicular to it. A worst case scale of fluctuation for the material properties is identified.

This chapter is based on Varkey *et al.* (2020).

4.1. INTRODUCTION

Much research, especially in 2D, has been done on the influence of spatial variability of the material properties, by utilising various modelling techniques. However, only a limited amount of research (Hicks & Spencer, 2010; Huang *et al.*, 2013; Griffiths *et al.*, 2009; Hicks *et al.*, 2014; Ji & Chan, 2014; Hicks & Li, 2018) has been done on the influence of 3D spatial variability of soil properties in the reliability based-assessment of slopes, especially using 3D RFEM owing to the large computational requirements. Researchers have previously conducted 3D reliability-based assessments assuming the same value for the scale of fluctuation of the shear strength properties for all directions in the horizontal plane. However, a detailed investigation of horizontal scales of fluctuation below a Dutch regional dyke (de Gast *et al.*, 2019, 2020) revealed the scale of fluctuation along the dyke to be much longer than across the dyke.

An additional idealisation in 3D embankment analyses has been to consider the slope geometry to be deterministic, although it is observed in practice that variations in the geometry occur along the length of a dyke. However, Juang *et al.* (2019) recently looked at variations in the height of an infinite slope combined with variations in the shear strength properties, and observed that the variations in the geometry had a less significant impact on slope reliability than the latter for the problem they analysed.

In recent years, the uncertainty arising due to stratigraphic heterogeneity of materials layers, i.e. the uncertainty in determining the exact location of different layers at unsampled locations, has received increasing attention. For modelling stratigraphic uncertainty, two approaches have been widely adopted: (i) a boundary-based model (Li *et al.*, 2016a) which assumes a continuous function to define the spatial correlation in the location (i.e. depth) of the boundary separating two materials; and (ii) a category-based model (Qi *et al.*, 2016) which predicts finite and discrete material categories using a coupled-Markov chain method (Elfeki & Dekking, 2001). Xiao *et al.* (2017) compared the pros and cons of the two approaches and developed a 2D heuristic approach combining the two models. They observed that the category-based model was a better approach to model the natural weathering process and complicated anisotropic material transitions in 2D, whereas the boundary-based model was suggested to be more suitable for uniformly stratified cases. It was also observed that the boundary-based model can incorporate material spatial variability and can easily be extended to the modelling of 3D stratigraphic uncertainty (Li *et al.*, 2016b), whereas extending the category-based model to 3D stratigraphic uncertainty modelling is rather difficult (Liang *et al.*, 2014). Deng *et al.* (2017) evaluated the reliability of a slope considering 2D soil spatial variability and stratigraphic uncertainty using the category-based model. They observed that the location, layout and number of boreholes had a significant influence on the reliability of the slope. Recently, Wang *et al.* (2019) introduced a clustering-based approach to identify subsurface stratification using CPT and borehole data. Meanwhile, Zhao & Wang (2020) proposed an interpolation technique for characterising multilayer soil property profiles from sparse measurements, in conjunction with the clustering-based approach for soil stratification.

This chapter investigates the influence of three forms of geometric uncertainty on the reliability of a 3D slope. These are due to anisotropic spatial variability of the shear strength parameters, spatial variability in the geometry of the slope along its length, and spatial variability in the depth of the boundary separating the slope and foundation

materials. These uncertainties have been modelled by random fields, as they are assumed to be stationary stochastic processes which can be defined by a trend and a variation with zero mean (Rackwitz, 2000), and linked with the finite element method within a Monte-Carlo framework. Note that, here and in Chapter 5, the term "reliability" is not linked to its general definition in EC7, defined as the ability of a structure to fulfil specified requirements during its service life, but rather to a confidence level in the factor of safety.

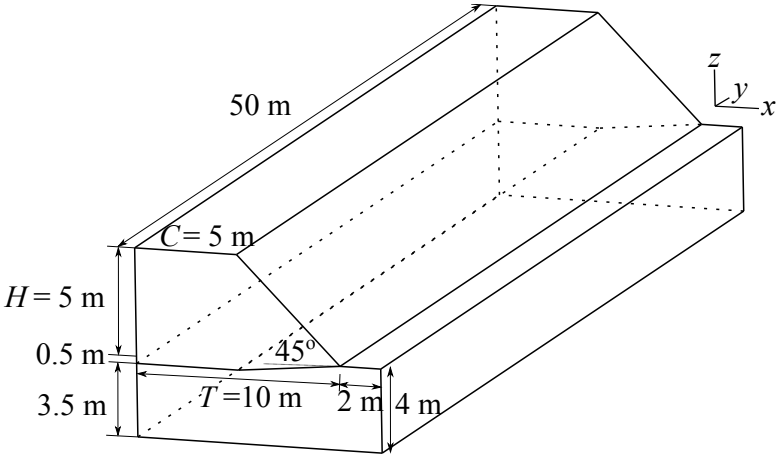

Figure 4.1: Geometry of the problem

4.2. DESCRIPTION OF THE EXAMPLE PROBLEM

Figure 4.1 shows an idealised 45° slope, 5 m high (H) and 50 m long (L), resting on a 4 m deep foundation layer, which has been used in this chapter as an example. A foundation settlement of 0.5 m has been assumed under the crest of the slope, and this reduces linearly under the sloping face of the slope to 0 m at the toe. The slope and foundation layer were meshed with a total of 8800, 20-node, regular hexahedral elements with approximate size of 0.5 m in depth and 1 m × 1 m in plan, and using a 2 × 2 × 2 Gaussian integration scheme. The mesh was fixed at the base, whereas 2D rollers on the y-z faces prevented movement in the x direction and 1D rollers on the x-z faces allowed movement only in the z direction (see Hicks & Li (2018); Spencer (2007) for an explanation of these boundary conditions). The parameters of the model are summarised in Table 4.1. A COV of 0.2 was used for the shear strength parameters (c' and ϕ') of both the slope and foundation, which is well within the typical range of values (Phoon & Kulhawy, 1999; Cherubini, 2000), and the other parameters were considered to be deterministic. A vertical scale of fluctuation of 1 m and a range of values for the horizontal scale of fluctuation of c' and ϕ' have been considered.

4.3. MODELLING STRATEGY

The spatial variability of the properties is mathematically represented using random fields, with an ensemble of random fields being used to represent the uncertainty in the spatial

Table 4.1: Soil parameter values

Parameter	Mean value	COV	θ_z	θ_x and θ_y
Cohesion (c')	10 kPa for slope and 8 kPa for foundation	0.2	1 m	1–2000 m
Friction angle (ϕ')	25° for slope and 20° for foundation	0.2	1 m	1–2000 m
Dilation angle	0°	0.0	-	-
Young's modulus	1×10^5 kPa	0.0	-	-
Poisson's ratio	0.3	0.0	-	-
Unit weight	20 kN/m^3	0.0	-	-

distribution. Each realisation (random field) is based on the same underlying statistics, but each will be different with respect to the spatial distribution of property values. In this chapter, the continuous random fields have been discretised as spatial averages using the LAS method (Fenton & Vanmarcke, 1990). Following generation and transformation to the physical space, the random field values are mapped to the finite elements at the Gauss point level and the boundary-value problem then analysed within a Monte Carlo framework using RFEM. The strength reduction method has here been used to analyse the slope and compute the factor of safety in each realisation of the Monte Carlo simulation. In this method, gravity loading is applied to generate the in-situ stresses. The resulting shear stresses are checked against the Mohr-Coulomb failure criterion and excess stresses are iteratively redistributed throughout the model. If equilibrium is achieved within 500 iterations, the shear strength parameters are reduced in a subsequent step and the whole process is repeated. The lowest strength reduction factor that triggers failure is the factor of safety of the slope for that realisation. A total of 500 Monte Carlo simulations have been carried out for each RFEM analysis presented in this chapter, which was found to be sufficient to ensure convergence of the output statistics (i.e. mean and standard deviation of F).

4.3.1. MODELLING OF GEOMETRIC UNCERTAINTY

Uncertainty in the form of different cross-sectional geometries along the slope length are considered in this chapter. Specifically, uncertainty in the various cross-sectional parameters of the slope, that is, height H, crest width C and toe width T, have been modelled as 1D random fields by LAS using the correlation function:

$$\rho(\tau_y) = \exp\left(-\frac{2\tau_y}{\theta_y}\right) \tag{4.1}$$

where τ_y is the lag distance and θ_y is the scale of fluctuation in the y direction.

Depending on the generated field values, in each realisation the nodes of the finite element mesh are moved in the x-z plane to generate different cross-sectional geometries in the slope length (y) direction. As illustrated in Figure 4.2, based on the generated field value for H at a certain location y, all nodes (of the slope, but not the foundation layer) in the x-z plane corresponding to the y-location are moved in the z direction. Similarly,

Table 4.2: Statistics of geometric and boundary parameters: (a) geometric uncertainty; (b) boundary uncertainty

(a)

Parameter	Mean (m)	COV	θ_y (m)	Resulting range of values (m)
Slope height H	5	0.03	10	4.55–5.45
Toe width T	10	0.03	10	9.1–10.9
Crest width C	5	0.03	10	4.55–5.45

(b)

Location (relative to toe)	Mean (m)	COV	θ_x (m)	θ_y (m)	Resulting range of values (m)
Under the crest (linearly decreasing to 0 m at the toe)	0.5	0.18	10	10	0.23–0.77

based on the generated field values for the crest and toe widths at each location y, all nodes in the x-z plane (in the slope and foundation layer) are translated in the x direction.

The point statistics of the normal distributions defining the uncertainties in the geometric parameters were chosen so as to give a range of possible values up to around 10 % either side of the mean (see Table 4.2a), which is on the conservative side based on fluctuations generally observed for Dutch regional dykes. The variations in crest and toe widths were correlated using the following equation:

$$\boldsymbol{\xi} = \mathbf{L}\boldsymbol{Z} \tag{4.2}$$

where $\mathbf{L}$ is the lower triangular matrix obtained by the decomposition of the correlation matrix $\mathbf{R}$ (Equation (2.20)), $\boldsymbol{\xi}$ and $\boldsymbol{Z}$ are the vectors of correlated and uncorrelated standard normal random variables. A value of 0.75 has been adopted for the cross-correlation coefficient between the crest and toe widths, whereas variations in H have been taken as uncorrelated with respect to these quantities. Note that, as a result of the variations in H, crest width and toe width, possible variations of up to +/- 5° in the slope angle have been generated, which are likely to be on the conservative side based on ground surface measurements of a regional dyke in the Netherlands de Gast (2020). Figure 4.3 illustrates the meshes generated in two realisations.

4.3.2. MODELLING OF BOUNDARY UNCERTAINTY

The uncertainty in the depth of the boundary between the slope and the underlying foundation layer has been modelled as a 2D random field by LAS using the correlation function:

$$\rho(\tau_x, \tau_y) = \exp\left(-\sqrt{\left(\frac{2\tau_x}{\theta_x}\right)^2 + \left(\frac{2\tau_y}{\theta_y}\right)^2}\right) \tag{4.3}$$

where τ_x is the lag distance and θ_x is the scale of fluctuation in the x direction.

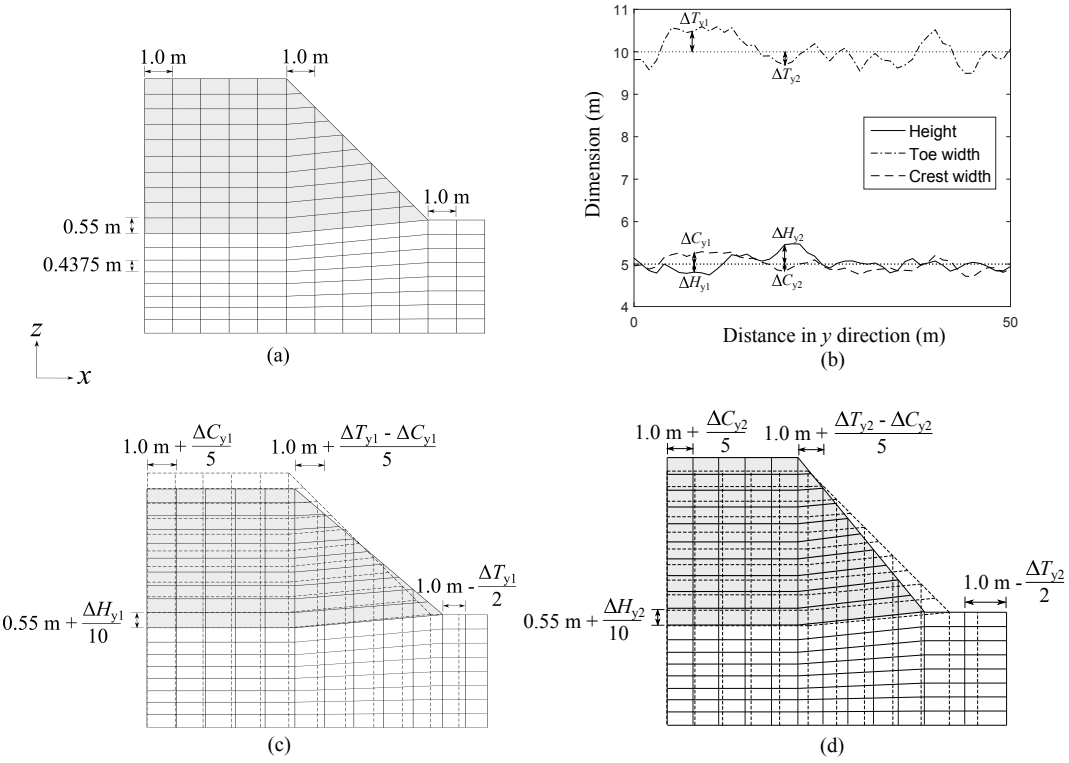

Figure 4.2: Generation of different cross-sections along the slope length: (a) original (reference) cross-section; (b) typical 1D random fields for slope height (H), toe width (T) and crest width (C) along the slope length; (c) cross-section generated at $y = y_1$ (shown by solid lines); (d) cross-section generated at $y = y_2$ (shown by solid lines)

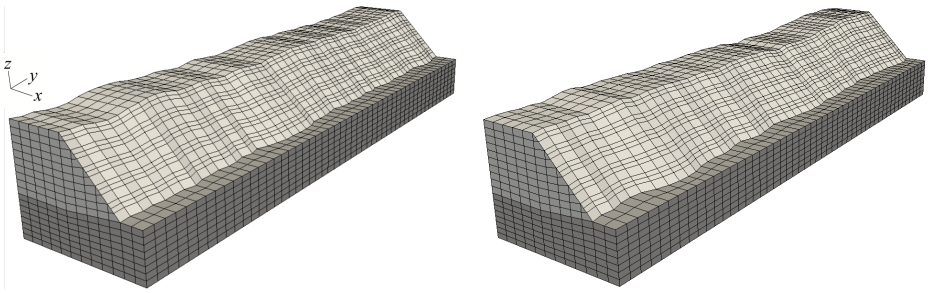

Figure 4.3: Typical mesh realisations considering geometric uncertainty

The point statistics of the normal distribution defining this uncertainty are listed in Table 4.2b. An isotropic horizontal correlation length of 10 m has been assumed for the boundary uncertainty, unless stated otherwise. Based on the field value at an x-y location corresponding to a column of nodes in the finite element mesh, the locations of

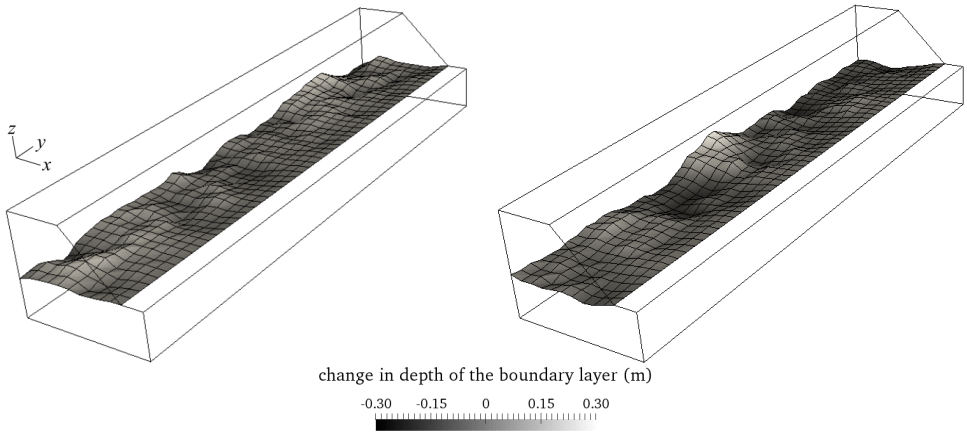

Figure 4.4: Typical realisations of material boundary depth profiles (deformations scaled-up by a factor of 5 for better visualisation)

all nodes of the finite element mesh, above and below the material boundary, are adjusted vertically. Figure 4.4 illustrates the depth profiles of the material boundary generated in two realisations. ection

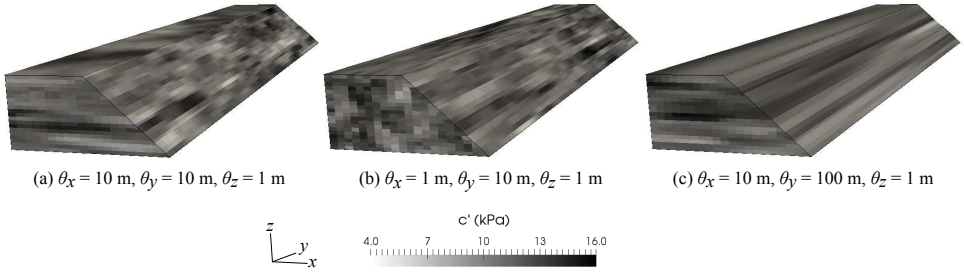

Figure 4.5: Typical realisations of c' generated from isotropic 3D random fields with $\theta = 10$ m, by: (a) squashing in the z direction, (b) squashing in the x and z directions, and (c) stretching in the y and squashing in the z directions

4.3.3. MODELLING OF ANISOTROPIC MATERIAL UNCERTAINTY

The spatial uncertainty in material properties is modelled using 3D random fields generated using the following 3D separable Gauss Markov correlation function:

$$\rho(\tau_x, \tau_y, \tau_z) = \exp\left(-\frac{2\tau_z}{\theta_z} - \sqrt{\left(\frac{2\tau_x}{\theta_x}\right)^2 + \left(\frac{2\tau_y}{\theta_y}\right)^2}\right) \tag{4.4}$$

where τ_z is the lag distance and θ_z is the scale of fluctuation in the z direction. The separation of the vertical (z) correlation structure from the two horizontal (x and y) directions was done to model the long-term depositional characteristic in the soil.

The method of random field generation follows Hicks & Spencer (2010) and Li (2017). It begins with generating standard normal fields with $\theta_x = \theta_y = \theta_z$ in Equation (4.4), followed by transformation to anisotropic random fields. This is carried out by squashing and/or stretching fields in the required directions. The generated standard normal fields are then transformed to their physical space and mapped to the Gauss points of the finite element mesh. Figure 4.5 illustrates typical random fields of c' mapped to an idealised 3D slope.

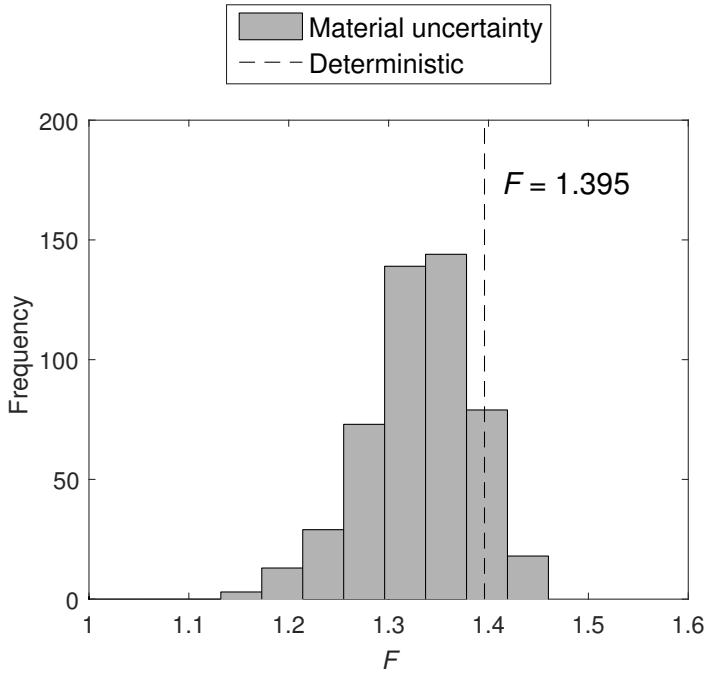

Figure 4.6: Histogram of F obtained based on material uncertainty, compared with the deterministic solution

4.4. RESULTS AND DISCUSSION

A deterministic analysis of the 3D slope using the mean parameters listed in Tables 4.1 and 4.2 resulted in a factor of safety of $F = 1.395$. Figure 4.6 shows the histogram of F obtained by analysing the slope accounting only for uncertainties in the material parameters, and using $\theta_x = \theta_y = 10\,\text{m}$ and $\theta_z = 1\,\text{m}$. As shown in the figure, the mean F from the stochastic analysis is lower than the deterministic F (shown as a dashed line), due to the greater influence of weaker zones on slope failures in a heterogeneous soil. The results obtained by analysing the slope with uncertainties in the material properties, as well as with uncertainties in the geometry and/or boundary between the slope and foundation layer, are discussed below. Normal distributions have been used for each of the uncertainties, due to the relatively low values assumed for the COVs of the various

parameters; that is, for COV < 0.33, there is negligible influence of truncating distributions to prevent negative values.

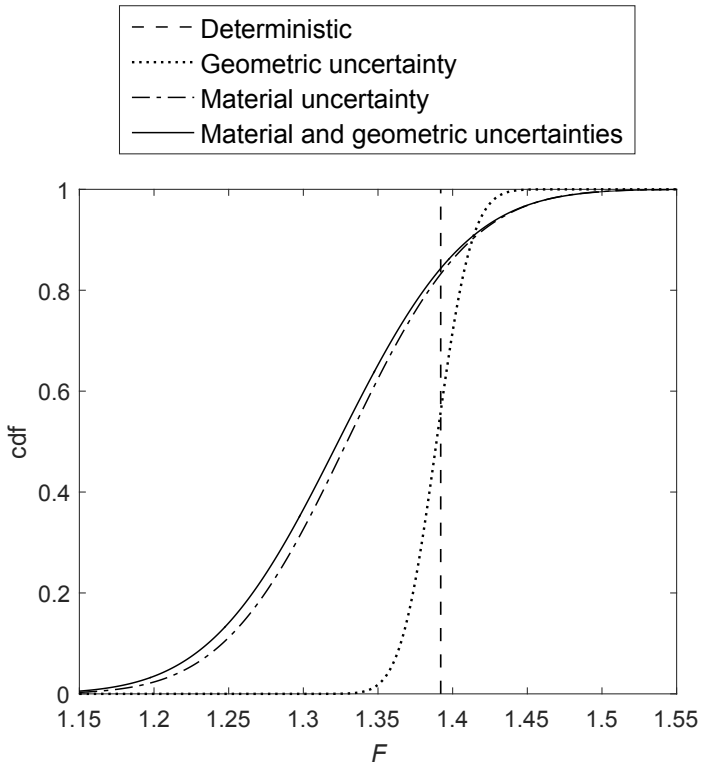

Figure 4.7: Cdfs of F obtained with geometric and material uncertainties

4.4.1. INFLUENCE OF 1D GEOMETRIC UNCERTAINTY

The cdf of F obtained by analysing the slope with uncertainty only in the external geometry, as defined by the point statistics and θ_y in Table 4.2a, is shown in Figure 4.7. Also shown in the figure are the cdfs of F obtained by considering uncertainty only in the material properties with $\theta_x = \theta_y = 10\,\text{m}$ and $\theta_z = 1\,\text{m}$, and that obtained by considering the geometric and material uncertainties together. The distribution of F obtained by considering only the geometric uncertainty is centred near the deterministic F, whereas those which include uncertainty in the material properties are shifted substantially to the left due to the presence of weaker zones attracting failure.

Figure 4.8 illustrates the relative impact of each uncertainty on the performance of the slope. Figure 4.8a compares the F obtained by considering the two uncertainties together, with the F obtained for the same realisation by considering only the geometric uncertainty. Similarly, Figure 4.8b compares the F obtained by considering the two uncertainties with

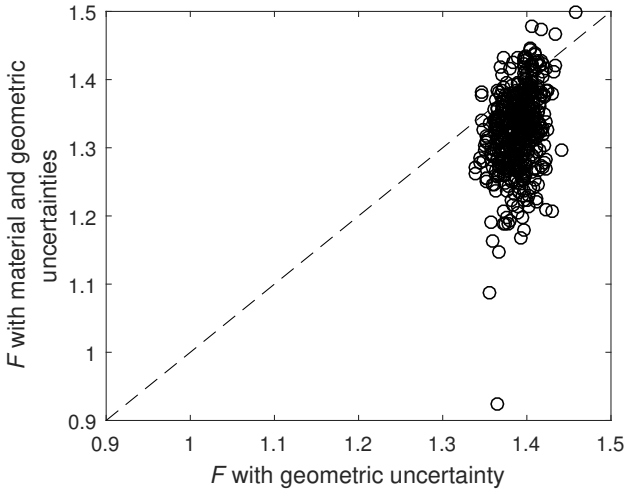

(a)

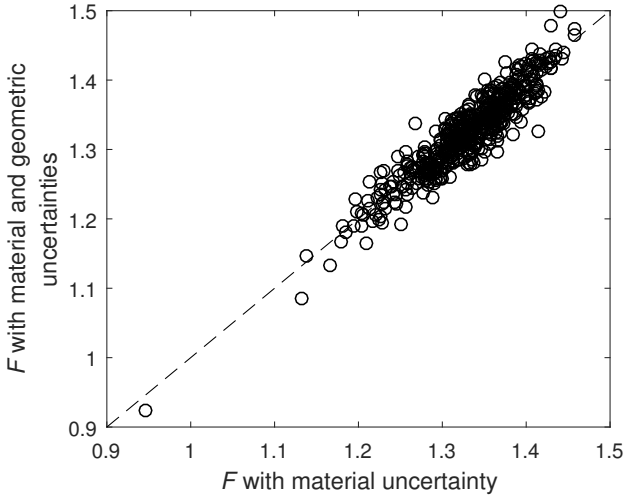

(b)

Figure 4.8: Comparing F obtained based on the material and geometric uncertainties, with F obtained in the same realisations based only on (a) geometric, and (b) material uncertainties

the F obtained in the same realisation by considering only the material uncertainty. The points are approximately aligned along the dashed 1:1 line in Figure 4.8b, whereas no definite correlation can be derived from the points in Figure 4.8a. Figures 4.7 and 4.8 clearly indicate the relatively small influence of the geometric uncertainty compared to the material uncertainty.

Thus, for the COVs of parameters considered in this chapter, which are within the

range reported in literature for material uncertainty and consistent with the maximum variations generally expected in geometry, the results indicate the larger relative influence of the spatial variability in the material properties. However, this inference may be restricted to the specific (simplified) problem considered in this chapter and therefore further research is warranted to arrive at a firm conclusion regarding the relative importance of the two uncertainties.

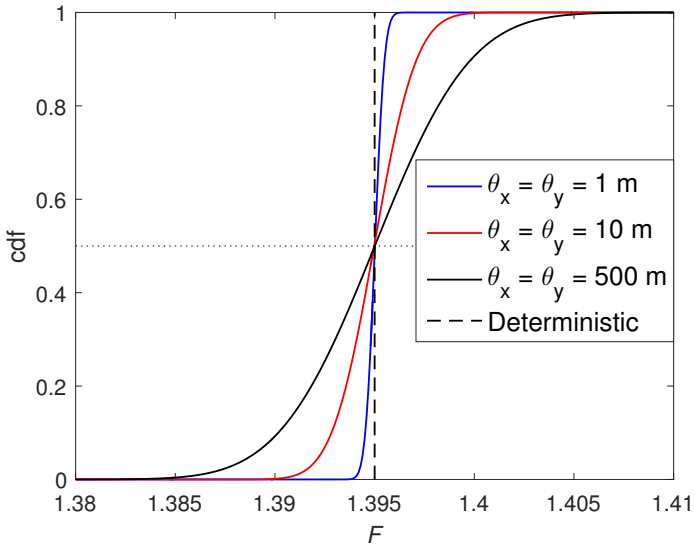

Figure 4.9: Cdfs of F obtained with various scales of fluctuation in the boundary uncertainty, compared with the deterministic solution

4.4.2. INFLUENCE OF 2D BOUNDARY UNCERTAINTY

The cdfs of F obtained by analysing the slope with uncertainty in the boundary location between the layers (i.e. between the slope material and the foundation layer) are shown in Figure 4.9. A range of values for the isotropic spatial variability ($\theta_x = \theta_y$) of the uncertainty in the boundary location have been considered in the analyses. As shown in the figure, a very small correlation length results in a narrower distribution of F compared with larger correlation lengths, although the means of the distributions are the same as the deterministic F (= 1.395). Moreover, a comparison of the range of responses in Figure 4.9 to those in Figure 4.7 indicates the very small influence of the boundary uncertainty on the slope reliability with respect to influences due to the geometric and/or material uncertainties.

To illustrate the above, Figure 4.10a compares the F obtained by considering all the three uncertainties (material, geometric and boundary) with those obtained in the same realisations considering only uncertainties in the geometric and material properties. Similarly, Figure 4.10b compares the F obtained by considering all three uncertainties together with those obtained in the same realisations with only the material uncertainty.

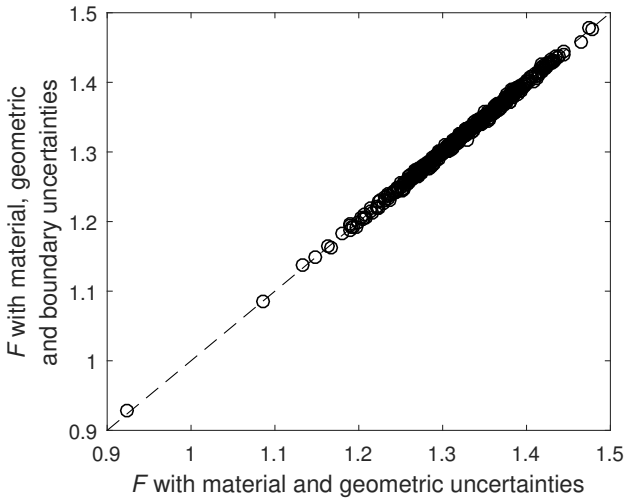

(a)

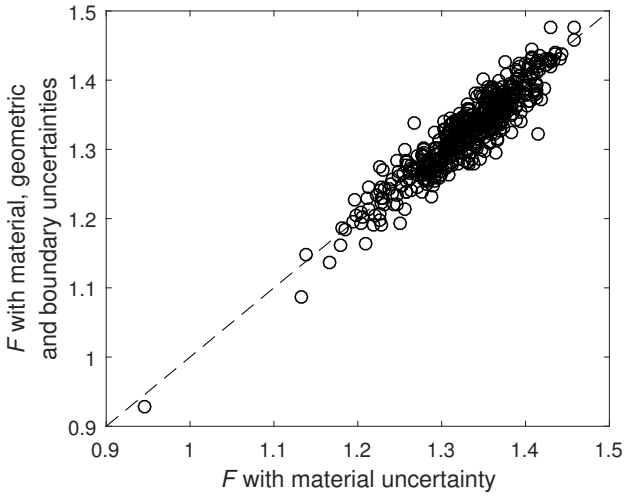

(b)

Figure 4.10: Comparing F obtained based on the material, geometric and boundary uncertainties, with F obtained in the same realisations based on (a) material and geometric uncertainties, and (b) only material uncertainty

These plots are based on the spatial statistics given in Table 4.2 for the geometric and boundary uncertainties, and on $\theta_x = \theta_y = 10\,\text{m}$ and $\theta_z = 1\,\text{m}$ for the material uncertainty. Figure 4.10 shows that the points are aligned along the 1:1 line (with those in Figure 4.10a having far less scatter). These results further demonstrate the significant influence of the material uncertainties on F, as well as the negligible influence of the boundary

uncertainty.

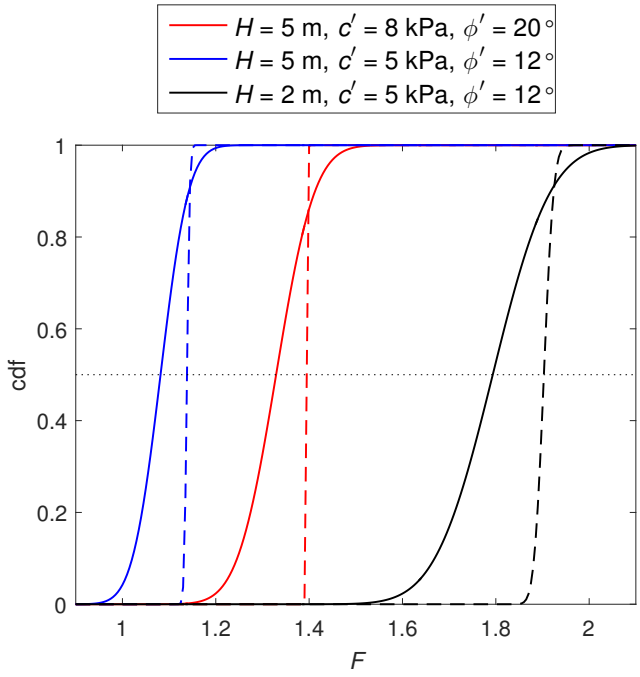

Figure 4.11: Cdfs of F obtained with various values of H and mean shear strength properties for the foundation material; solid curves are based on only material uncertainty and dashed curves are based on only boundary uncertainty

However, the above inference could be dependent on the relative shear strength properties in the two layers and on the geometry of the problem itself. Hence, further analyses were carried out with different slope geometries and with different mean c' and mean ϕ' for the foundation material. The cdfs of F obtained in the various cases are shown in Figure 4.11. It is clear that the responses of the slopes are significantly influenced by the material uncertainties, whereas the boundary uncertainty has a minor or negligible influence. For the various cases considered here, the point statistics defining the uncertainty in the slope material and the boundary between the layers are the same as in Table 4.1 and Table 4.2b, and the COV of the shear strength parameters for the foundation material is fixed at 0.20.

Note that, since the geometric and boundary uncertainties have been modelled by distorting the elements in the finite element mesh (see Sections 4.3.1 and 4.3.2), this modelling approach will also distort (to some extent) the spatial correlation structure of the material properties, as the material correlation structure is modelled relative to an undistorted mesh. Figure 4.12 shows covariances of the standard normal random fields of the material properties averaged over 500 realisations, as well as the exact covariances in the respective directions. For each realisation, the covariance (C) was calculated using

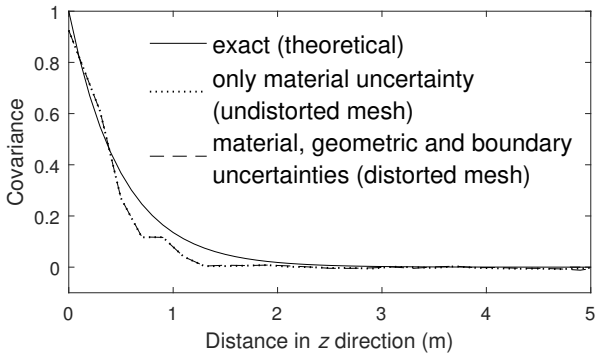

(a)

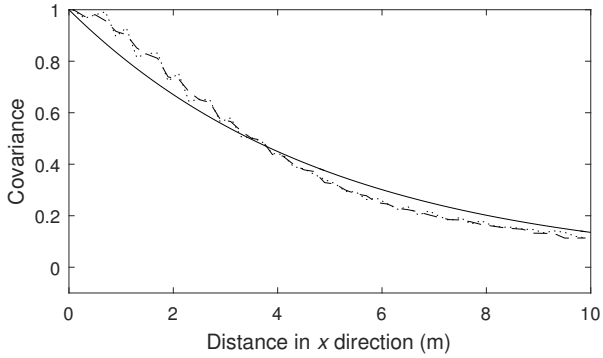

(b)

Figure 4.12: Covariances back-calculated from the standard normal 3D random fields of material properties, in (a) the vertical (z) direction (with $\theta_z = 1\,\text{m}$), and (b) the horizontal (x) direction (with $\theta_x = 10\,\text{m}$)

the following equation:

$$C_{j,k} = \frac{1}{n-j} \sum_{i=1}^{n-j} (Z_i \times Z_{i+j}) \tag{4.5}$$

where n is the number of cell values considered in the k direction, and Z_i and Z_{i+j} are the standard normal values at cell locations i and $i+j$ in the k direction. The exact covariance in each direction was calculated using Equation (4.4), by using only the associated terms in that direction. Figure 4.12 shows that the calculated covariances agree well with the expected covariances in the respective directions, illustrating that the spatial correlation structures of the material properties were preserved despite the distorted mesh.

4.4.3. INFLUENCE OF 3D ANISOTROPIC MATERIAL UNCERTAINTY

A recent detailed investigation of the horizontal scale of fluctuation derived from CPT data, for a Dutch regional dyke (de Gast *et al.*, 2019, 2020), has shown that the horizontal

scales of fluctuation may be quite different parallel to the dyke and perpendicular to it. This may be due, for example, to dykes often being located along ancient river channels, so that the correlation length along the dyke (and foundation layer) is greater than that across the dyke (i.e. $\theta_y > \theta_x$). Therefore, different scales of fluctuation in the two horizontal directions and 1 m in the vertical direction have been considered here. For this investigation, only uncertainty in the shear strength properties has been considered. Also, the slope in Figure 4.1 without the foundation layer has been analysed, in order to make a consistent comparison with the previous findings (Hicks & Spencer, 2010; Hicks & Li, 2018; Hicks *et al.*, 2014).

The mean and standard deviation of F obtained for various values of the horizontal scales of fluctuation are plotted in Figure 4.13. These results have been obtained by carrying out 500 Monte Carlo realisations for each combination of θ_x and θ_y. Figure 4.13a shows the influence of θ_y on the computed values of F (for different values of θ_x), whereas Figure 4.13b shows the influence of θ_x on F (for different values of θ_y). The dashed line in the figure shows the deterministic value of $F(= 1.417)$ obtained for the slope without a foundation layer. The results obtained for isotropic horizontal spatial variability ($\theta_x = \theta_y = \theta_h$) in each case have been highlighted as filled circles. As shown in the figure, with an increase in the value of θ_y, the range of possible solutions increases, as reflected by the higher standard deviation of F, and this increase in the range of solutions is greater than that due to a similar increase in θ_x.

Figure 4.13 shows that the responses for the mean and standard deviation of F are, in general, more influenced (with respect to the isotropic case) by a change in θ_y than a change in θ_x. Figure 4.13a shows that, for a given θ_x, there is a worst case θ_y with respect to the mean F, which for this example seems to range between approximately 10 m ($= 2H$) and 20 m ($= 4H$). However, over the whole range of θ_x considered, the worst case θ_y is around 16 m. Conversely, Figure 4.13b shows that, for a given θ_y, the most conservative approach is to assume a large θ_x, there not being an intermediate value of θ_x constituting a worst case. Overall, Figure 4.13 demonstrates that θ_y is the most influential scale of fluctuation and that, for $\theta_y > H$, it is sufficient (and generally conservative) to take $\theta_x = \theta_y$.

For very large and very small values of θ_y with respect to L, continuous long failures were observed in many realisations. For intermediate values of θ_y, smaller discrete failures were generally observed and sometimes multiple discrete failures, although these occurred in relatively few realisations. This is because of the relatively short length of slope, compared to that analysed in Hicks & Li (2018), making it difficult for multiple failure mechanisms to fully develop without interaction from the mesh ends. In order to give a general impression of trends, the failure lengths in each realisation have here been calculated as the number of continuously linked elements along the slope toe having an average out-of-face displacement greater than a certain threshold value (Hicks & Li, 2018). This threshold value was calibrated using the procedure described in Hicks *et al.* (2014) and, for the slope analysed here, it was calibrated as 37 % of the maximum out-face-displacement in that realisation. Although the failure lengths computed using this threshold-crossing method are only approximate, they are a good indication of trends.

The mean failure lengths obtained over all realisations for various values of θ_x and θ_y are plotted in Figure 4.14. The mean failure lengths for the isotropic horizontal spatial

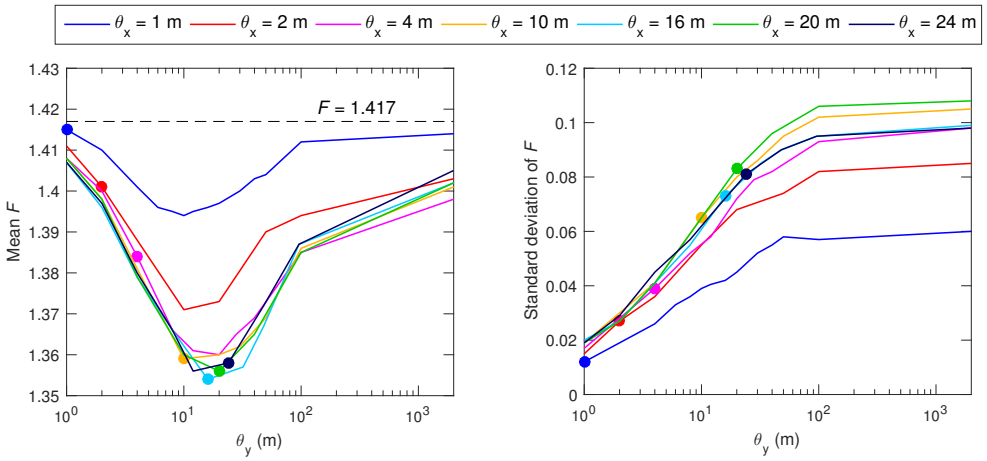

(a)

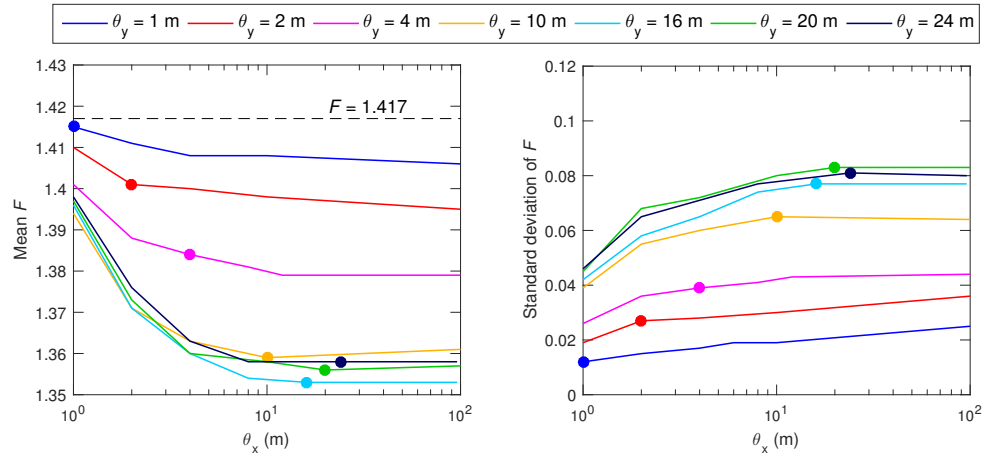

(b)

Figure 4.13: Mean and standard deviation of F as a function of θ_x and θ_y: (a) for fixed θ_x; and (b) for fixed θ_y. Dashed line is the deterministic value and the filled circles are for isotropic horizontal spatial variability.

variability in each case have also been highlighted as filled circles in the figure, and are in good agreement with the relationship for the mean discrete failure length (= $2H + \theta_h/2$) proposed in Chapter 5 (based on Hicks & Li (2018) for intermediate values of θ_h). Figure 4.14 shows that, as for the mean and standard deviation of F in Figure 4.13, the mean failure lengths are more influenced by a change in θ_y than a change in θ_x.

Based on the results in Figures 4.13 and 4.14, the responses obtained with anisotropic horizontal spatial variability, may be significantly different compared to those based

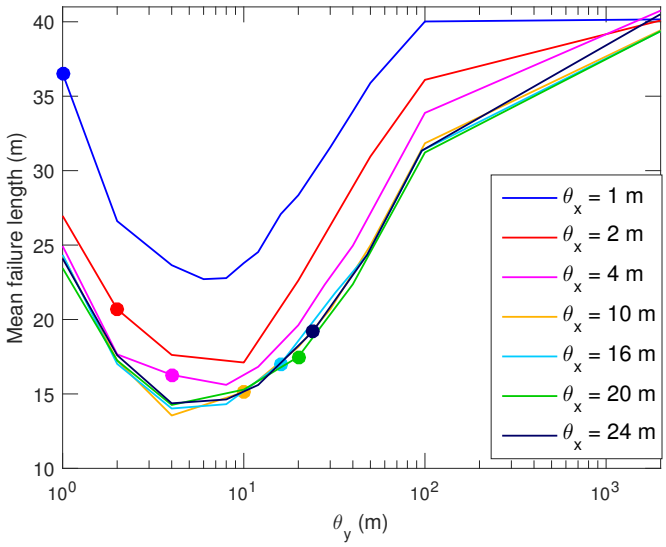

(a)

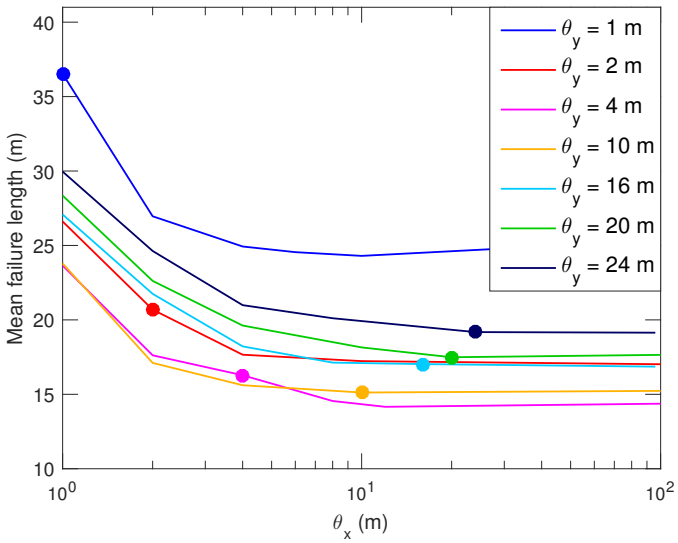

(b)

Figure 4.14: Mean failure lengths as a function of θ_x and θ_y: (a) for fixed θ_x; and (b) for fixed θ_y. Filled circles are for isotropic horizontal spatial variability.

on isotropic horizontal spatial variability. However, the results suggest that it would be reasonable (and conservative) to assume isotropic spatial variability in the horizontal

plane based on the value of θ_y, and that, in the absence of detailed knowledge of the site, to assume a worst case value of θ_y. In this investigation, the worst case value of θ_y was found to be around $3H \pm H$.

4.5. CONCLUSIONS

RFEM has been used to study the influence of three forms of uncertainty on the reliability of an idealised 3D embankment slope: these were due to 1D spatial variability in the external geometry of the slope along its length, 2D spatial variability in the depth of the boundary between the embankment material and the foundation layer, and 3D spatial variability in the shear strength properties of the slope and foundation materials.

It was observed that the uncertainties relating to the external geometry and inter-layer boundaries had little to negligible influence on slope reliability compared to spatial variability in the shear strength properties of the slope and foundation materials. Moreover, it was demonstrated that anisotropy of soil spatial variability in the horizontal plane can have a significant influence on embankment reliability and failure consequences, with the spatial correlation of material properties along the embankment length (θ_y) having a much greater influence than the spatial correlation structure of properties perpendicular to its length (θ_x).

The results indicated that assuming an isotropic spatial variability in the horizontal plane could give conservative or unconservative solutions. However, a conservative solution is generally obtained by assuming isotropic variability based only on the scale of fluctuation along the embankment. For those cases in which an accurate knowledge of θ_y is not available, a worst case value of $\theta_y \approx 3H \pm H$ was found for the embankment analysed. However, further research is recommended to give more insight into the likely range of worst values for θ_y.

REFERENCES

Cherubini, C. (2000). Reliability evaluation of shallow foundation bearing capacity on *c'*, *ϕ'* soils. *Canadian Geotechnical Journal* **37**, No. 1, 264–269.

de Gast, T. (2020). *Dykes and embankments: A geostatistical analysis on soft terrain*. Ph. D. thesis, Delft University of Technology, The Netherlands.

de Gast, T., Vardon, P. J. & Hicks, M. A. (2019). Observations and considerations regarding estimating horizontal scales of fluctuation around linear infrastructure. In *Proceedings of 7th International Symposium on Geotechnical Safety and Risk*, Taipei, Taiwan, pp. 340–345.

de Gast, T., Vardon, P. J. & Hicks, M. A. (2020). Assessment of soil spatial variability for linear infrastructure using cone penetration tests. *Géotechnique* Under review.

Deng, Z.-P., Li, D.-Q., Qi, X.-H., Cao, Z.-J. & Phoon, K.-K. (2017). Reliability evaluation of slope considering geological uncertainty and inherent variability of soil parameters. *Computers and Geotechnics* **92**, 121–131.

Elfeki, A. & Dekking, M. (2001). A Markov Chain Model for subsurface characterization: theory and applications. *Mathematical Geology* **33**, No. 5, 569–589.

Fenton, G. A. & Vanmarcke, E. H. (1990). Simulation of random fields via Local Average Subdivision. *Journal of Engineering Mechanics* **116**, No. 8, 1733–1749.

Griffiths, D. V., Huang, J. & Fenton, G. A. (2009). On the reliability of earth slopes in three dimensions. In *Proceedings of the Royal Society of London: A Mathematical, Physical and Engineering Sciences*, pp. 3145–3164.

Hicks, M. A. & Li, Y. (2018). Influence of length effect on embankment slope reliability in 3D. *International Journal for Numerical and Analytical Methods in Geomechanics* **42**, No. 7, 891–915.

Hicks, M. A., Nuttall, J. D. & Chen, J. (2014). Influence of heterogeneity on 3D slope reliability and failure consequence. *Computers and Geotechnics* **61**, 198–208.

Hicks, M. A. & Spencer, W. A. (2010). Influence of heterogeneity on the reliability and failure of a long 3D slope. *Computers and Geotechnics* **37**, No. 7-8, 948–955.

Huang, J., Lyamin, A. V., Griffiths, D. V., Krabbenhoft, K. & Sloan, S. W. (2013). Quantitative risk assessment of landslide by limit analysis and random fields. *Computers and Geotechnics* **53**, 60–67.

Ji, J. & Chan, C. L. (2014). Long embankment failure accounting for longitudinal spatial variation – A probabilistic study. *Computers and Geotechnics* **61**, 50–56.

Juang, C. H., Zhang, J., Shen, M. & Hu, J. (2019). Probabilistic methods for unified treatment of geotechnical and geological uncertainties in a geotechnical analysis. *Engineering Geology* **249**, 148–161.

Li, X. Y., Zhang, L. M. & Li, J. H. (2016a). Using conditioned random field to characterize the variability of geologic profiles. *Journal of Geotechnical and Geoenvironmental Engineering* **142**, No. 4, 04015096.

Li, Y. (2017). *Reliability of long heterogeneous slopes in 3D*. Ph.D. thesis, Delft University of Technology, The Netherlands.

Li, Z., Wang, X., Wang, H. & Liang, R. Y. (2016b). Quantifying stratigraphic uncertainties by stochastic simulation techniques based on Markov random field. *Engineering Geology* **201**, 106–122.

Liang, Y.-R., Wang, Z.-Z. & Guo, J.-H. (2014). Reservoir lithology stochastic simulation based on Markov random fields. *Journal of Central South University* **21**, No. 9, 3610–3616.

Phoon, K.-K. & Kulhawy, F. H. (1999). Characterization of geotechnical variability. *Canadian Geotechnical Journal* **36**, No. 4, 612–624.

Qi, X. H., Li, D.-Q., Phoon, K.-K., Ciao, Z.-J. & Tang, X. S. (2016). Simulation of geologic uncertainty using coupled Markov chain. *Engineering Geology* **207**, 129–140.

Rackwitz, R. (2000). Reviewing probabilistic soils modelling. *Computers and Geotechnics* **26**, No. 3, 199–223.

Spencer, W. A. (2007). *Parallel stochastic and finite element modelling of clay slope stability in 3D*. Ph. D. thesis, University of Manchester, UK.

Varkey, D., Hicks, M. A. & Vardon, P. J. (2020). Uncertainties in geometry, material boundary and shear strength properties of a 3D slope To be submitted.

Wang, X., Wang, H., Liang, R. Y. & Liu, Y. (2019). A semi-supervised clustering-based approach for stratification identification using borehole and cone penetration test data. *Engineering Geology* **248**, 102–116.

Xiao, T., Zhang, L.-M., Li, X.-Y. & Li, D.-Q. (2017). Probabilistic stratification modeling in geotechnical site characterization. *ASCE-ASME Journal of Risk and Uncertainty in Engineering Systems, Part A: Civil Engineering* **3**, No. 4, 04017019.

Zhao, T. & Wang, Y. (2020). Interpolation and stratification of multilayer soil property profile from sparse measurements using machine learning methods. *Engineering Geology* **265**, 105430.

5

AN IMPROVED SEMI-ANALYTICAL METHOD FOR 3D RELIABILITY ASSESSMENTS OF SLOPES IN SPATIALLY VARIABLE SOIL

An improved semi-analytical method for calculating the reliability of 3D slopes with spatially varying shear strength parameters is proposed. The response of an existing semi-analytical method has been compared with that of the computationally more intensive, but more general, RFEM demonstrating that the simpler method underestimates the failure probability. An alternative relationship for the expected failure length and two correction factors are proposed, which modify the original formulation of the simpler method. The proposed approach gives substantially improved results that compare favourably with those obtained by RFEM, and therefore provides a more accurate simplified solution.

This chapter is based on Varkey *et al.* (2017, 2019a,b).

5.1. INTRODUCTION

Much research has been done in 2D slope reliability analysis to understand the influence of various levels of anisotropy of the heterogeneity in the mechanical and hydraulic parameters (Arnold & Hicks, 2011), and in making use of inverse analysis techniques to reduce the uncertainty in hydraulic conductivity by using pore pressure measurements (Vardon *et al.*, 2016). These studies are based on the simplifying assumption that the mechanical and hydraulic parameters are correlated over an infinite distance in the third dimension. However, this is not the case, which indicates a need for 3D reliability analysis. So far, only a limited amount of research has been done in 3D, due (at least in part) to the large computational requirements. This is especially true for RFEM, which does not make any prior assumptions regarding the location and shape of the failure mechanism, and hence requires large computational time and memory to carry out multiple finite element analyses. Spencer & Hicks (2007) and Hicks & Spencer (2010) used 3D RFEM to investigate the influences of anisotropy of the heterogeneity in the undrained shear strength and slope length in the third dimension on the estimation of the failure probability. They also grouped the failure modes into three categories, which were based on the horizontal scale of fluctuation of the shear strength relative to the slope dimensions. Meanwhile, Hicks *et al.* (2008, 2014) and Huang *et al.* (2013) developed strategies to quantify the failure consequences in terms of slide volume by using a threshold crossing technique linked to the out-of-face displacements and the K-means clustering method, respectively.

Vanmarcke (1977, 1980) pioneered 3D reliability assessments of slopes by making certain (important) simplifying assumptions, and thereby developed a simplified method which gives a quick and convenient solution. Li *et al.* (2015) and Varkey *et al.* (2017) compared the performance of this method with that of RFEM for reliability predictions of an idealised 3D slope, for cohesive and c–ϕ soils, respectively, and have highlighted those instances in which the two methods give similar results, as well as those in which there are significant differences. Moreover, Hicks & Li (2018) investigated slope length dependency for cohesive soils by comparing 3D RFEM with the Vanmarcke (1977) method and the "2.5 D" method of Calle (1985).

This chapter further investigates the differences in 3D solutions obtained by RFEM and Vanmarcke's method for a slope with a fixed length in the third dimension and, having established the differences to be due to simplifying assumptions in Vanmarcke's method, proposes an approach to improve its performance.

5.2. RANDOM FINITE ELEMENT METHOD

In this chapter, independent (i.e. uncorrelated) random fields for both shear strength variables have been generated using local average subdivision (LAS) Fenton & Vanmarcke (1990), which requires only the mean (μ), standard deviation (σ) and scales of fluctuation (i.e. spatial correlation distances) in the three dimensions ($\theta_x, \theta_y, \theta_z$), where θ_z is the vertical scale of fluctuation (θ_v) and $\theta_x = \theta_y$ are the horizontal scales of fluctuation (θ_h). The random fields are here generated using the Markov covariance function:

$$\beta_M(\tau_x, \tau_y, \tau_z) = \sigma^2 \exp\left(-\frac{2\tau_z}{\theta_z} - \sqrt{\left(\frac{2\tau_x}{\theta_x}\right)^2 + \left(\frac{2\tau_y}{\theta_y}\right)^2} \right) \tag{5.1}$$

where τ_x, τ_y and τ_z are the lag distances in the respective directions. A random field is initially generated using $\theta = \theta_x = \theta_y = \theta_z$ in Equation (5.1), and this field is then post-processed by squashing and/or stretching in the respective directions to generate the required level of anisotropy; see Hicks & Samy (2002, 2004) and Hicks & Spencer (2010) for details.

Following the random field generation, the field values are mapped to the Gauss points of a finite element mesh, and the boundary value problem is analysed by finite elements. In this chapter, the strength reduction method is used to determine the factor of safety of the slope in each realisation, and multiple realisations are performed to generate a distribution of safety factors.

Hicks & Spencer (2010) conducted similar 3D RFEM analyses for a cohesive slope with θ_v equal to one fifth of the slope height, and proposed three categories of failure mode, for different values of θ_h with respect to the slope height (H) and slope length (L):

(i) Mode 1 ($\theta_h < H$): Failure propagates through weak and strong zones alike, resulting in considerable averaging of property values along the entire slope length. This is similar to a 2D analysis based on the mean property values.

(ii) Mode 2 ($H < \theta_h < L/2$): Failure propagates through semi-continuous weaker zones, resulting in discrete 3D failures and a wide range of possible solutions.

(iii) Mode 3 ($\theta_h > L/2$): Failure propagates through weak zones and there is a wider range of possible solutions. The failure impacts the entire slope length, and the solution is analogous to that for a 2D stochastic analysis.

Hicks *et al.* (2014) investigated the modes of failure in more detail, by automatically computing failure geometries in 3D RFEM. It was thereby shown that the Mode 2 category of failure is widespread, and may also occur for the relatively small and large values of θ_h normally associated with failure mode categories Mode 1 and Mode 3.

5.3. VANMARCKE'S METHOD

Vanmarcke (1977) considered 3D slope reliability by extending a circular slip circle to a cylindrical failure surface with resisting end-sections within a probabilistic framework. The load (due to self weight) and cross-sectional characteristics were assumed to be constant along the slope axis. Hence, only the uncertainty due to the natural variability of the soil strength mobilised along the failure surface was considered. Vanmarcke (1977) first considered the spatial variability in undrained shear strength, and later considered a slope with spatial variability in drained soil shear strength along with several other extensions (Vanmarcke, 1980).

The general method predicts the failure length b, along the embankment axis, which maximises the probability of failure occurring when centred at a specific location (see Figure 5.1). Using the classical circular-arc stability approach, the factor of safety of the slope is given by

$$F_b = \frac{(s_b L_a b) r_b + R_e}{(W b) a_W} \tag{5.2}$$

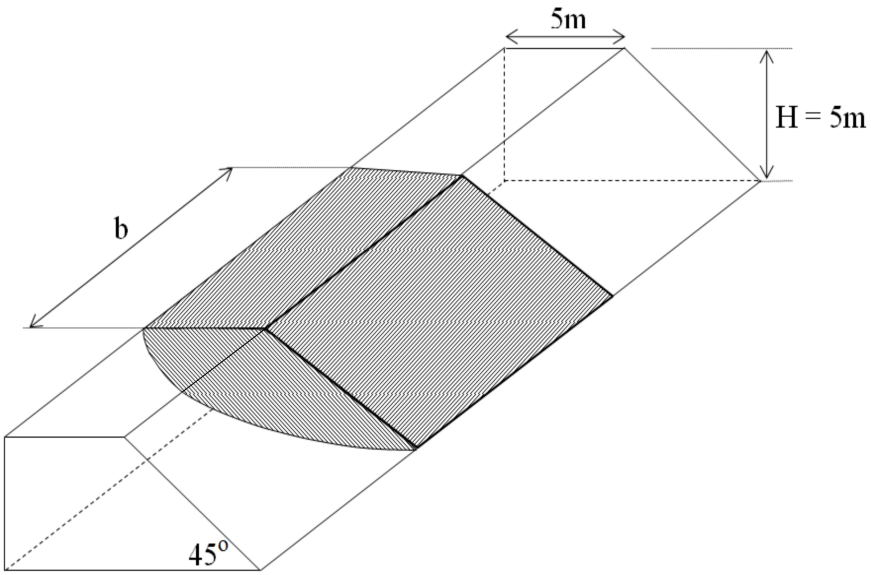

Figure 5.1: Failure mass within a 3D slope (based on Vanmarcke (1977))

$$R_e = (2 s_e A) r' \tag{5.3}$$

where s_b is the averaged shear strength along the failure surface of length b, L_a is the length of the cross-sectional failure arc, r_b is the lever arm of the resisting moment about the centre of rotation, R_e is the resisting moment of the end-sections defined by Equation (5.3), W is the weight per unit length of the sliding mass, a_W is the lever arm of the centre of gravity of the sliding mass about the same centre of rotation, s_e is the shear strength over the two end-sections, A is the area of each end-section and r' is the effective rotation arm for the end sections.

For a spatially variable shear strength, and by assuming a deterministic overturning moment and neglecting any variance in the end-resistance, the mean and standard deviation (denoted by a 'bar' and 'tilde', respectively, above the random variable) of the factor of safety are given by

$$\overline{F_b} = \frac{(\overline{s_b} L_a b) r_b + (2 \overline{s_e} A) r'}{(W b) a_W} \tag{5.4}$$

$$\widetilde{F_b} = \frac{(\widetilde{s_b} L_a b) r_b}{(W b) a_W} \tag{5.5}$$

For a stationary random field of the shear strength parameters, the averaged shear strength on the end-sections ($\overline{s_e}$) and the averaged shear strength along the failure surface ($\overline{s_b}$) are assumed to be equal to the mean of all point shear strength values ($\overline{s}$) throughout the slope Vanmarcke (1977). Following Vanmarcke (1977) and assuming $r' = r_b$, Equation (5.4) simplifies to

$$\overline{F_b} = \frac{(\overline{s} L_a) r_b}{W a_W} \left[1 + \frac{d}{b}\right] \tag{5.6}$$

and thereby to

$$\overline{F_b} = \overline{F_2} \left[1 + \frac{d}{b}\right] \tag{5.7}$$

where $\overline{F_2}$ is the 2D factor of safety based on the mean values of the soil parameters, which can be calculated via any appropriate method, and d is the effective width of the end-sections given by

$$d = 2A/L_a \tag{5.8}$$

The random shear strength at any point, as well as the mean and variance of all point shear strength values, are respectively given by (Vanmarcke, 1980)

$$s = c + \sigma_n \tan(\phi) \tag{5.9}$$

$$\overline{s} = \overline{c} + \overline{\sigma_n} \tan(\overline{\phi}) \tag{5.10}$$

$$\widetilde{s}^2 = \widetilde{c}^2 + \overline{\sigma_n}^2 (\tan(\widetilde{\phi}))^2 \tag{5.11}$$

where c is the cohesion, ϕ is the friction angle and σ_n is the stress normal to the failure surface.

Assuming that the failure surface is known, the averaged value of shear strength over the failure length (s_b) is calculated as the average of spatial averages of strength over the failure surface for embankment segments of unit length (s_1) perpendicular to the cross-section. The greater the length of the failure arc for an embankment segment of unit width, over which the point shear strength values are averaged, the more the fluctuations in shear strength cancel each other out, resulting in a reduction in the standard deviation. Moreover, the greater the length of the cylindrical surface along the embankment axis, over which s_1 is averaged, the more the fluctuations in s_1 cancel each other out, resulting in a further reduction in the standard deviation. Hence, Equation (5.5) may be expressed as

$$\begin{aligned} \widetilde{F_b} &= \frac{\Gamma(L_a)\Gamma(b)(\widetilde{s} L_a b) r_b}{(W b) a_W} \\ \widetilde{F_b} &= \Gamma(L_a)\Gamma(b) V_s \overline{F_2} \end{aligned} \tag{5.12}$$

where V_s is the coefficient of variation of the point shear strength ($= \widetilde{s}/\overline{s}$), and $\Gamma(L_a)$ and $\Gamma(b)$ are the reduction factors relating to the standard deviation along the failure arc and failure length, respectively. $\Gamma(b)$ is given by

$$\begin{aligned} &\Gamma(b) = \sqrt{(\theta_{\mathrm{h}}/b)}; \quad && \theta_{\mathrm{h}} < b \\ &\Gamma(b) = 1; && \theta_{\mathrm{h}} \geqslant b \end{aligned} \tag{5.13}$$

and $\Gamma(L_a)$ is obtained by replacing b with L_a and θ_h with the equivalent scale of fluctuation (based on both θ_h and θ_v) along the failure arc (for details, see Vanmarcke (1977)).

Both $\overline{F_b}$ and $\widetilde{F_b}$ are dependent on the failure length (b). When the probability of failure is considered for a length centred at a specific location, there is a critical length (b_c) which maximises the probability of failure occurring at that location. Vanmarcke (1977) proposed the following equation for the expected failure length:

$$\begin{aligned} b = b_c = \frac{\overline{F_2}}{\overline{F_2} - 1} d; \quad & b_c > \theta_h \\ b = \theta_h; \quad & b_c \leqslant \theta_h \end{aligned} \tag{5.14}$$

5.4. COMPARISON OF VANMARCKE AND RFEM SOLUTIONS

A 50 m long slope, with the geometry shown in Figure 5.1, has been analysed by Vanmarcke's method and RFEM. The finite element model was meshed by 4000, 20-node hexahedral elements, which were 0.5 m deep and 1 m × 1 m in plan (except along the slope face), and used 2 × 2 × 2 Gaussian integration. The mesh was fixed at the base, with rollers on the back face preventing movement perpendicular to the face, and rollers on the two end-faces allowing movement only in the vertical direction. The end-faces were fixed against horizontal movements because Spencer (2007) found that allowing horizontal movement on the end-faces appeared to result in a bias of failures congregating towards the ends of the slope; this was thought to be due to the implied symmetry of the random field about the mesh end boundaries. A further investigation and explanation of the boundary conditions is given in Hicks & Li (2018).

In each realisation of the RFEM analysis, an independent random field was generated for each shear strength parameter. The parameter values were then assigned to the finite element mesh at the Gauss point level, and the finite element analysis carried out using the strength reduction method. Gravity loading was applied to the model to generate the in situ stresses, and the resulting shear stresses at the integration points were checked against the Mohr–Coulomb failure criterion. If the stresses exceeded the failure criterion, the excess stresses were iteratively redistributed throughout the model. If equilibrium could not be achieved within 500 iterations the analysis was deemed to have reached failure; otherwise, the shear strength parameters were reduced in the subsequent step and the whole process repeated until failure occurred. The lowest factor by which the shear strength parameters needed to be reduced to induce failure was taken to be the safety factor for that realisation.

The soil parameter values are listed in Table 5.1, and a normal distribution was considered appropriate for both c and ϕ. Note that the coefficients of variation (= SD/mean) of cohesion and friction angle were set at 0.2, which is well within the typical range reported in Cherubini (2000) and small enough to avoid the possibility of negative values with the normal distribution. The vertical scale of fluctuation was taken to be 1 m for all analyses (see de Gast *et al.* (2017, 2020) for typical values), whereas a wide range of θ_h was considered.

Based on the mean values of the shear strength parameters listed in Table 5.1, the plane strain factor of safety was found to be 1.4, with failure involving an $A = 12\,m^2$ block

Table 5.1: Table of parameter values

Parameter	Mean	SD	θ_v	θ_h
Cohesion, c	10 kPa	2 kPa	1 m	1–10^4 m
Friction angle, ϕ	25°	5°	1 m	1–10^4 m
Dilation angle, ψ	0°	-	-	-
Young's modulus, E	1×10^5 kPa	-	-	-
Poisson's ratio, ν	0.3	-	-	-
Unit weight, γ	20 kN/m^3	-	-	-

of soil (per unit length) sliding along an approximately circular arc of length $L_a = 9.3$ m, giving a value of d of 2.58 m. The failure geometry was determined using finite elements and the ridge finding procedure described in Hicks *et al.* (2014). These derived parameters were used to compute Vanmarcke's solution (Equations (5.7) and (5.12)) for the same problem. Meanwhile, a total of 500 Monte Carlo realisations were carried out to make predictions using RFEM.

Figure 5.2 compares the mean and standard deviation of the 3D factor of safety (F) by the two methods, for different values of θ_h. The mean and standard deviation of F_b (i.e., in Vanmarcke's solution) are largely dependent on the predicted failure length b, as seen in Equations (5.7) and (5.12).

Figure 5.3 compares the mean failure length obtained by the two methods (see Varkey *et al.* (2017) for comparison of slide volumes). For each RFEM realisation, the integrated failure length was calculated from the total number of elements in the row directly above the slope toe in which out-of-face displacement was greater than a calibrated threshold value (representing failure), and follows the procedure described in detail in Hicks *et al.* (2014). Also for each realisation, the discrete failure lengths were calculated from the number of continuously linked elements in the row directly above the slope toe in which out-of-face displacements were greater than the same threshold value (as described in Hicks & Li (2018)). For this investigation, the threshold displacement was calibrated to be 37 % of the maximum computed out-of-face displacement. The mean integrated failure length and the mean discrete failure length in the RFEM analyses were obtained by averaging over all the realisations for each θ_h. Note that although the integrated and discrete failure lengths are approximately equal at very small and very large θ_h, at intermediate values of θ_h the two differ, due mostly to the increased probability of multiple failures of shorter length relative to the slope length. Since the integrated failure length is more closely related to the slope length, discrete failure lengths are considered in the remaining part of this chapter as a more independent measure of the failure length. Overall, Figure 5.3 shows that the RFEM solutions are consistent with the 3 categories of failure mode identified previously by Hicks & Spencer (2010); i.e., an overriding disposition to shorter discrete 3D failures (Mode 2), but with an increased likelihood of long failures (Modes 1 and 3) at very small and very large θ_h. In contrast, the Vanmarcke solution predicts a small failure length for very small θ_h. For larger θ_h, the predicted failure length by Vanmarcke's method is equal to θ_h (Equation (5.14)), but is here limited to a maximum of 50 m due to the finite length of the slope in this study.

The large difference between the mean F of the two solutions at small θ_h is mainly

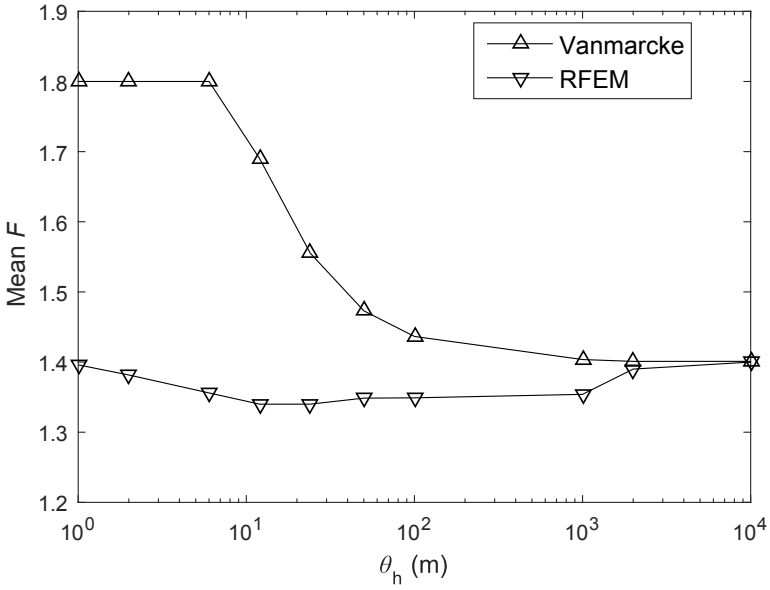

(a)

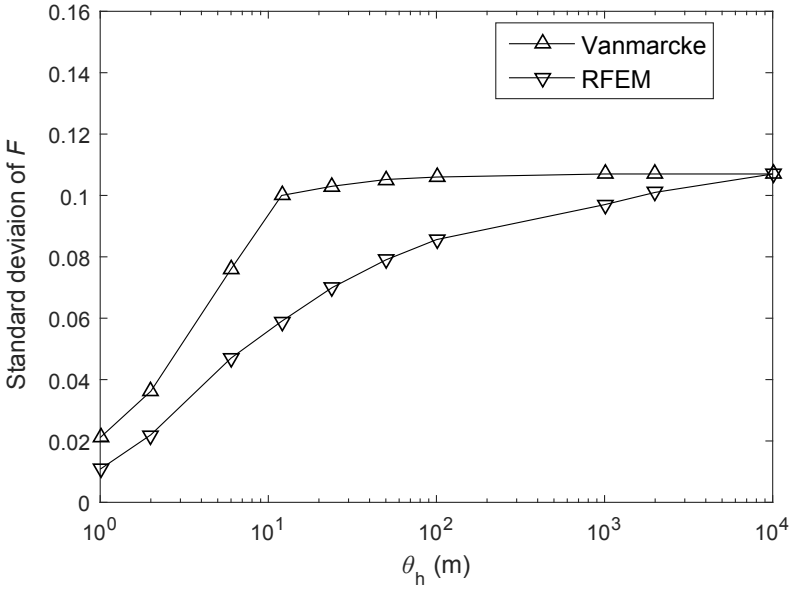

(b)

Figure 5.2: Comparison of (a) mean and (b) standard deviation of factor of safety by the two methods

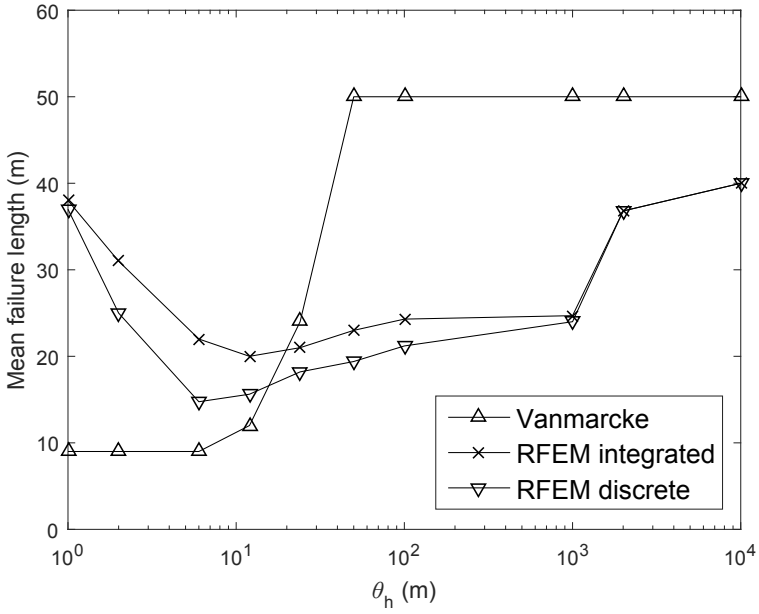

Figure 5.3: Comparison of mean failure length by the two methods

due to the differences in predicted failure length, coupled with an exaggerated influence of the cylinder ends in Vanmarcke's method. At small θ_h there is considerable averaging of properties, resulting in a longer failure length in the RFEM analysis; however, Vanmarcke's method predicts short failure lengths, which results in a relatively larger contribution from the end-resistance and thereby bigger factors of safety relative to RFEM. In contrast, at very large θ_h, the two methods converge to the same F as the 2D solution. For intermediate values of θ_h, an additional cause of the higher F in the Vanmarcke solution is that it takes no account of failure being attracted to weaker zones; i.e., the solution is driven by the means of the property distributions.

Finally, convergence to a 2D solution at high θ_h with two random variables in Figure 5.2 is slower compared to a similar investigation involving variability in only undrained shear strength (one random variable) in Li *et al.* (2015). Note that for very large θ_h, the failure length computed by RFEM is limited to the finite length of the slope considered. Also, Figure 5.3 shows that failure lengths computed by RFEM for very small and very large θ_h are shorter than the slope length. This is attributed to the failed zone not reaching the ends of the mesh, due to the boundary conditions which have a greater influence due to the non-zero friction angle.

5.5. CORRECTIONS TO VANMARCKE'S METHOD

This section further investigates the reasons behind the differences in results by the two methods and proposes a way to correct for them. Firstly, three causes for the differences

are evaluated as follows:

5.5.1. END-RESISTANCE DUE TO GEOMETRIC ASSUMPTIONS

The 3D cylindrical slip surface in Vanmarcke's method includes an additional resistance from both ends of the cylinder. However, this end-resistance is overestimated, as demonstrated by Li *et al.* (2015) and reinforced by Figure 5.2a. The reason for the overestimation is partly the shape effect, as illustrated in Figure 5.4. Vanmarcke assumes vertical end-sections, whereas the failure obtained in a typical RFEM analysis has a very different geometry (shown by coloured elements in Figure 5.4) influenced by spatial variability and 3D effects. Moreover, Equation (5.4) further overestimates the resisting moment by taking $r' \approx r_b$.

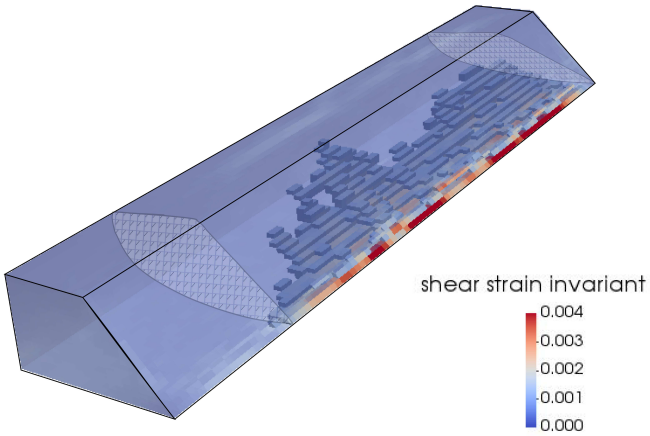

Figure 5.4: RFEM realisation illustrating iso-surfaces of shear strain invariant at failure within slope, superimposed on Vanmarcke's 3D cylindrical model

To correct for the overestimation in the end-resistance due to the geometric assumptions, finite element analyses were carried out for different slope lengths based only on the mean shear strength parameters. The ratio of the factors of safety obtained by finite elements using the strength reduction method and by Vanmarcke's method, for the same failure length, is denoted as β and used here as a correction factor to account for the overestimation of end-resistance in the Vanmarcke method. Thus, the mean factor of safety $\overline{F_b}$ in Equation (5.7) becomes

$$\overline{F_b} = \overline{F_2}\left[1 + \frac{d}{b}\right]\beta \tag{5.15}$$

The end-resistance correction factor (β) values calibrated for a slope with the cross-sectional geometry shown in Figure 5.1 are plotted in Figure 5.5 with respect to failure length, for the set of parameters listed in Table 5.1 and for cases representing high and low friction angles. As expected, the impact of the geometric assumptions in Vanmarcke's method reduces as the length of the failure increases. The value of β varies from 0.8 for short failures to 0.98 for very long failures, for the range of scenarios considered.

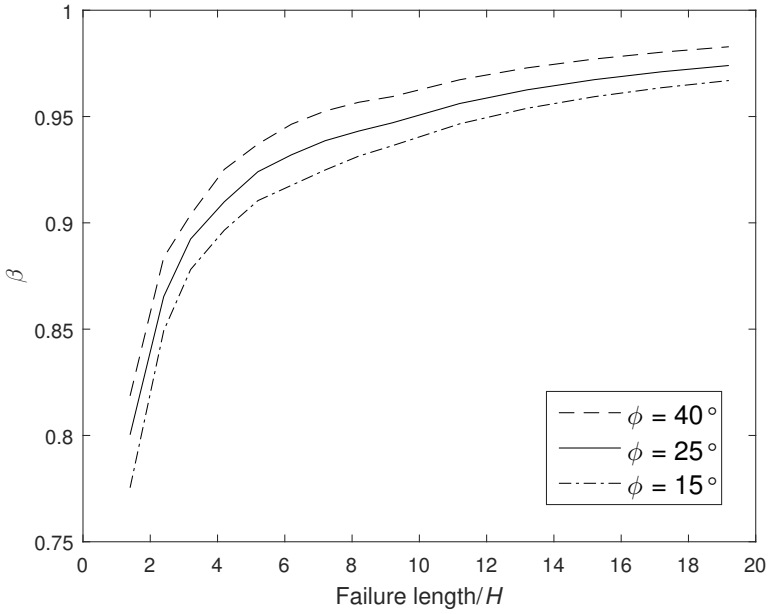

Figure 5.5: Calibrated values of end-resistance correction factor (β)

5.5.2. AVERAGED STRENGTH ALONG SLIP SURFACE

Equation (5.7) is based on the assumption that the averaged mean shear strength over the failure surface ($\overline{s_b}$) is the same as the mean point shear strength ($\overline{s}$) throughout the slope. However, RFEM results indicate that weak zones have a greater influence on the failure mechanism than strong zones in each realisation, as has been highlighted in numerous previous slope reliability studies (e.g. Hicks & Spencer (2010); Hicks & Samy (2002)). Similar findings have also been reported by Ching & Phoon (2013) and Ching *et al.* (2016), who showed that the mean shear strength over the failure surface is typically lower than $\overline{s}$ for various 2D boundary value problems. All these studies have highlighted the difference between spatial averaging over the whole domain and spatial averaging over an emergent slip surface, which is the solution of a boundary value problem over a spatially variable domain and hence changes from realisation to realisation.

This chapter quantifies the difference between the two spatial averages and proposes a reduction factor (α) for the mean safety factor equal to the ratio of $\overline{s_b}$ to $\overline{s}$. This reduction factor is not applied to the resistance from the end-sections, even though Vanmarcke's method also assumes $\overline{s_e} = \overline{s}$ in Equation (5.4), as the vertical sides of the failure surface generally pass through a spatially more variable domain due to a relatively low value of the vertical scale of fluctuation compared to H (de Gast *et al.*, 2017). Thus, the mean factor of safety in Equation (5.15) changes to

$$\overline{F_b} = \overline{F_2}\left[\alpha + \frac{d}{b}\right]\beta \tag{5.16}$$

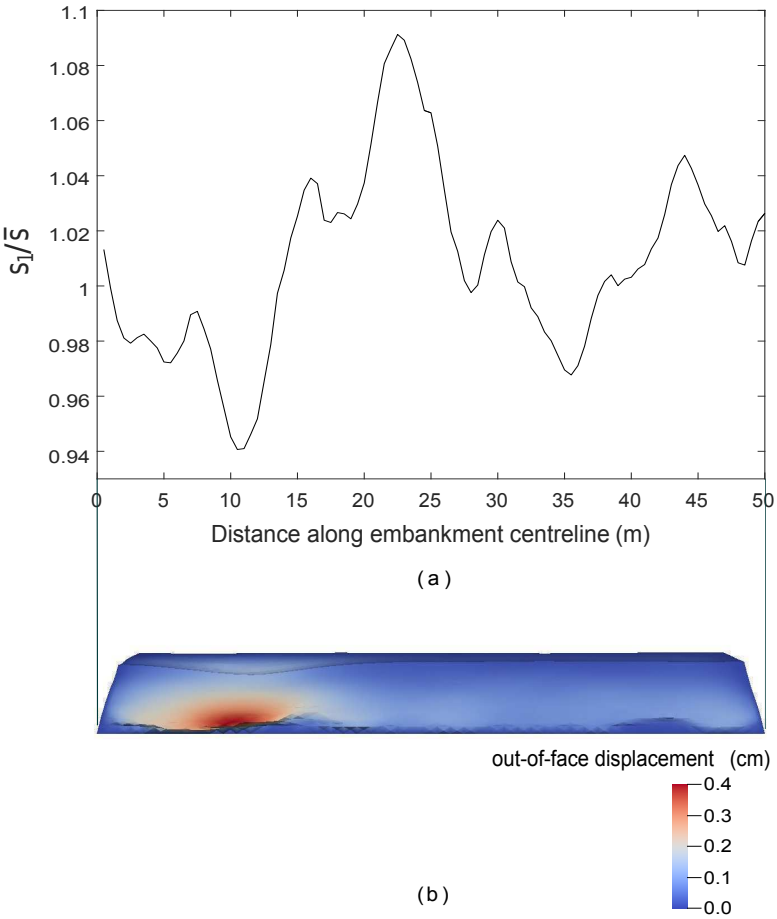

Figure 5.6: RFEM result for a typical realisation showing failure centred at a critical position: (a) variation in average cross-sectional strength per unit length; (b) failure mechanism

Figure 5.6 shows the results for a typical RFEM realisation, illustrating that failure is often located around the point where the averaged shear strength per unit cross-section (s_1) is a minimum (in this case, at 10 m along the slope). This critical point is considered as the centre of the most-probable failure surface for the purpose of estimating α. The steps to compute α are:

- Generate 3D random fields of the shear strength parameters (e.g., using LAS).
- For each realisation:
  - Identify the critical cross-section, i.e., the one with the minimum s_1 (as in Figure 5.6), along the embankment length;
  - Compute the average shear strength over the expected failure length (s_b),

centred at the critical position.

- Repeat the above process for all realisations.
- $\overline{s_b}$ = average of s_b over all the realisations.
- $\alpha = \overline{s_b}/\overline{s}$.

Since an actual slip surface is a function of the boundary value problem and spatial variability in each realisation, its shape and orientation cannot be determined without doing a finite element analysis. Therefore, the averaging of shear strength is carried out over a three dimensional domain (of dimensions comparable to the expected failure cross-section and length) that can encompass an emergent slip surface. Although this will tend to give an upper bound to the actual $\overline{s_b}$, due to the actual slip surface being attracted to the weaker zones, it nevertheless provides a reasonable first approximation.

5.5.3. EXPECTED FAILURE LENGTH

Since RFEM results indicate the influence of weak zones on the failure mechanism (cf. Calle (1985), who suggested that the real failure, if it occurs, coincides with the length of a potentially unstable zone), the averaging of shear strength needs to be carried out along the potential failure zone which is centred at the critical position. However, the length of the potential failure does not necessarily coincide with the critical failure length predicted by Vanmarcke (1977), since the latter does not take into account the influence of weak zones.

Hicks & Li (2018) compared the failure length computed using RFEM, Vanmarcke's method and the "2.5 D" method of Calle for very long slopes in cohesive soils. They showed that Calle's method and Vanmarcke's method underestimate the potential failure length at small θ_h. For very small θ_h relative to H, the failure length calculated by RFEM tends to be very long, extending over the entire length of slope in each realisation. For larger θ_h, the mean RFEM failure length tends towards Calle's solution. Since neither of the two methods (Vanmarcke's method nor Calle's 2.5 D method) predict the failure length accurately for all values of θ_h, it was proposed to use the mean failure length calculated by RFEM as the averaging length in the modified Vanmarcke's method (MVM). However, because the use of RFEM to determine the averaging length is computationally expensive, which rather defeats the purpose of using MVM, an approximate equation for the mean failure length (based on RFEM) is proposed in this chapter.

Figures 5.7a to 5.7e show the sensitivity of the mean failure length (computed using RFEM) to several parameters: H, slope angle, ϕ, θ_v, θ_h and slope length (L). Figure 5.8 shows the histogram of failure lengths obtained from multiple 3D RFEM realisations of a 5 m high slope with $\theta_h = 6$ m, for the various values of slope angle, friction angle and θ_v considered in Figures 5.7b to 5.7d. Based on this sensitivity analysis, the failure length is clearly a complex function of the soil spatial variability, as well as of the geometry of the boundary value problem. The median and mean of the histogram of failure lengths, obtained for the range of possible values of parameters considered, are approximately equal to $2H + \theta_h/2$ and $2H + \theta_h$, respectively (see Figure 5.8), and are used here as approximate solutions instead of the complex function of failure length for intermediate values of θ_h (i.e., for $H < \theta_h < L/2$, as consistent with Mode 2 failures in Hicks & Spencer (2010)).

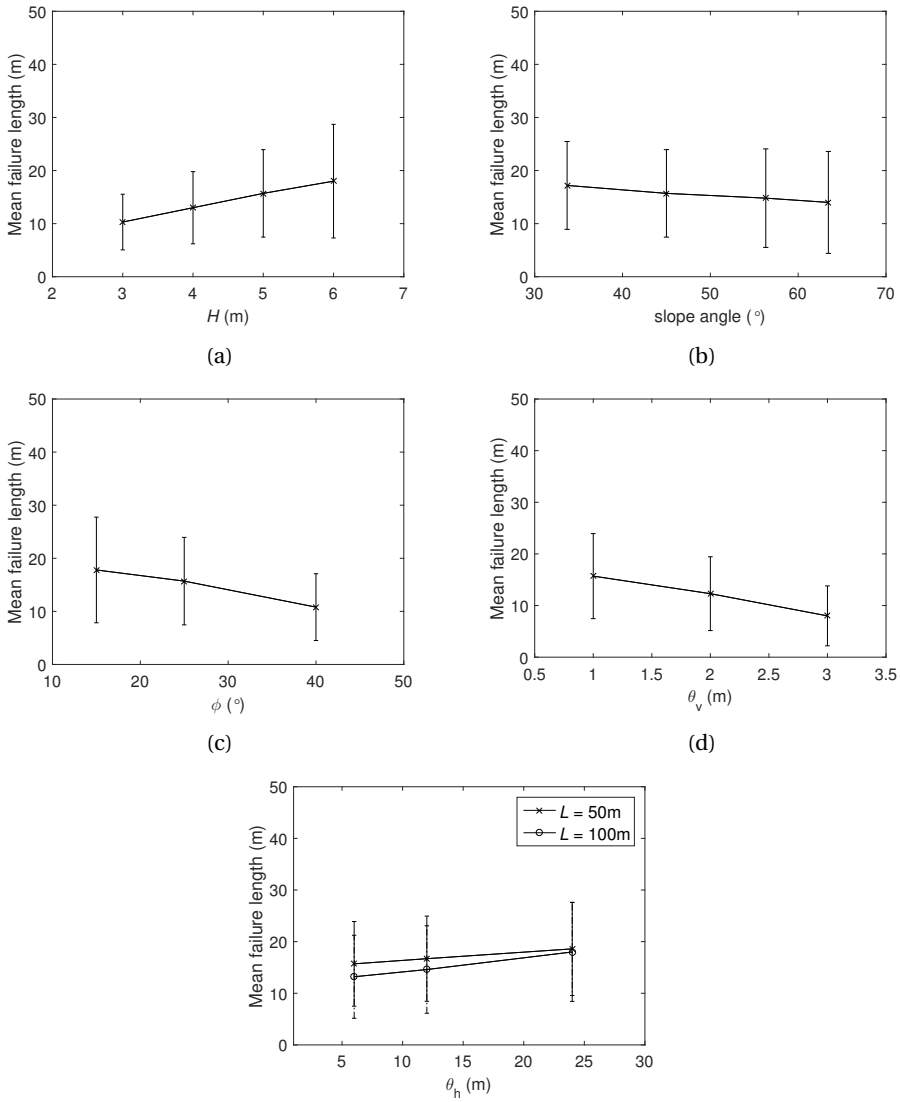

Figure 5.7: Mean failure lengths with the associated one standard deviation error bar obtained by RFEM versus: (a) slope height (H); (b) slope angle; (c) friction angle (ϕ); (d) vertical scale of fluctuation (θ_v); (e) horizontal scale of fluctuation (θ_h)

5.5.4. RECOMMENDED VALUES FOR CORRECTION FACTORS

Based on the RFEM computations of the mean failure length, Figure 5.9 shows the values of the correction factor α for the range of parameter values considered in Figures 5.7a to 5.7e. Since α is calculated as the ratio of the averaged shear strength over a

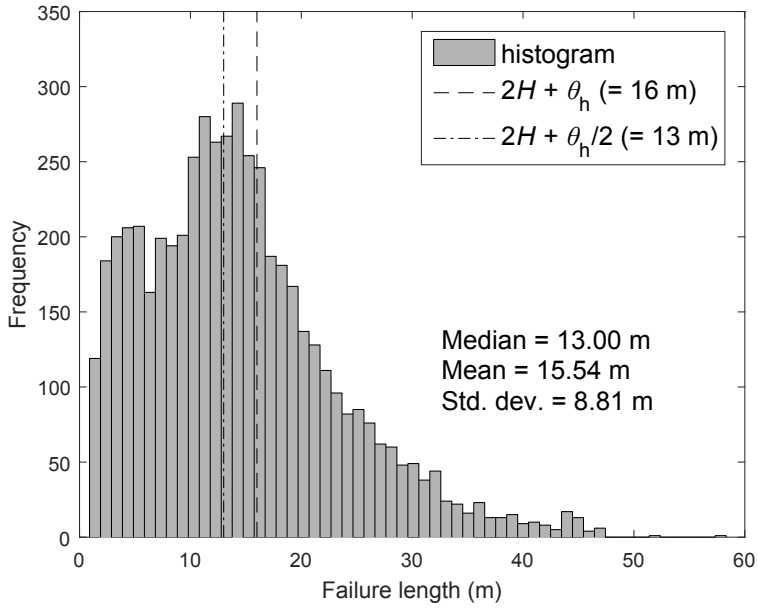

Figure 5.8: Histogram of failure lengths obtained in each realisation of 3D RFEM analyses of a 5 m high slope for the various scenarios considered in Figures 5.7b to 5.7d

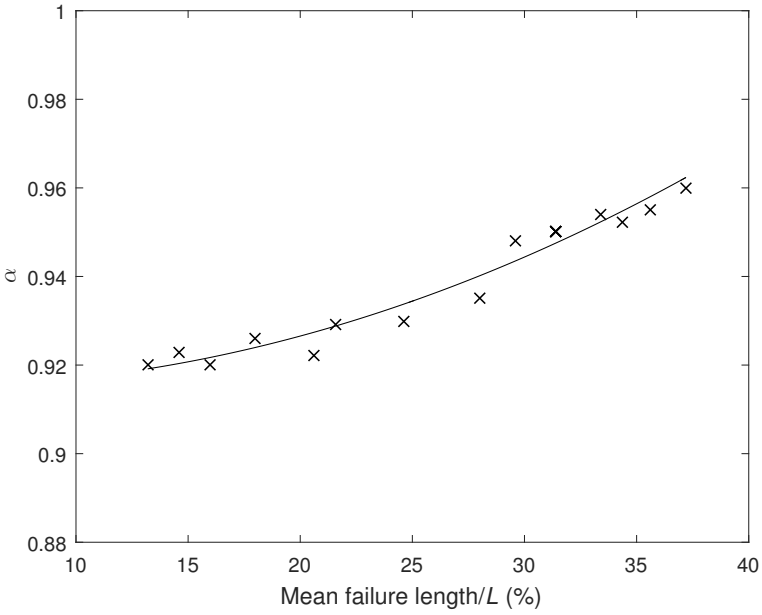

Figure 5.9: α for all cases considered in Figures 5.7a to 5.7e

Table 5.2: Table of recommended correction factor values

Mean failure length/H	β	Mean failure length/L (%)	α
1–2	0.80–0.85	< 15	0.920
2–3	0.85–0.89	15–22	0.920–0.930
3–5	0.89–0.92	22–28	0.930–0.940
5–20	0.92–0.97	28–37	0.940–0.965
> 20	0.97–1.00	> 37	0.965–1.000

failed segment to the averaged shear strength over the entire slope, the failure length is normalised by L in Figure 5.9. The value of α approaches unity for very long failures relative to L, whereas for intermediate failure lengths relative to L, α lies between 0.92 and 0.96. The recommended values of β and α for a range of values of the failure length are summarised in Table 5.2 (based on Figures 5.5 and 5.9, respectively). Note that the β values reported in Table 5.2 correspond to a soil with a friction angle of 25°. Slight variations in the value of β, with respect to those reported in Table 5.2, are expected for cases with higher or lower values of friction angle (see Figure 5.5).

5.6. METHODOLOGY AND ANALYSIS

The steps followed to compute the mean F (and standard deviation of F) of slopes with the proposed modified Vanmarcke method are:

- Calculate $\overline{F_2}$.
- Calculate the effective width d of the end-sections using Equation (5.8).
- Calculate the approximate failure length using either $2H + \theta_h/2$ or $2H + \theta_h$.
- Obtain β from Figure 5.5 or use the recommended values in Table 5.2.
- Obtain α from Figure 5.9 or use the recommended values in Table 5.2.
- Calculate the mean F using Equation (5.16).
- Calculate the standard deviation of F using Equation (5.12).

In order to test the methodology the 5 approaches listed in Table 5.3 have been compared for a base case problem. Note that approach MVM-1, which uses the mean failure length obtained by RFEM analysis, has been considered in order to check which one of the two simpler expressions for the failure length is a good approximation.

A 50 m long slope, again with the cross-sectional geometry shown in Figure 5.1, the soil parameters listed in Table 5.1 and a vertical scale of fluctuation of 1 m has been considered. The mean failure lengths obtained by RFEM for different values of θ_h and the corresponding correction factors are summarised in Table 5.4 and represent the base case. The mean F obtained by using the different methods and the relative influence of each correction factor (in MVM-1) towards improving the mean F for the base case are plotted in Figure 5.10. At very small θ_h the major improvement is due to considering the correct failure length and correcting for the overestimated contribution in resistance from the

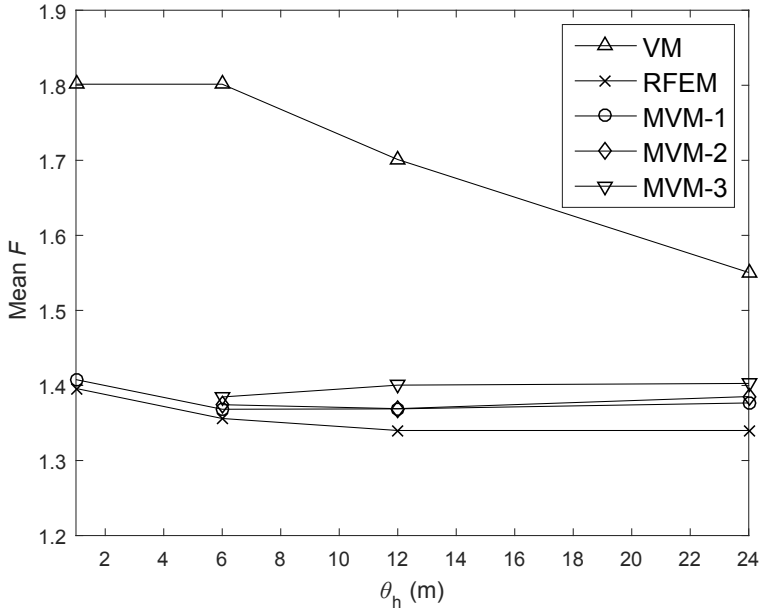

(a)

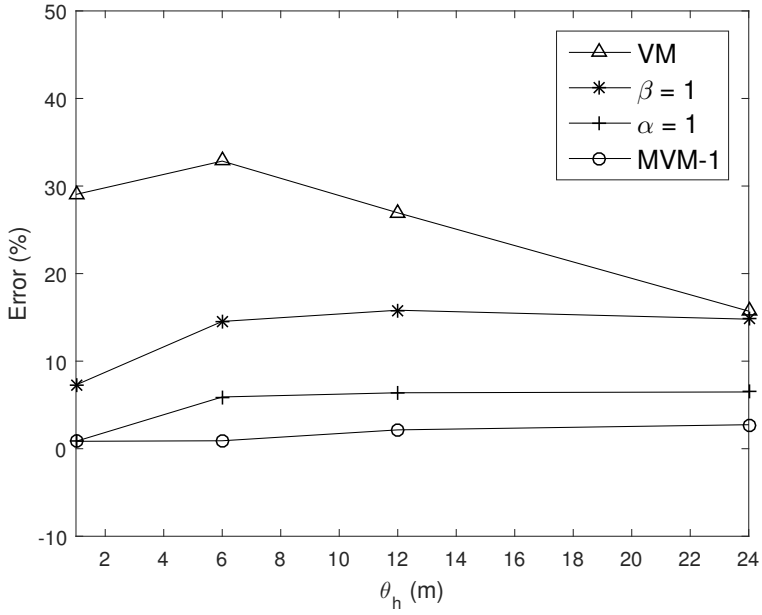

(b)

Figure 5.10: Comparison of mean F by the different methods and relative influence of correction factors for the base case: (a) Mean F as a fuction of θ_h, and (b) Error in mean F by VM and MVM-1 with respect to mean F by RFEM

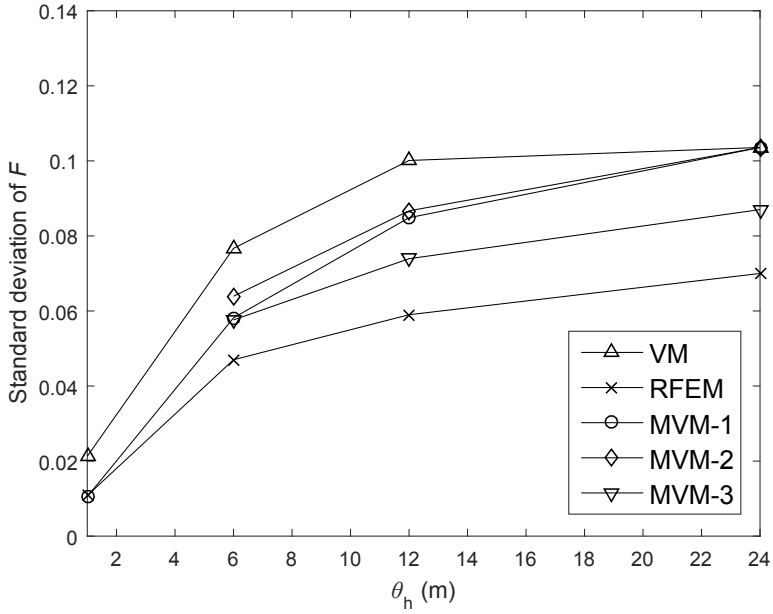

Figure 5.11: Comparison of standard deviation of F by the different methods for the base case

Table 5.3: List of compared approaches

Approach	Description
RFEM	Random finite element method
VM	Vanmarcke's method
MVM-1	MVM based on the mean failure length obtained by RFEM
MVM-2	MVM based on the failure length given by $2H+\theta_h/2$
MVM-3	MVM based on the failure length given by $2H+\theta_h$

Table 5.4: Mean failure lengths obtained by RFEM, corresponding correction factors and mean F calculated by using MVM-1 for the base case

θ_h (m)	Mean failure length (m)	β	α	Mean F
1	37.0	0.940	1.000	1.408
6	15.7	0.881	0.950	1.375
12	16.7	0.882	0.954	1.369
24	18.6	0.895	0.960	1.377

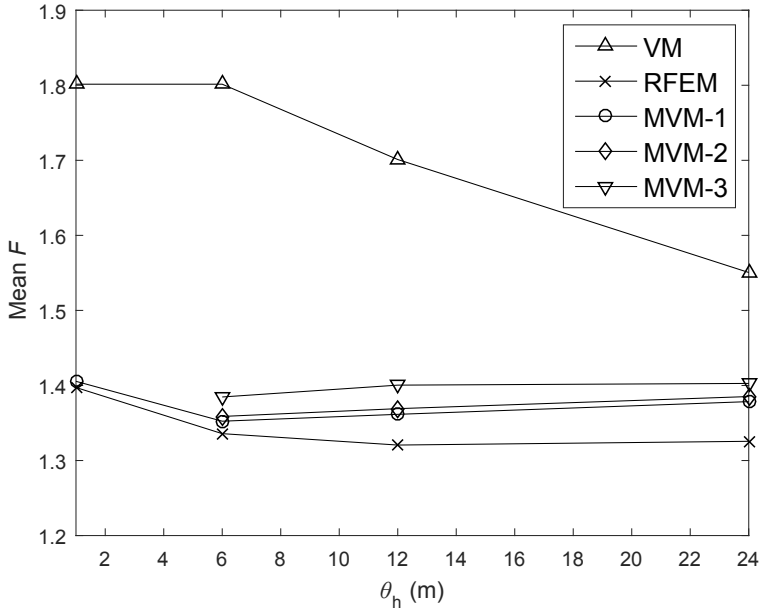

(a)

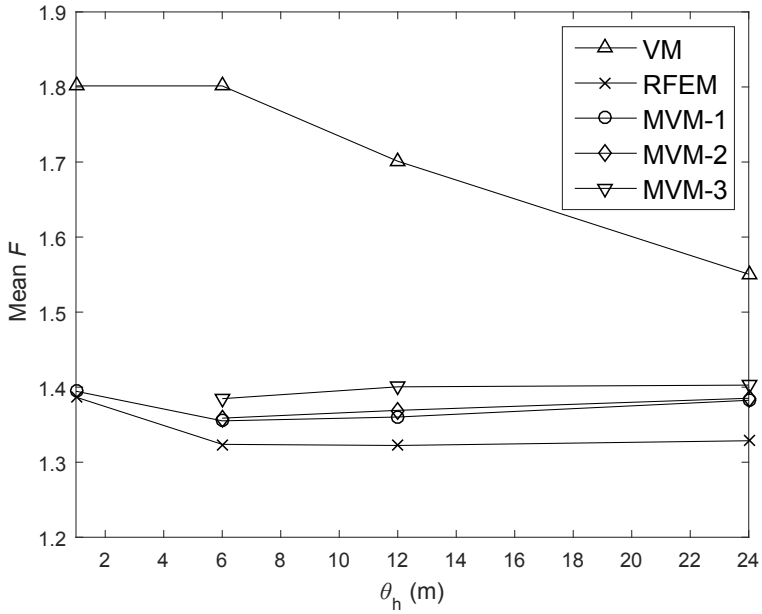

(b)

Figure 5.12: Comparison of mean F by RFEM, VM and MVM for two additional cases: (a) $\theta_v = 2\,\text{m}$, and (b) $L = 100\,\text{m}$

end-sections. For intermediate values of θ_h, each correction factor has a considerable influence on the results, although α has relatively lower importance than the other two factors for this particular example. The small remaining error in the MVM-1 analysis may be attributed to an overestimated α, due to the averaging of shear strength being carried out over entire cross-sections of the slope segments, since the exact shape of the failure surface is not known a priori.

Figure 5.11 compares the standard deviation of the F obtained by the different methods. The standard deviation has not improved as significantly as the mean, but it remains above that obtained using RFEM and is thus conservative. The difference between the VM and MVM results is mainly due to the different failure lengths used in the two methods. The main difference between the MVM and RFEM results may be attributed to the approximate form of the variance reduction factor used in Vanmarcke's method, compared to the variance reduction factor derived from the covariance function used in the RFEM model in this chapter. Note that in Figure 5.10a and Figure 5.11, the mean and standard deviation of F are not calculated for very small values of θ_h ($< H$) by MVM-2 and MVM-3, since the approximate equation for the failure length does not hold true for this range of θ_h.

Two additional cases with the same cross-sectional geometry have been considered: one with a higher value of θ_v and the other with a longer slope length ($L = 100$ m). The mean F obtained by using the different methods considered in this chapter are plotted in Figure 5.12. Overall, Figures 5.10 and 5.12 show that the mean F obtained by MVM, based on the mean failure length obtained by RFEM, or based on the failure length calculated by $2H + \theta_h/2$, are in good agreement with the RFEM mean F for all cases considered. Thus the proposed simplified expression ($b = 2H + \theta_h/2$) for the failure length seems a good approximation, although good results have also been obtained using $b = 2H + \theta_h$. Note that Hicks & Li (2018) conducted 3D RFEM analysis on much longer slopes with undrained shear strength parameters, where the boundary effects have negligible influence on the calculated failure length and F. Their study also implied a mean discrete failure length approximately equal to $2H + \theta_h/2$ (see Hicks & Li (2018)) and thus reinforces the findings in this chapter.

Figures 5.10 to 5.12 are based on the 3D F computed for slopes with the specific cross-sectional geometry shown in Figure 5.1. However, the influence of different cross-sectional geometry parameters, such as H and slope angle, on the expected failure length (Figures 5.7a and 5.7b and Figure 5.8) were taken into account in deriving the correction factors for the modified Vanmarcke method, implying that the applicability of the proposed method is not restricted to the one cross-section. Hence, in order to demonstrate its wider applicability, additional cases of slopes with different cross-sectional geometries (H and slope angle) have been considered. These further analyses have been based on slopes that are 50 m long in the third dimension, the soil parameters listed in Table 5.1 and a vertical scale of fluctuation of 1 m. The results, expressed in terms of percentage error in the mean F computed by VM and MVM-2 relative to the mean F computed by RFEM, are plotted in Figure 5.13, and the failure lengths obtained by the various approaches are listed in Tables 5.5 and 5.6. Figure 5.13 shows that the mean F computed by MVM-2 has an error $< 8\%$ (relative to the mean F computed by RFEM) and is substantially better than the mean F computed by VM (with an error of approximately 15–50 %, and a tendency

Table 5.5: Failure lengths obtained by VM and MVM-2, and mean failure lengths obtained by RFEM, for slopes of different height and slope angle = 45°

θ_h (m)	$H = 3$ m				$H = 4$ m				$H = 5$ m				$H = 6$ m			
	$\overline{F_2}$	Failure length (m)			$\overline{F_2}$	Failure length (m)			$\overline{F_2}$	Failure length (m)			$\overline{F_2}$	Failure length (m)		
		VM	MVM-2	RFEM		VM	MVM-2	RFEM		VM	MVM-2	RFEM		VM	MVM-2	RFEM
6	1.92	6.0	9.0	12.5	1.60	6.1	11.0	14.4	1.40	9.0	13.0	15.7	1.29	13.6	15.0	15.9
12	1.92	12.0	12.0	14.3	1.60	12.0	14.0	15.8	1.40	12.0	16.0	16.7	1.29	13.6	18.0	16.8
24	1.92	24.0	18.0	18.0	1.60	24.0	20.0	18.2	1.40	24.0	22.0	18.6	1.29	24.0	24.0	21.1

Table 5.6: Failure lengths obtained by VM and MVM-2, and mean failure lengths obtained by RFEM, for slopes of different slope angle and $H = 5$ m

θ_h (m)	slope angle = 26.56°				slope angle = 45°				slope angle = 63.43°			
	$\overline{F_2}$	Failure length (m)			$\overline{F_2}$	Failure length (m)			$\overline{F_2}$	Failure length (m)		
		VM	MVM-2	RFEM		VM	MVM-2	RFEM		VM	MVM-2	RFEM
6	2.08	6.0	13.0	16.7	1.40	9.0	13.0	15.7	1.10	27.4	13.0	12.7
12	2.08	12.0	16.0	17.4	1.40	12.0	16.0	16.7	1.10	27.4	16.0	14.2
24	2.08	24.0	22.0	20.2	1.40	24.0	22.0	18.6	1.10	27.4	22.0	18.1

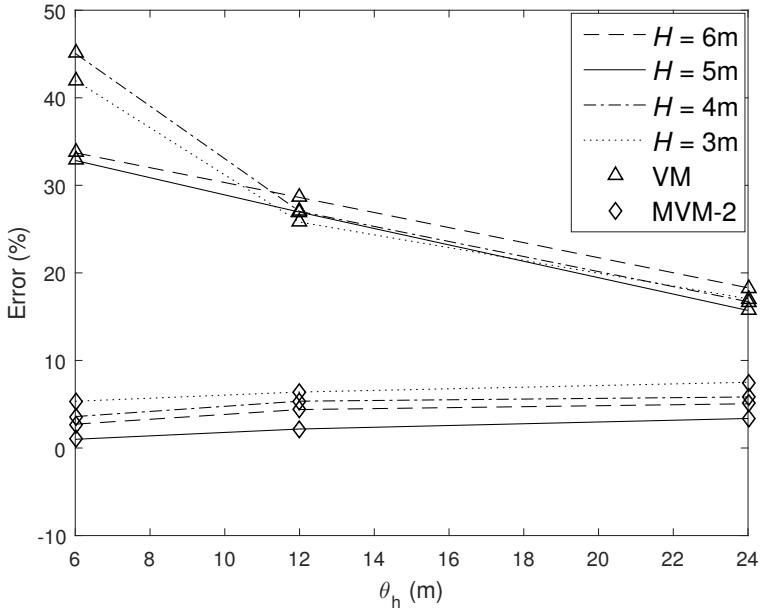

(a)

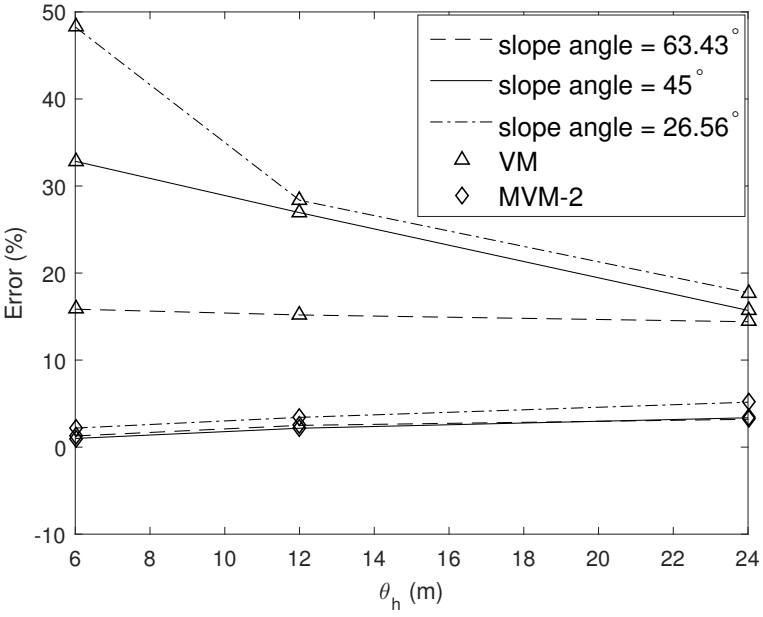

(b)

Figure 5.13: Error in mean F by VM and MVM-2 (relative to RFEM) for different cross-sectional geometries: (a) Slope angle = 45°, and (b) $H = 5\,\text{m}$

for larger errors at lower θ_h) for the range of parameters considered. This improvement is partly driven by the improved estimates of the failure lengths shown in Tables 5.5 and 5.6. Note that the relatively higher error in the mean F computed by VM at $\theta_h = 6\,m$, for slopes with $H = 3\,m$, $H = 4\,m$ and slope angle = 26.56°, is due to the very short failure length predicted by VM (see Tables 5.5 and 5.6) in these cases.

The proposed method has been shown to work well for all test cases considered in this chapter. However, a few limitations of the proposed method, which are beyond the scope of this research, are that it cannot be applied to slopes in which the failure surface passes through multiple soil layers, to slopes with cross-sections or soil layer depths varying along the embankment length, or to slopes made up of soils with multiple scales of fluctuation of the inherent shear strength.

5.7. CONCLUSIONS

A modified semi-analytical method for slope reliability has been proposed based on Vanmarcke's method (Vanmarcke, 1977). A comprehensive numerical investigation identified 3 significant areas which required improvement. These were corrected by an alternative relationship for the expected failure length (equal to $2H + \theta_h/2$ for intermediate values of θ_h) and a modified equation (Equation (5.16)) for the mean F that utilises two correction factors, α and β. Calibration curves for the correction factors are provided and recommended values for these factors are summarised in Table 5.2. These suggest that, for very long embankments, $\alpha \approx 0.92$ and $0.85 \leq \beta \leq 0.92$ may be reasonable first approximations. The mean F obtained by using the modified method was in good agreement with the mean F obtained by RFEM for all cases considered in this chapter.

REFERENCES

Arnold, P. & Hicks, M. A. (2011). A stochastic approach to rainfall-induced slope failure. In *Proceedings of 3rd International Symposium on Safety and Risk*, Munich, pp. 107–115.

Calle, E. (1985). Probabilistic analysis of stability of earth slopes. In *Proceedings of 11th International Conference on Soil Mechanics and Foundation Engineering*, California, pp. 809–812.

Cherubini, C. (2000). Reliability evaluation of shallow foundation bearing capacity on *c'*, *ϕ'* soils. *Canadian Geotechnical Journal* **37**, No. 1, 264–269.

Ching, J., Hu, Y.-G. & Phoon, K.-K. (2016). On characterizing spatially variable soil shear strength using spatial average. *Probabilistic Engineering Mechanics* **45**, 31–43.

Ching, J. & Phoon, K.-K. (2013). Mobilized shear strength of spatially variable soils under simple stress states. *Structural Safety* **41**, 20–28.

de Gast, T., Vardon, P. J. & Hicks, M. A. (2017). Estimating spatial correlations under man-made structures on soft soils. In *Proceedings of 6th International Symposium on Geotechnical Safety and Risk*, Colorado, USA, pp. 382–389.

de Gast, T., Vardon, P. J. & Hicks, M. A. (2020). Assessment of soil spatial variability for linear infrastructure using cone penetration tests. *Géotechnique* Under review.

Fenton, G. A. & Vanmarcke, E. H. (1990). Simulation of random fields via local average subdivision. *Journal of Engineering Mechanics* **116**, No. 8, 1733–1749.

Hicks, M. A., Chen, J. & Spencer, W. A. (2008). Influence of spatial variability on 3D slope failures. In *Proceedings of 6th International Conference on Computer Simulation in Risk Analysis and Hazard Mitigation*, Kefalonia, pp. 335–342.

Hicks, M. A. & Li, Y. (2018). Influence of length effect on embankment slope reliability in 3D. *International Journal for Numerical and Analytical Methods in Geomechanics* **42**, 891–915.

Hicks, M. A., Nuttall, J. D. & Chen, J. (2014). Influence of heterogeneity on 3D slope reliability and failure consequence. *Computers and Geotechnics* **61**, 198–208.

Hicks, M. A. & Samy, K. (2002). Influence of heterogeneity on undrained clay slope stability. *Quarterly Journal of Engineering Geology and Hydrogeology* **35**, No. 1, 41–49.

Hicks, M. A. & Samy, K. (2004). Stochastic evaluation of heterogeneous slope stability. *Italian Geotechnical Journal* **38**, No. 2, 54–66.

Hicks, M. A. & Spencer, W. A. (2010). Influence of heterogeneity on the reliability and failure of a long 3D slope. *Computers and Geotechnics* **37**, No. 7, 948–955.

Huang, J., Lyamin, A. V., Griffiths, D. V., Krabbenhoft, K. & Sloan, S. (2013). Quantitative risk assessment of landslide by limit analysis and random fields. *Computers and Geotechnics* **53**, 60–67.

Li, Y., Hicks, M. A. & Nuttall, J. D. (2015). Comparative analyses of slope reliability in 3D. *Engineering Geology* **196**, 12–23.

Spencer, W. A. (2007). *Parallel stochastic and finite element modelling of clay slope stability in 3D*. Ph.D. thesis, University of Manchester, UK.

Spencer, W. A. & Hicks, M. A. (2007). A 3D finite element study of slope reliability. In *Proceedings of 10th International Symposium on Numerical Models in Geomechanics*, Rhodes, pp. 539–543.

Vanmarcke, E. H. (1977). Reliability of earth slopes. *Journal of the Geotechnical Engineering Division* **103**, No. 11, 1247–1265.

Vanmarcke, E. H. (1980). Probabilistic stability analysis of earth slopes. *Engineering Geology* **16**, No. 1-2, 29–50.

Vardon, P. J., Liu, K. & Hicks, M. A. (2016). Reduction of slope stability uncertainty based on hydraulic measurement via inverse analysis. *Georisk: Assessment and Management of Risk for Engineered Systems and Geohazards* **10**, No. 3, 223–240.

Varkey, D., Hicks, M. A. & Vardon, P. J. (2017). Influence of spatial variability of shear strength parameters on 3D slope reliability and comparison of analysis methods. In *Proceedings of 6th International Symposium on Geotechnical Safety and Risk*, Colorado, USA, pp. 400–409.

Varkey, D., Hicks, M. A. & Vardon, P. J. (2019a). An improved semi-analytical method for 3d slope reliability assessments. *Computers and Geotechnics* **111**, 181–190.

Varkey, D., Hicks, M. A. & Vardon, P. J. (2019b). Modified semi-analytical method for 3D slope reliability. In *Proceedings of 7th International Symposium on Geotechnical Safety and Risk*, Taipei, Taiwan, pp. 406–411.

6

CONCLUSIONS AND RECOMMENDATIONS

6.1. INTRODUCTION

Uncertainties in soil properties, including the spatial nature of their variability and their impact on reliability-based assessments of 2D geotechnical structures have been extensively researched. For example, many researchers have used the random finite element method (RFEM), which combines finite elements with random fields of soil properties representing the spatial variability, to carry out full probabilistic assessments of geotechnical structures. This method is versatile and it does not make any prior assumptions regarding the location or shape of the failure mechanism. The significance of considering the spatial variability of soil properties in three dimensions is also now well recognised. Specifically, the range of critical values of isotropic correlation lengths of soil variability in the horizontal plane which result in the lowest mean F have been identified. In addition to calculating the probabilities of failure, research has been carried out to quantify the failure consequences, including the modelling of the dynamics of the sliding process, thereby allowing a complete assessment of the risks involved. So far, only a limited amount of research has been conducted in 3D reliability-based assessments owing to the large computational requirements, which is especially true for RFEM.

Although RFEM has been widely used by researchers, it is yet to find its way into practice, due to its complexity and computational requirements. However, there are alternative semi-analytical methods giving quick and convenient solutions based on certain simplifying assumptions, although these need to be thoroughly examined before applying them in everyday engineering practice. The work presented in this thesis has investigated these questions through three main chapters. While all major findings are discussed in detail throughout this thesis and are summarised in the conclusions of the respective chapters, the following sections give an overview of the research carried out by highlighting the major findings and providing an outlook for further research.

6.2. CHARACTERISTIC SOIL PROPERTY VALUES FOR THE RELIABILITY-BASED ASSESSMENT OF A DYKE

The reliability-based assessment and re-design of a representative cross-section of an existing dyke in the Netherlands were carried out using RFEM. The characteristic soil property values resulting in the 5-percentile system response for the dyke section, consistent with the requirements of Eurocode 7, were back-calculated. It was observed that the back-calculated characteristic values represented a significant increase in strength capacity over simpler interpretations of Eurocode 7 based only on the point statistics.

As described in Section 2.3.1 of Chapter 2, geotechnical engineering practice often uses a simplified deterministic approach based on characteristic soil property values and partial factors for reliability-based assessments of structures. Although a range of values for the partial factors is usually available in the National Annexes of the Eurocode, there is either limited or no guidance in the code regarding the determination of characteristic values, making the determination of the latter rather subjective. As such, for reasons of simplicity and conservatism, the geotechnical engineering practice sometimes uses 5-percentile soil property values as the characteristic values for reliability-based assessments of dykes. Chapter 3 describes a case study involving the re-assessment and re-design of an historical dyke section in the Netherlands. As part of the regular safety as-

sessment, the dyke section was originally analysed by a water board using a deterministic approach based on 5-percentile (characteristic) soil property values; that is, a simplistic but often adopted interpretation of Eurocode 7.

Chapter 3 begins by recapping an interpretation of the definition of characteristic soil property values found in Eurocode 7, as explained by a consideration of the scale of fluctuation relative to the size of the problem domain. A comparison was made between the original deterministic assessment of the dyke section and the reliability-based safety factor calculated using RFEM (which is consistent with the requirements of Eurocode 7). The results indicated that a proper accounting of soil spatial variability via RFEM leads to a significantly higher reliability-based factor of safety compared to the deterministic solution based on 5-percentile characteristic values. Furthermore, a re-design of the dyke section to meet national safety requirements was carried out using the two methods. It was shown that a consideration of the soil spatial variability, while re-designing the dyke section, resulted in a significant economic gain and far less intrusive mitigation measure compared to that using the simpler deterministic approach.

An advantage of the RFEM approach is that it gives accurate solutions satisfying the requirements of Eurocode 7, without the need to explicitly calculate the characteristic property values. Nevertheless, back-calculated characteristic soil property values, consistent with the requirements of Eurocode 7, were compared with those derived based on the frequently adopted approach of ignoring the scale of fluctuation (i.e. the 5-percentile values), as well as with others derived using alternative simple approaches, some of which indirectly incorporate the scale of fluctuation by reducing the variance of the underlying property distributions. It was observed that the back-calculated characteristic values using RFEM represented a significant increase in strength capacity over simpler interpretations of Eurocode 7 based on 5-percentile property values. Aside from the over-conservative solution computed using 5-percentile property values, most other methods gave factors of safety within 10% of the benchmark solution (both conservative and unconservative).

To summarise:

1. RFEM may be used to give accurate solutions satisfying the requirements of Eurocode 7, without the need to explicitly calculate the characteristic property values. In doing so, it fully accounts for uncertainties that arise due to the spatial variability of soil properties.

2. The reliability-based factor of safety of the dyke cross-section computed using RFEM was significantly higher than the deterministic solution based on 5-percentile characteristic values.

3. Re-designing of the dyke section using RFEM resulted in a far less costly and less intrusive mitigation measure compared to that using the deterministic approach based on 5-percentile characteristic values.

4. The characteristic soil property values resulting in a 5-percentile system response were back-calculated. It was found that the same system response could be computed using 34-percentile property values in a deterministic analysis.

5. Alternative simple approaches for calculating characteristic values mostly gave factors of safety within 10% of the RFEM solution.

6.3. GEOMETRIC UNCERTAINTIES AND ANISOTROPIC SOIL SPATIAL VARIABILITY

Material uncertainty has been shown to have a significantly greater impact on embankment reliability than geometric uncertainties. The spatial correlation of material properties along the length of the embankment has been shown to significantly influence the embankment reliability and failure consequences. In addition, a worst case horizontal correlation length has been identified. These findings allow reliability analyses to be undertaken with a significantly reduced computational effort.

The significance of considering spatial variability of the parameters in all three dimensions has begun to be well recognised amongst researchers, including the identification of the critical range of correlation length in the horizontal plane that maximises the probability of failure. Isotropic correlation lengths are typically assumed in the horizontal plane, mainly due to insufficient data to prove otherwise. However, a recent detailed site investigation (de Gast *et al.*, 2020) along a Dutch regional dyke has shown that the correlation lengths may be quite different in different horizontal directions. This may be due, for example, to dykes often being located along ancient river channels, so that the correlation length along the dyke is higher than that across the dyke. In addition, another common assumption in literature relates to a constant dyke cross-section for each designed dyke segment, even though variations in geometry of a dyke along its length are usually observed in practice.

Chapter 4 investigated the influence of the following three forms of uncertainty on the reliability of an idealised embankment slope: 1D spatial variability in the geometry of the slope along its length, 2D spatial variability in the depth of the boundary between the slope and foundation layer, and 3D spatial variability in the shear strength properties of the slope and foundation materials. The strategies adopted for modelling the uncertainties were discussed. The relative influence of these uncertainties were investigated by comparing the responses obtained using RFEM analyses for an idealised 3D slope. It was observed that the spatial variability in the geometric parameters had relatively less influence on the reliability of the slope compared to that due to the spatial variability of material properties within soil layers. It was shown that the uncertainty in the depth of the boundary between the slope and foundation layers, relating to incomplete knowledge regarding the layering of the construction and foundation soils, had almost negligible influence on the reliability of the slope compared to that due to heterogeneity within the layers themselves.

Having established that the reliability of slopes is most sensitive to spatial variability in the material parameters compared to spatial variability in the geometry and/or in the layering, the influence of considering anisotropy in the soil spatial variability in the horizontal plane was also investigated. It was observed that the responses were more sensitive to soil spatial variability along the embankment length than perpendicular to it. Furthermore, a critical horizontal correlation length along the embankment direction was identified as $3H \pm H$. It was also demonstrated that carrying out a reliability-based

analysis assuming isotropic horizontal spatial variability based on this critical value would give a reasonably conservative estimate of the structural response.

To summarise:

1. Uncertainties relating to the external geometry of the slope and the location of the boundary between the embankment and foundation materials had little to negligible influence on slope reliability compared to the spatial variability in the shear strength properties of the slope and foundation materials.

2. The spatial correlation of material properties along the length of the embankment had a greater influence on embankment reliability and failure consequence than the spatial correlation of material properties perpendicular to it.

3. A worst case horizontal scale of fluctuation for the material properties along the embankment length was identified as $3H \pm H$.

4. Assuming isotropic spatial variability in the horizontal plane based on this critical value gave a reasonably conservative estimate of the structural response.

6.4. IMPROVED SEMI-ANALYTICAL METHOD FOR SLOPE RELIABILITY ASSESSMENTS

A semi-analytical method has been improved to allow a quick estimation of slope reliability, taking into account soil spatial variability. This means that reliability analyses can be undertaken in vastly reduced times, although limitations of the analytical conceptualisation (e.g. single soil layer) remain.

In this thesis, the realisations of an RFEM analysis have been carried out simultaneously using the Grid computing technique. The requirement of a large number of realisations, and thereby a large computational effort, limits the application of RFEM for reliability assessments using stand-alone PCs, especially for long geotechnical structures such as dykes, and thereby limits its applicability in engineering practice. Alternative semi-analytical methods are available however, such as the simplified method developed by Vanmarcke (1977) for predicting the reliability of heterogeneous 3D slopes, based on spatial averages of shear strength along a predefined failure surface with resisting end-sections. The performance of RFEM compared with Vanmarcke's method for reliability assessments of an idealised 3D slope is presented in Chapter 5. Specifically, the mean and standard deviation of the 3D F and the expected failure lengths obtained for a range of horizontal scales of fluctuation θ_h of the soil shear strength parameters were compared. It was observed that the two methods gave similar solutions for very large values of θ_h with respect to slope length. For very small values of θ_h, Vanmarcke's method predicted a much shorter failure length, which resulted in a relatively larger contribution from the end-resistance and thereby to an overestimated mean F. For intermediate values of θ_h, which are generally more likely, an additional cause of the higher mean F in the Vanmarcke solution was that it takes no account of failure being attracted to weaker strength zones.

Based on a comprehensive numerical investigation, 3 significant areas needing improvement were identified: an overestimated end-resistance due to geometric assumptions;

an overestimated spatially averaged strength along the slip surface due to no account being taken of failure being attracted to weaker strength zones; and the predicted failure length not coinciding with the weak strength zones as in the RFEM solutions. These were corrected by proposing two correction factors to account for the first two issues, and an alternative relationship (equal to $2H + \theta_h/2$) for the expected failure length based on a detailed sensitivity analysis of the failure length to several parameters. The methodology adopted for calibrating the correction factors, the calibration curves and the recommended values for the factors were also provided. Based on these correction factors, a modified version of the Vanmarcke method was proposed which gave substantially improved results that compared favourably with those obtained by RFEM, and therefore provided a more accurate simplified solution. Additional cases of slopes with different cross-sectional geometries were also considered, demonstrating a wider applicability of the proposed simplified method.

To summarise:

1. A detailed comparative analysis between RFEM and Vanmarcke's method identified those instances (i.e. very small values of θ_h) in which the two methods give similar results, as well as those instances (i.e. intermediate and large values of θ_h) in which there are significant differences.

2. Three main assumptions in Vanmarcke's method that resulted in the differences were identified: the end-resistance was overestimated, the spatially averaged shear strength along the slip surface was overestimated and the predicted failure length did not coincide with the weaker strength zones.

3. A modified formulation of the Vanmarcke method was proposed based on an alternative relationship ($= 2H + \theta_h/2$) for the expected failure length, as well as two correction factors α and β to account for the overestimated average shear strength and end-resistance, respectively.

4. Calibration curves for the two correction factors were provided, and $\alpha \approx 0.92$ and $0.85 \leq \beta \leq 0.92$ were recommended for very long embankments.

5. The modifications proposed to the Vanmarcke method gave substantially improved results that were in good agreement with the RFEM solution.

6.5. RECOMMENDATIONS FOR FURTHER RESEARCH

There are certain limitations of the work presented in thesis which require attention. Recommendations providing an outlook on future research are listed below:

- Spatial variability in the material properties was the only form of uncertainty (relating to soil properties) considered in this research, and any uncertainties in measurements and transformations from in-situ tests were ignored. Although the random part of these uncertainties may average out, the systematic part of the transformation uncertainty, which does not average out, may influence some of the conclusions of this dissertation and needs further investigation.

- To make reliability-based methods feasible in everyday engineering practice, simplifications to a certain extent are required, but without losing sight of the true physical processes. Results in Chapter 3 showed that, aside from the over-conservative F computed using 5-percentile property values, most other simplified methods gave F within 10% of the benchmark solution. Given the problem-dependent nature of these characteristic values, further studies are recommended for a more general insight. As long as there is no best simplified method that can accurately determine the reliability-based characteristic values for all types of problems, the advantages of a more accurate RFEM solution may outweigh its limitations relating to computational requirements.

- The reliability-based assessment in Chapter 3 is based on using distributions factored down by partial factors and calculating the 5-percentile system response, which converges in far fewer realisations of a Monte Carlo simulation than, for example, the weak tail of the response distribution. However, more advanced methods such as subset simulation (van den Eijnden & Hicks, 2017) may be required for accurately estimating the system response directly at very low probabilities of failure (i.e. at the target reliability level).

- In Chapter 3, independent spatial variation in c' and $\tan\phi'$ was assumed. However, based on the discussion in Section 2.4, a negative correlation between these parameters is usually suggested, which generally results in a narrower range of responses. It would be valuable to investigate what difference including this correlation makes in the reliability-based assessments of the dyke section and in the back-figured characteristic values.

- In Chapter 3, the phreatic surface is considered to be deterministic. An important extension, although ambitious, would be to account for uncertainty in the phreatic surface due to soil-atmospheric interactions (Jamalinia *et al.*, 2019) coupled with a hydro-mechanical analysis of slopes in heterogeneous unsaturated soil (Arnold, 2016).

- Chapter 4 demonstrates that anisotropy in the horizontal soil spatial variability is a major influential factor for computing the reliability of, and failure consequences associated with, long heterogeneous slopes. For the idealised slope considered in the chapter, a range of worst case correlation lengths in the horizontal plane, with respect to the computed mean F, has been proposed. Basing any analysis on such a range of worst case correlation lengths would result in reasonably conservative estimates of reliability, by-passing the need to accurately compute the in-situ soil variability and thereby resulting in significant economic advantages. Although the range of worst case correlation lengths worked well for the specific problem analysed in the chapter, the applicability of the proposed range to different problems warrants further research.

- In recent years, the uncertainty arising due to the stratigraphic heterogeneity of material layers has received an increasing amount of attention. Chapter 4 investigates the influence of this form of uncertainty via continuous random fields to model the boundaries between different layers, and is relevant to Dutch dykes. However, in practice it is seldom observed that thin clay layers underlying peat layers below the dykes extend along the entire length of the dyke. It would therefore be interesting to model discrete

zones of material categories at the unsampled locations, for example using the Markov Chain Monte Carlo method (Section 4.1), and investigate its influence on the results.

- The proposed modifications to the Vanmarcke method in Chapter 5 are shown to work well for all the cases considered. However, a few limitations of this improved method are that it cannot yet be applied to slopes in which:
  - the failure surface passes through multiple soil layers;
  - cross-sections or soil layer depths vary along the embankment length;
  - soils exhibit anisotropy in the horizontal spatial variability, or;
  - soils have multiple scales of fluctuation of the inherent shear strength.

  The applicability of the proposed method under these circumstances warrants further research.
- In this thesis, the failure lengths in each realisation were computed as the number of elements along the slope toe having an out-of-face displacement greater than a certain threshold value, as calibrated using the threshold-crossing technique (Hicks *et al.*, 2014). Although the failure lengths computed by this simple, yet effective, procedure were a good indication of the trends for comparative purposes, a more accurate procedure needs to be developed for risk-based assessments of real engineering problems which sometimes exhibit sequential and/or retrogressive failures. For example, the material point method (González Acosta *et al.*, 2020) could be used in conjunction with random fields and the Monte Carlo method (Wang *et al.*, 2019).
- This thesis has used a simple soil model, since the focus was to investigate the influence of uncertainties on reliability-based assessments of structures and to benchmark simpler probabilistic methods. A direct (and important) extension of the current work would be to include more realistic aspects of soil behaviour, although the same methodology for probabilistic assessment would still be applicable.

REFERENCES

Arnold, P. (2016). *Probabilistic modelling of unsaturated slope stability accounting for heterogeneity*. Ph.D. thesis, University of Manchester, UK.

de Gast, T., Vardon, P. J. & Hicks, M. A. (2020). Assessment of soil spatial variability for linear infrastructure using cone penetration tests. *Géotechnique* Under review.

González Acosta, J. L., Vardon, P. J., Remmerswaal, G. & Hicks, M. A. (2020). An investigation of stress inaccuracies and proposed solution in the material point method. *Computational Mechanics* **65**, 555–581.

Hicks, M. A., Nuttall, J. D. & Chen, J. (2014). Influence of heterogeneity on 3D slope reliability and failure consequence. *Computers and Geotechnics* **61**, 198–208.

Jamalinia, E., Vardon, P. J. & Steele-Dunne, S. C. (2019). Tthe effect of soil–vegetation–atmosphere interaction on slope stability: a numerical study. *Environmental Geotechnics* , 1–12.

van den Eijnden, A. P. & Hicks, M. A. (2017). Efficient subset simulation for evaluating the modes of improbable slope failure. *Computers and Geotechnics* **88**, 267–280.

Vanmarcke, E. H. (1977). Reliability of earth slopes. *Journal of the Geotechnical Engineering Division* **103**, No. 11, 1247–1265.

Wang, B., Hicks, M. A. & Vardon, P. J. (2019). Slope failure analysis using the random material point method. *Géotechnique Letters* **6**, No. 2, 113–118.

ACKNOWLEDGEMENTS

I wish to express my deepest gratitude to my promotor Prof. Michael Hicks whose vast knowledge and experience in this field helped me realise the goal of this project. The clarity and perfection that he brought to the research articles have always added a different perspective and elevated their value. I am grateful to him for giving me this opportunity to work with him. I also would like to express my sincere gratitude and appreciation to my promotor Dr. Phil Vardon for his valuable comments and encouragement throughout this project. I express my deepest gratitude to my supervisory team for their constant guidance, encouragement and for demonstrating belief in me.

I would like to thank my PhD committee for their valuable time and insightful comments, which have greatly helped me to improve the clarity of my thesis. I would like to extend my thanks to Ir. Henk van Hemert for being instrumental in carrying out the case study with the support of the water board HHNK. I would like to thank NWO and industry sponsors for financing this research programme and the SURF Foundation for their support in carrying out the analyses on the Dutch National e-infrastructure.

I especially would like to thank Bram for helping me with understanding the concepts, helping with developing the models and for always being available for our various discussions on this topic. I would like to thank Tom for helping me with the translations, discussions and for all the good times. I also would like to thank Prof. Cristina Jommi for her valuable insights, Anne-Catherine, Aparajita, Stefano, Haoyuan, Weiyuan, Leon, Elahe, Arash, Varenya, Ivo, Ali, Aoxi, Jiani, Shirish, Andre, Poly, all my past and present colleagues and friends who have supported me throughout this journey and for the wonderful time we have spent together. I would like to thank all my teachers, whose guidance and encouragement have brought me to this stage, especially Dr. Jakka, Dr. Mukerjee and Dr. Jayasree.

This thesis would not have come to this shape, if not for the support and unwavering love of my parents, Kuckuli, Eldho and the rest of my family. I cannot thank Eldho enough for his constant support and understanding during these years.

CURRICULUM VITÆ

Divya VARKEY

18-03-1991 Born in Bhilai, India.

EDUCATION

2009–2013 Bachelor of Technology in Civil Engineering
Department of Civil Engineering
College of Engineering Trivandrum, Trivandrum, India

2013–2015 Master of Technology in Soil Dynamics
Department of Earthquake Engineering
Indian Institute of Technology Roorkee, Roorkee, India

2015–2020 Ph.D. in Geo-engineering
Section of Geo-Engineering, Faculty of Civil Engineering and Geosciences
Delft University of Technology, Delft, The Netherlands

RESEARCH EXPERIENCE

2014–2015 Research intern (DAAD IIT Master sandwich programme)
Institute of Geotechnical Engineering
University of Stuttgart, Stuttgart, Germany

2015–2020 Ph.D. candidate
Section of Geo-Engineering, Faculty of Civil Engineering and Geosciences
Delft University of Technology, Delft, The Netherlands

2020–present Post-doc researcher
Section of Geo-Engineering, Faculty of Civil Engineering and Geosciences
Delft University of Technology, Delft, The Netherlands

List of Publications

Journal Publications

- Varkey, D., Hicks, M.A. & Vardon, P.J. (2019). An improved semi-analytical method for 3D slope reliability assessments. *Computers and Geotechnics*, **111**, 181–190.
- Hicks, M.A., Varkey, D., van den Eijnden, A.P. , de Gast, T. & Vardon, P.J. (2019). On characteristic values and the reliability-based assessment of dykes. *Georisk: Assessment and Management of Risk for Engineered Systems and Geohazards*, **13**(4), 313–319.
- Varkey, D., Hicks, M.A., van den Eijnden, A.P. & Vardon, P.J. On characteristic values for calculating factors of safety for dyke stability. *Géotechnique letters*, **10**(2), 353–359.
- Varkey, D., Hicks, M.A., & Vardon, P.J. Uncertainties in geometry, material boundary and shear strength properties of a 3D slope. *To be submitted*.

Conference Publications

- Varkey, D., Hicks, M.A. & Vardon, P.J. (2017). Influence of spatial variability of shear strength parameters on 3D slope reliability and comparison of analysis methods, *Proceedings of 6th International Symposium on Geotechnical Safety and Risk*, Colorado, USA, pp. 400–409.
- Varkey, D., Hicks, M.A. & Vardon, P.J. (2018). 3D slope stability analysis with spatially variable and cross-correlated shear strength parameters, *Proceedings of 9th European Conference on Numerical Methods in Geotechnical Engineering*, Porto, Portugal, pp. 498–503.
- Varkey, D., Hicks, M.A., Vardon, P.J., & van den Eijnden, A.P. (2019). Influence of spatial variability of shear strength parameters on reliability-based assessment of dykes, *Proceedings of 27th European Young Geotechnical Engineers Conference*, Bodrum, Turkey, pp. 153–160.
- Varkey, D., Hicks, M.A. & Vardon, P.J. (2019). Modified semi-analytical method for 3D slope reliability, *Proceedings of 7th International Symposium on Geotechnical Safety and Risk*, Taipei, Taiwan, pp. 406–411.